1953

LIBRARY
FISH & WILDLIFE SERVICE
PACIFIC OCEANIC FISHERY
INVESTIGATIONS

SEARS FOUNDATION FOR MARINE RESEARCH
BINGHAM OCEANOGRAPHIC LABORATORY, YALE UNIVERSITY

# JOURNAL OF MARINE RESEARCH

VOLUME XI, 1952

NUMBER 2

ISSUED NOVEMBER 15, 1952, NEW HAVEN, CONN., U. S. A.

# JOURNAL OF MARINE RESEARCH

PUBLISHED BY

SEARS FOUNDATION FOR MARINE RESEARCH

BINGHAM OCEANOGRAPHIC LABORATORY, YALE UNIVERSITY

---

BOARD OF EDITORS

*Chairman:* A. E. PARR
*American Museum of Natural History*
*New York*

C. O'D. ISELIN
*Woods Hole Oceanographic Institution*

H. U. SVERDRUP
*Norsk Polarinstitutt*
*Oslo, Norway*

DANIEL MERRIMAN
*Bingham Oceanographic Laboratory*

C.-G. ROSSBY
*Institut für Meteorologi*
*Stockholm, Sweden*

THOMAS G. THOMPSON
*Oceanographic Laboratories*
*University of Washington*

MANAGING EDITOR

YNGVE H. OLSEN
*Bingham Oceanographic Laboratory*
*Yale University*
*New Haven, Conn.*

SEARS FOUNDATION FOR MARINE RESEARCH
BINGHAM OCEANOGRAPHIC LABORATORY, YALE UNIVERSITY

JOURNAL OF
MARINE RESEARCH

VOLUME XI 1952 NUMBER 2

# DETERMINATION OF OCEAN TRANSPORTS AND VELOCITIES BY ELECTROMAGNETIC EFFECTS

By

W. V. R. MALKUS AND M. E. STERN

*Woods Hole Oceanographic Institution*[1]
*Woods Hole, Massachusetts*

## ABSTRACT

The electric potentials in and about an ocean current are shown to be related in a simple fashion to the total fluid transport. In many waters, surface measurements alone permit the determination of this total transport. It is also established that the local vertical potential gradient is a measure of the local velocity. Several techniques of measurement, including the "Geomagnetic electrokinetograph" method, and the errors which may be involved in each, are discussed.

## INTRODUCTION

In reinvestigating[2] the electric potentials induced in ocean currents by the magnetic field of the earth, this work determines the relation between the total potentials across the current and the total volume transport of fluid.[3] The validity of interpreting local electric effects as indicative of the local velocity structure of the fluid stream is discussed, and thus the usefulness of the vertical potential gradient for this purpose is established. Though various methods of measurement

[1] Contribution No. 608 from the Woods Hole Oceanographic Institution.

[2] Previous work has included the papers of: Faraday (1832); Longuet-Higgins (1949); Stommel (1948); von Arx (1950).

[3] Kolin (1945) and Arnold (1951), among others, have arrived at similar relations for the flow of fluid in a pipe.

are possible, the measurements from shipboard are stressed. A ship moving with the fluid stream, however, induces an additional potential; hence an analysis of the relation between shipboard measurement and velocity structure is made for both magnetic field components.

In this paper, (I) the relations between the total transports and electric potentials are deduced and the approximations involved in relating local electric observables to local velocities are determined, and (II) the limitations imposed by the techniques of measurement are discussed and possible future experiments are suggested.

## DISCUSSION

I. It will be recalled that the motion of a conductor at right angles to a magnetic field produces an electric field whose magnitude is $V \times H \times 10^{-8} \frac{\text{volts}}{\text{cm}}$ and which is at right angles to both the motion and the magnetic field (where $V$ is the velocity of the conductor and $H$ the magnetic field). Therefore, as a result of its motion relative to the earth's magnetic field, an ocean stream will have a certain electromotive force induced in it at every point. These emf's set up electric currents and electric fields, and at every point in the fluid the electric current density is proportional to the *effective* electric field and the conductivity of the medium. That is to say,

$$\rho \boldsymbol{i} = \boldsymbol{E} + \boldsymbol{V} \times \boldsymbol{H}, \tag{1}$$

where $\rho$ = resistivity of the water, $\boldsymbol{V}$ = vector velocity of the water, $\boldsymbol{H}$ = earth's magnetic field, $\boldsymbol{i}$ = electric current density, and $\boldsymbol{E}$ = electric field vector.

It is assumed first that the electric and magnetic forces on the ions in the sea are small compared to the hydrodynamic forces, that the electric currents which flow do not appreciably alter the earth's magnetic field, and that a steady state exists. Then the electric field may be represented by a potential function $\varphi$, $\boldsymbol{E} = -\nabla\varphi$ (since $\nabla \times \boldsymbol{E} = 0$). Hence

$$\nabla\varphi = \boldsymbol{V} \times \boldsymbol{H} - \rho \boldsymbol{i}, \tag{2}$$

or

$$\frac{\partial \varphi}{\partial x} = (V_y H_z - V_z H_y) - \rho i_x, \tag{3}$$

$$\frac{\partial \varphi}{\partial y} = (V_z H_x - V_x H_z) - \rho i_y, \tag{4}$$

$$\frac{\partial \varphi}{\partial z} = (V_x H_y - V_y H_x) - \rho i_z, \tag{5}$$

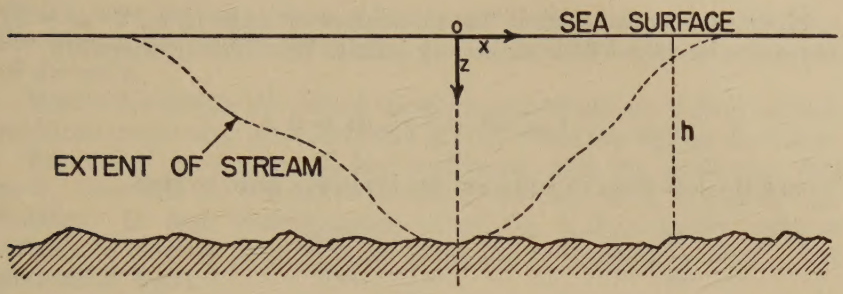


Figure 1.

where the subscripts $x$, $y$, $z$ denote the components of velocity, magnetic field, and electric current in those directions.

Now one considers a coordinate frame with the $y$-axis (into the paper) along the mean direction of an ocean stream, as in Fig. 1. The total surface integrals of equations (3) and (5) to a constant depth $z$ in the $x,z$ plane may be written as

$$\int_{-\infty}^{+\infty}\int_{0}^{z} \frac{\partial \varphi}{\partial x}\, dx\, dz = \int_{-\infty}^{+\infty}\int_{0}^{z} \Big[(V_y H_z - V_z H_y) - \rho i_x\Big]\, dx\, dz\,, \qquad (6)$$

and

$$\int_{-\infty}^{+\infty}\int_{0}^{z} \frac{\partial \varphi}{\partial z}\, dx\, dz = \int_{-\infty}^{+\infty}\int_{0}^{z} \Big[(V_x H_y - V_y H_z) - \rho i_z\Big]\, dx\, dz\,. \qquad (7)$$

In actual ocean streams $\int_{-\infty}^{+\infty}\int_{0}^{z} V_z\, H_y\, dx\, dz$ is very much smaller than $\int_{-\infty}^{+\infty}\int_{0}^{z} V_y H_z\, dx\, dz$ except on the magnetic equator, while $\int_{-\infty}^{+\infty}\int_{0}^{z} V_x H_y dx\, dz$ is very much smaller than $\int_{-\infty}^{+\infty}\int_{0}^{z} V_y\, H_z\, dx\, dz$ except in the rare situation where $H_z$ falls to zero. Partially integrating the potential gradients in equations (6) and (7), one obtains

$$\int_{0}^{z} [\varphi(\infty, z) - \varphi(-\infty, z)]\, dz = \int_{-\infty}^{+\infty}\int_{0}^{z} H_z\, V_y\, dx\, dz - \int_{-\infty}^{+\infty}\int_{0}^{z} \rho i_x\, dx\, dz, \qquad (8)$$

and

$$\int_{-\infty}^{+\infty} [\varphi(x,0) - \varphi(x,z)]\, dx = \int_{-\infty}^{+\infty}\int_{0}^{z} H_x V_y dx\, dz - \int_{-\infty}^{+\infty}\int_{0}^{z} \rho i_z\, dx\, dz\,. \qquad (9)$$

Since the electric current has no sources or sinks (i. e., $\nabla \cdot \rho \boldsymbol{i} = 0$), there can be no net flow across any infinite line (plane); therefore

$$\int_{-\infty}^{+\infty} \rho i_z \, dx = \int_{0}^{\infty} \rho i_z \, dz = 0 \,.^4$$

Hence the last term in equation (9) is always zero, so that

$$\int_{-\infty}^{+\infty} [\, \varphi(x, 0) - \varphi(x, z)] \, dx = \int_{-\infty}^{+\infty} \int_{0}^{z} H_x \, V_y \, dx \, dz \,,$$

and if $H_x$ has small spatial variation across the stream, one may write

$$\oint \varphi dx = H_x T_z \,, \tag{10}$$

where $\oint$ denotes integration around an infinite rectangular contour bounded by $z = 0$ and any other arbitrary $z$, and where $T_z$ is the total volume transport of fluid through that contour. Note that this result is independent of the depth of the sea or of bottom conductivity. The last term in equation (8) is not zero in general, but in the case of a nonconducting bottom, $\int_0^h \rho i_z dz = \int_0^\infty \rho i_z dz = 0$, since no current flows below $z = h$; hence

$$\int_{0}^{h} [\varphi(\infty, h) - \varphi(-\infty, h)] \, dz = \int_{-\infty}^{+\infty} \int_{0}^{h} H_z \, V_y \, dx \, dz \,.$$

Since, at some large distance from the stream, $\varphi$ does not vary with depth, the relation above may be rewritten as

$$(\varphi_{+\infty} - \varphi_{-\infty}) = \frac{H_z T}{h} \,, \tag{11}$$

where $H_z$ is again assumed to have small spatial dependence, $T$ is the total volume transport of fluid, $\varphi_{+\infty} - \varphi_{-\infty}$ is the total potential difference across the stream, and $h$ is the mean depth of the bottom. Estimates of the effect of bottom conductivity in reducing $\varphi_{+\infty} - \varphi_{-\infty}$ have been made by using a three layer analysis developed by Stommel

[4] The electric current in the $y$ direction has been neglected in this equation in comparison with $i_z$. This corresponds to the observation that

$$\int_{-\infty}^{+\infty} \int_{0}^{z} V_x H_y dx \, dz \ll \int_{-\infty}^{+\infty} \int_{0}^{z} V_y H_x d \quad dz$$

and is an approximation of the same magnitude.

(1948); they indicate errors of less than 1% at a few kilometers from the edge of the stream for bottom conductivities one thousandth that of the sea's.

Before discussing the actual measurements made by a ship, several relations permitting interpretation of local velocities will be discussed.

Returning to equation (5) and neglecting again the small term due to $V_x$, note that $\rho i_z = 0$ at the surface of the sea and $\rho i_z \approx 0$ at the sea bottom. In fact, determination of $\rho i_z$ for various model streams similar to those in nature indicate that it is never more than a few percent of $V_y H_x$.

Hence

$$\frac{\partial \varphi}{\partial z} = - V_y H_x ,$$

or

$$V_y = - \frac{1}{H_x} \frac{\partial \varphi}{\partial z} . \tag{12}$$

The approximations involved in this useful equation seem small compared to the possible errors in measurement to be discussed in Section II.

A second approximate relation involves a definition of a quantity

$$k = \frac{H_z V_y}{\rho i_x} . \tag{13}$$

Previous authors (von Arx, 1950; Stommel, 1948) have shown that $k$ is related to the average "equivalent" depth near the region of observation, i. e.,

$$k \approx \frac{h}{h - h_1} ,$$

where $h_1$ is a depth such that $V_y(x, 0)\ h_1$ is the transport per unit section of the stream at the point $x$. Differentiating equation (8) with respect to $z$ one obtains

$$(\varphi_{+\infty} - \varphi_{-\infty}) = \int_{-\infty}^{+\infty} H_z V_y \, dx - \int_{-\infty}^{+\infty} \rho i_x \, dx$$

$$= \int_{-\infty}^{+\infty} \rho i_x (k - 1) dx = \frac{H_z T}{h} . \tag{14}$$

Hence a point to point knowledge of $k$ and $\rho i_x$ permit the determination of the total transport, while

$$V_y \approx \frac{\rho i_x}{H_z} \tag{15}$$

if $k$ is quite close to one, as it may be in equatorial currents.

Another defined quantity,

$$K = \frac{\int_{-\infty}^{+\infty} H_z V_y dx}{\int_{-\infty}^{+\infty} \rho i_x dx}, \tag{16}$$

also has proved to be quite useful. From equations (8) and (11)

$$\varphi_{+\infty} - \varphi_{-\infty} = \frac{H_z T}{h} = (K - 1) \int_{-\infty}^{+\infty} \rho i_x dx, \tag{17}$$

and, since $K$ is the ratio of two integrals, the local random errors and fluctuations of the observations of $V_y$ and $\rho i_x$ are smoothed out. Perhaps a more significant aspect of $K$ is its relation to the mean depth of the total fluid stream. Hence $K$ may be a constant or near-constant for a particular section of the stream, or it might be deduced from theoretical relations between the horizontal and vertical velocity profiles.

A cable laid on or anchored to the ocean bottom could directly measure the potentials in the preceding relations. A ship, however, induces an additional potential between any electrodes it may tow due to its own motion. Considerable discussion has been given to the problems of electrodes towed in line behind a ship (von Arx, 1950). In the absence of wind drift at right angles to the electrodes' heading, the measured potential gradient is

$$(\nabla \varphi)_{measured} = \nabla \varphi - \boldsymbol{V} \times \boldsymbol{H} = - \rho \boldsymbol{i}. \tag{18}$$

Since the total potential across the stream is

$$\int_{-\infty}^{+\infty} \nabla \varphi \cdot d\boldsymbol{l} = \int_{-\omega}^{+\infty} (\boldsymbol{V} \times \boldsymbol{H} - \rho \boldsymbol{i}) \cdot d\boldsymbol{l} \qquad \text{(measured at surface)}$$

where $d\boldsymbol{l}$ is the increment of path of the ship as it crosses the stream, a navigational determination of this path can provide the integral $\int_{-\infty}^{+\infty} \boldsymbol{V} \times \boldsymbol{H} \cdot d\boldsymbol{l}$; this knowledge, plus the measured potential, provides $\int_{-\infty}^{+\infty} \rho \boldsymbol{i} \cdot d\boldsymbol{l}$. The total fluid transport is then found from equations (11) or (17).

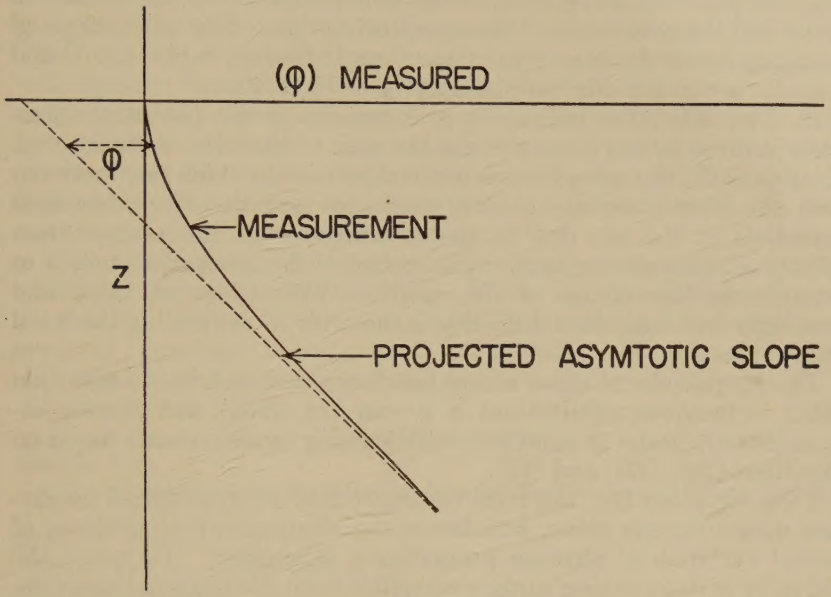


Figure 2.

For an electrode which is let down from a ship to determine the potential between a surface electrode and depth $z$,

$$\varphi_{measured} = \boldsymbol{V}_B \times \boldsymbol{H} \cdot \boldsymbol{s} - \int_0^{\boldsymbol{s}} \nabla\varphi \cdot d\boldsymbol{s}\,, \tag{19}$$

where $\boldsymbol{s}$ is the vector distance between the surface and deep electrode and $\boldsymbol{V}_B$ is the velocity of the ship with respect to the earth. In the simple case of the ship drifting or moving such that the deep electrode departs only slightly from due upstream or due downstream in its horizontal displacement from the surface electrode, the measured potential becomes:

$$\varphi_{measured} = V_B \times \boldsymbol{H} \cdot \boldsymbol{z} - [\varphi(x, z) - \varphi(x, 0)]\,. \tag{20}$$

(One assumes that the depth $z$ can be determined from the pressure at the deep electrode.) The gradient of $(\varphi)_{measured}$ permits the determination of $[V_B - V_y(x, 0)]$ as well as the variation of $V_y$ with depth from equation (12), and, if the measurements are made to sufficient depth to be below the stream (i. e. $\frac{\partial\varphi}{dz} \to 0$), then $V_y$ $(x, 0)$ and $V_B$ separately are determined. Fig. 2 shows a theoretical measurement from a drifting ship and may help to clarify these conclusions.

$\varphi$, the potential at depth $z$, is the potential between the measured curve and the projection of its asymptotic slope. The initial slope of $(\varphi)_{measured}$ for a drifting ship is zero, as indicated, while the initial slope for a moving ship determines $[V_B - V_y(x, 0)]$.

II. The difficulties encountered in measuring the potential differences induced by the motion of the sea seem to have two main sources. The first is the changing electrochemical potentials which exist between even the most carefully chosen electrodes and the electrochemical potentials in the sea due to spatial variation in the temperature, salinity and oxygen content. The second is the navigational error in determining the change of ship position with time. A third and seemingly less important difficulty is the error in estimating the wind drift of the ship.

The magnitude of these errors has been analyzed in considerable detail in previous publications, e. g. von Arx (1950), and those computations are borne in mind here in discussing measurements based on equations (10), (11), and (12).

From equation (11) the total transport may be determined by surface measurements alone, and hence the electrochemical problem of spatial variation of physical properties is minimized. However, the difficulty of determining surface velocities from navigational measurements is exaggerated by the subtraction of $\int_{-\infty}^{+\infty} \rho \boldsymbol{i} \cdot d\boldsymbol{l}$ from $\int_{-\infty}^{+\infty} \boldsymbol{V} \times \boldsymbol{H} \cdot d\boldsymbol{l}$, for both of these experimental quantities may be large, while their difference, proportional to the total transport, may be small in comparison. A criterion for the usefulness of equation (11) is $K$, defined in equation (16) as

$$K = \frac{\int_{-\infty}^{+\infty} \boldsymbol{V} \times \boldsymbol{H} \cdot d\boldsymbol{l}}{\int_{-\infty}^{+\infty} \rho \boldsymbol{i} \cdot d\boldsymbol{l}}.$$

The probable error is then at least $\frac{1}{K-1}$ greater than the integrated navigational error. (Preliminary surveys of the Gulf Stream area [von Arx, 1951] suggest that $K$ lies in the range of 1.1 to 1.5. Equatorial waters may be expected to have small $K$'s, and since there is no Loran network in these areas, the usefulness of equation [11] would be small.)

From equations (10) and (12) one might deduce both local velocities and total transport in all waters, yet here the electrochemical problem

is most serious. While the determination of temperature with depth can easily be made and corrections to the observed potential established, the variation of oxygen with depth can produce potentials considerably in excess of those due to the fluid transport. Several suggestions have been advanced to shield the electrodes from these concentration gradients. Surrounding the deep electrode with water carried from the surface seemed the most feasible of these, but no assurance of the success of this method can be given until adequate experiments have been performed.

The authors would like to acknowledge with gratitude the assistance of Henry Stommel and William von Arx of the Woods Hole Oceanographic Institution in the many discussions of the theoretical and practical problems arising in the application of electromagnetic methods to measurements in the ocean.

## REFERENCES

Arnold, J. S.
1951. Electromagnetic flowmeter for transient flow studies. Rev. sci. Instrum., *22* (1): 43–47.

Faraday, Michael
1832. Phil. Trans. Roy. Soc., p. 175.

Kolin, Alexander
1945. An alternating field induction flow meter of high sensitivity. Rev. sci. Instrum., *16* (5): 109–116.

Longuet-Higgins, M. S.
1949. The electrical and magnetic effects of tidal streams. Mon. Not. R. astr. Soc., geophys. Suppl., *5* (8): 285–307.

Stommel, Henry
1948. The theory of the electric field induced in deep ocean currents. J. mar. Res., *7* (3): 386–392.

von Arx, W. S.
1950. An electromagnetic method for measuring the velocities of ocean currents from a ship under way. Pap. phys. Oceanogr. Meteor., *11* (3): 1–62.

von Arx, W. S.
1951. Some measurements of the surface velocities of the Gulf Stream. W. H. O. I. Tech. Rep., Ref. No. 51–96, December.

# SALINITY DISTRIBUTION AND CIRCULATION IN THE CHESAPEAKE BAY ESTUARINE SYSTEM[1,2]

By

D. W. PRITCHARD

*Chesapeake Bay Institute of The Johns Hopkins University*

## ABSTRACT

The salinity distribution in a coastal plain estuary governs the dynamic structure. In the estuaries studied, the salinity increases with depth, the salinity-depth curve having the general shape of an inverse tangent function. Though there is a layer of relatively rapid increase in salt content with depth, separating an upper less saline layer from a lower more saline layer, this halocline is still sufficiently weak to allow a downward random flux of fresh water as well as an upward random flux of salt. The longitudinal salinity gradient is approximately uniform with depth. The salinity is on the average higher on the right side of the estuary (looking downstream) than on the left.

Superimposed upon the oscillatory tidal motion there is a net circulation in which the upper less saline layer moves seaward and the lower more saline layer moves up the estuary. The boundary between the two layers of net flow has a slight lateral slope, being deeper on the right side of the estuary than on the left.

As a result of considerations of the salt balance, a net upward vertical motion is implied. A combination of the concepts of salt continuity and volume continuity allow the successful computation of the mean net horizontal velocity in the two opposite flowing layers.

## INTRODUCTION

The Chesapeake Bay and its tributary estuaries may be classed in a group of coastal indentations called coastal plain estuaries. This type of estuary has been formed by the drowning of a former river valley either as a result of subsidence of the land or of a rise in sea level. This body of water, into which rivers empty, takes the shape of an elongated indentation of the Atlantic Coastline. The depths are relatively shallow, so that mixing of at least moderate magnitude extends to all depths.

The analysis to be presented here is based upon a series of extensive surveys of the physical and chemical properties of the waters of Chesapeake Bay and its major tributaries. The data were collected

[1] Contribution No. 6 from the Chesapeake Bay Institute.

[2] Results of work carried out for the Office of Naval Research of the Navy Department, the State of Maryland (Department of Research and Education), and the Commonwealth of Virginia (Virginia Fisheries Laboratory), under contract with The Johns Hopkins University.

between July 1949 and January 1951. During this period ten separate cruises were undertaken in the Bay and its tributaries, with an average of 120 stations occupied on each cruise.

A total of 5,830 salinity measurements were made, of which approximately 2,027 were obtained by means of the conductivity-temperature-indicator developed at the Chesapeake Bay Institute for rapid *in situ* measurements. Most of the samples were also analyzed for pH, phosphate, dissolved oxygen, and turbidity.

Temperature measurements were made chiefly with the bathythermograph, though an electronic temperature device was used extensively after August 1950. Some 1,200 surface temperatures were obtained by means of a bucket thermometer, and approximately 800 subsurface temperatures were taken by means of reversing thermometers. These thermometer temperatures were employed primarily for calibration of the bathythermographs.

The above data have been compiled in the Chesapeake Bay Institute Data Reports 1 through 7, which are available in the majority of oceanographic libraries in the United States.

Current velocity was measured with a modified Jacobsen drag current meter, which has been described by Pritchard and Burt (1951). Approximately 1,650 individual current measurements were obtained and analyzed for this study, the majority of them from the James River estuary. Current observations made in the Chesapeake Bay by the Coast and Geodetic Survey were also used in the analysis.

## TREATMENT OF DATA

For each station the temperature and salinity, as well as other chemical properties, were plotted against depths. Vertical sections and horizontal charts for each survey were then prepared from these individual station curves. The charts showed the distribution of temperature and salinity at the surface and at depths of 10, 20, 30, 40, and 60 feet. In each case consideration was given to the probable effect of tidal motion on the individual measurements.

The study of the salt balance is based upon an extensive field investigation of the James River estuary. Approximately 1,530 salinity and 1,600 current velocity measurements were made during two periods, the first from 17 June through 21 July 1950, the second from 30 August to 3 September 1950. In this analysis it was necessary to use data averaged with respect to the periodic tidal fluctuations.

The James River data were divided into four periods, each period covering at least six tidal cycles. The salinity data were then averaged for each period in such a way that the average vertical gradients were

maintained. This was accomplished by averaging with respect to a characteristic inflection point on the vertical salinity curve rather than with respect to depth. While the resulting average curve gives slightly different salinities at individual depths than a straight averaging process would, the mean salinity from top to bottom is the same in both cases.

The current velocities were for the most part directed along the longitudinal axis of the estuary, either in the ebb direction (toward the mouth of the estuary) or in the flood direction (toward the head of the estuary). The appropriate ebb or flood component of all velocity observations was plotted against a time scale for each five feet of depth. (See Fig. 5 as an example of the type of plot.) The areas under the resulting velocity time curve were then planimetered, taking ebb areas as positive and flood areas as negative. The final mean velocity figures for each depth and for each period were obtained by dividing the net velocity-time areas by the total time in each period.

## DISCUSSION OF THE OBSERVED DISTRIBUTION OF SALINITY AND CURRENT VELOCITY

The Chesapeake Bay and its major tributaries may be considered an estuarine system composed of a number of estuaries of different size and character leading into the lower Chesapeake Bay. This estuarine system is shown in Fig. 1. The Chesapeake Bay is approximately 165 nautical miles long, extending from the mouth of the Susquehanna at Havre de Grace, Maryland, to the Virginia Capes. If the upper limit of the estuarine region is defined as the mean limit of measurable salt water intrusion, then the area of the Chesapeake Bay estuarine system is 3,014 square miles (nautical).

The 20 and 60 foot depth contours are shown in Fig. 1. Approximately 50% of the estuarine system (i. e., Bay plus tributaries) is less than 20 feet deep. Thirty-five per cent of the total area has depths greater than 30 feet, 18% greater than 40 feet, and only 8% greater than 60 feet. The corresponding figures for Chesapeake Bay alone are 57% of the area greater than 20 feet in depth, 44% greater than 30 feet, 24% greater than 40 feet, and 10% greater than 60 feet.

The Susquehanna River contributes 49% of the annual fresh water inflow into the Bay, but it contributes 87% of that above the mouth of the Potomac. Thus the Bay above the mouth of the Potomac may be considered the estuary of the Susquehanna.

The Potomac River estuary is the second largest in the system, the salt water intruding in measurable quantity nearly 60 miles above Chesapeake Bay proper. The Potomac River contributes about 18% of the total fresh water inflow into the Bay.

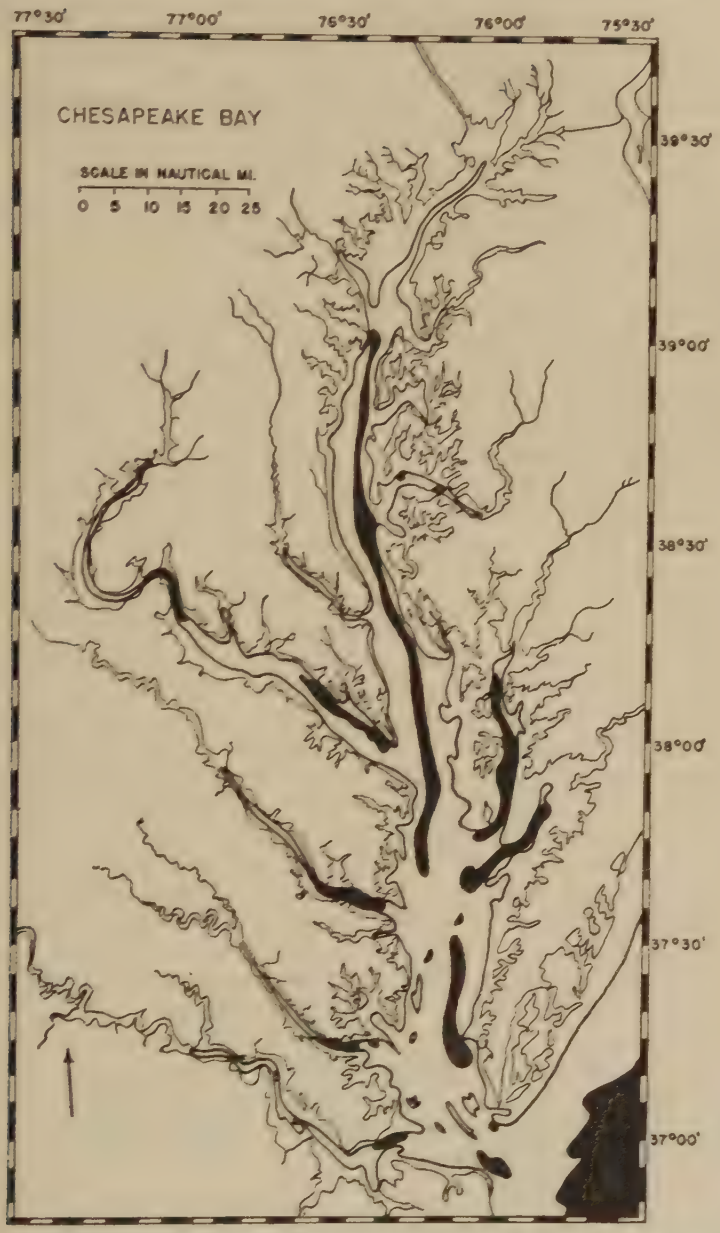


Figure 1. The Chesapeake Bay Estuarine System. Heavy line is 20-foot contour. Black areas represent depths greater than 60 feet.

About 16% of the annual contribution of fresh water is supplied by the James River, which enters the Bay only 15 miles from the Virginia Capes; the Rappahannock River contributes about 4% of the fresh water inflow, the York River about 2%. Only 7% is contributed by the rivers and streams entering from the eastern shore of the Bay, the remaining 4% being supplied by the small streams entering from the western shore.

The total fresh water inflow entering the Bay and its tributaries each year is slightly greater than the total volume of the estuarine system.

The lower Chesapeake Bay, from the Potomac southward, may be considered as a composite estuary, parent to the estuaries of the Susquehanna, Potomac, Rappahannock, York, and James rivers. This composite estuary is considerably more complicated than the tributary estuaries, each of which has essentially only one source of fresh water.

The typical horizontal salinity distribution is shown in Fig. 2. A characteristic feature of this distribution is the obliqueness of the isohalines, resulting in higher salinity on the left side and lower salinity on the right side of the estuary. (Directions are taken in reference to facing toward the mouth of the estuary.) In the lower Chesapeake Bay proper this feature may be related to the greater fresh water inflow from the western shore. However, above the mouth of the Potomac, where the major source of fresh water is the Susquehanna, the lateral distortion of the salinity pattern is also present though somewhat less pronounced. Whenever detailed surveys involving time series of observations have been made in the tributary estuaries of the Potomac, Rappahannock, and James rivers, slightly higher mean salinities have been found on the left side of the estuary. In these narrower estuaries the differences have been slight but definite. In Fig. 2 the mean salinities on either side of three cross sections in the James River have been entered to indicate the magnitude of the lateral salinity gradient in this relatively narrow estuary. Since this cross-stream gradient has been found in other estuaries where observations have been sufficiently detailed, it appears that this phenomenon is due to the earth's rotation rather than peculiar geographical features.

In the upper Bay and in each of the tributary estuaries there are considerable seasonal variations in salinity which diminish in magnitude toward the mouth of the Bay. In spring the high river flow is reflected in minimal salinities throughout the estuary while in summer and fall the decreased river flow results in maximum salinities during the latter season.

In contrast to the fairly regular salinity field, the temperature distribution over much of the year shows no clear-cut pattern. The summer

Figure 2. Typical surface salinity pattern in Chesapeake Bay and tributary estuaries.

temperature distribution indicates that the temperatures are controlled primarily by the local weather conditions. In winter the surface isotherms follow a more regular pattern, with temperatures increasing from the head of the estuary towards the ocean.

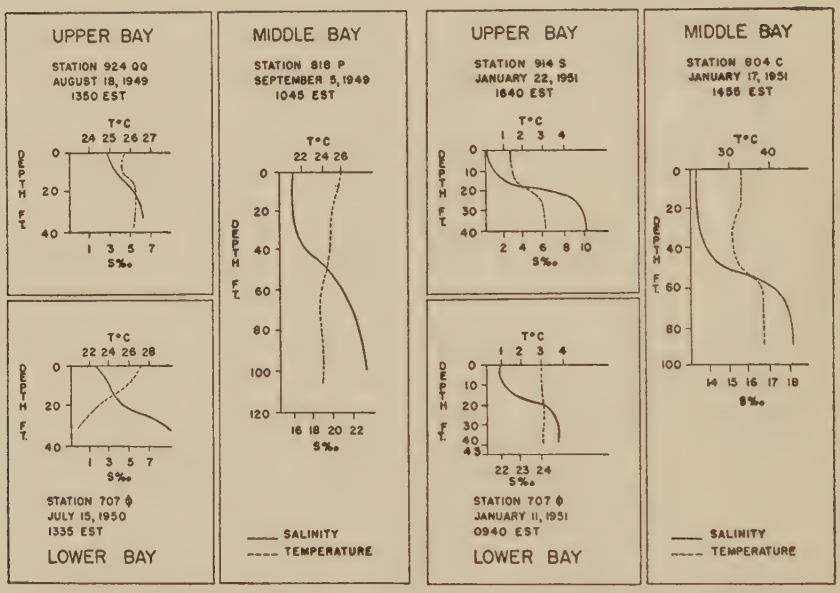


Figure 3. Examples of vertical profiles of temperature and salinity in the Chesapeake Bay: (left) summer; (right) winter.

Fig. 3 shows examples of summer and winter station curves in the Chesapeake Bay. Throughout the year the salinity-depth curves have the general shape of an inverse tangent function with an inflection point at mid-depth. The temperature curves frequently show a positive gradient at the depth of maximum salinity change, particularly in winter.

During the summer of 1950 an extensive field study of the oyster seed bed area in the James River estuary was undertaken. The large amount of data obtained in this study permitted a more detailed examination of the salinity distribution and of the concomitant physical structure than was possible for other areas. Thus it has been possible to describe in some detail the horizontal salinity distribution over approximately 15 miles of this estuary at a particular phase of the tide. Figs. 4 shows surface salinities at high and low water on 2 September 1950. Though the general features of distribution are the same

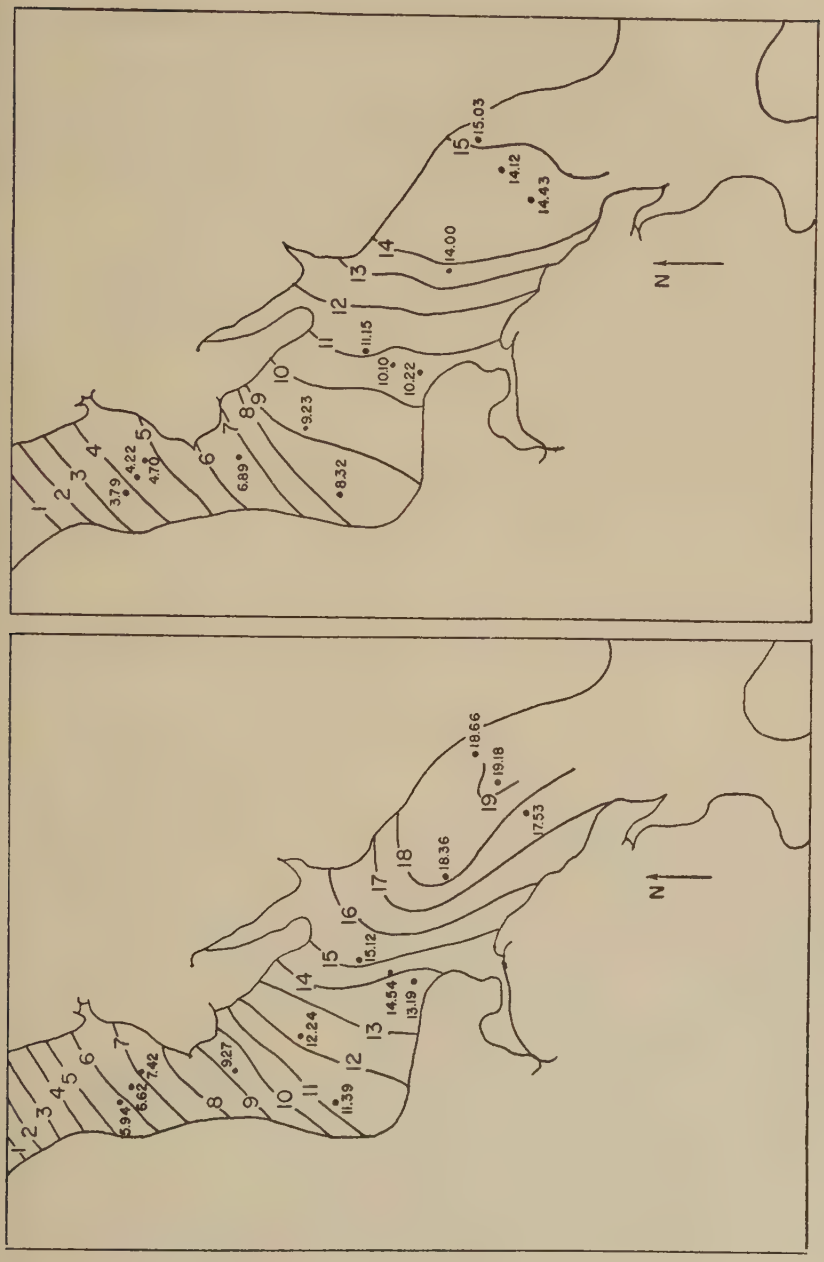


Figure 4. Surface salinity distribution in the James River estuary: (left) high water; (right) low water.

at both stages of the tide, the salinity at high water averages about 4°/₀₀ higher than that at low water.

Fig. 5 shows the variation in salinity with time at the surface and at 10 and 20 feet for a single station in the James River estuary. The observed currents at each depth are plotted on the same graph. The

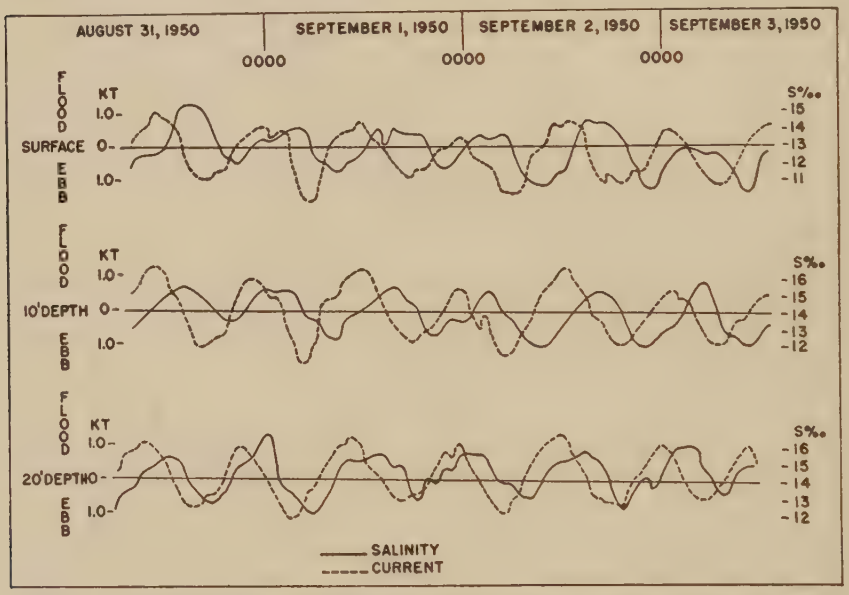


Figure 5. Time variations in current and salinity at a station in the James River estuary.

periodic character of the time changes in the current due to the tide are evident from this graph. Data of the type shown in Fig. 5 were analyzed to find the mean variation in salinity and current over a tidal cycle (Fig. 6). It is seen from the latter figure that the surface salinity reaches a maximum after the surface current has shifted to ebb. This is due to the fact that the shift in current from flood to ebb occurs first at the surface. Consequently the salinity in the lower layers is still increasing due to the flooding tide even when the surface waters are ebbing. The mixing of this higher salinity water from below causes the surface salinity maximum to occur after the ebb shift in current.

Three mean salinity-depth curves for stations in the James River estuary are presented in Fig. 7. The region of high salinity gradient at mid-depths, pointed out previously for data taken in the Bay proper, appears in these curves, which have the general shape of an inverse tangent function. However, the more detailed observations reveal regions of increased gradient near the surface and near the bottom.

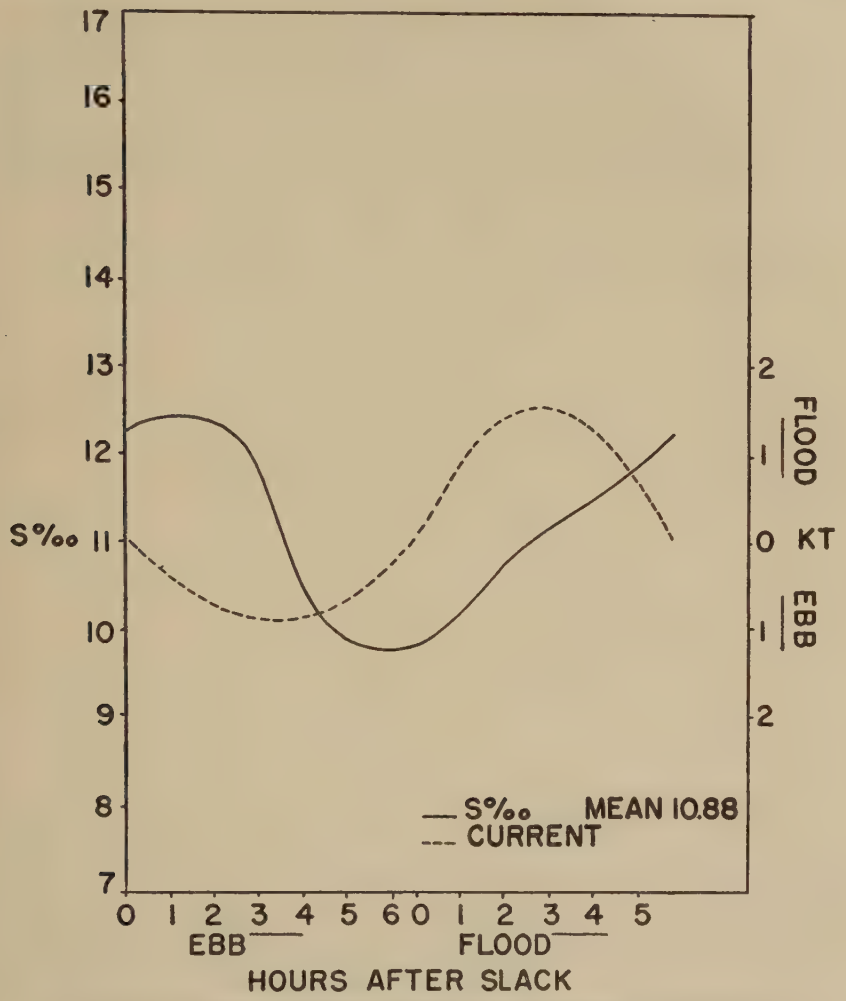


Figure 6. Mean time variation of salinity and current for one tidal cycle.

Although the surface gradient disappears under conditions of high winds, it is present in the mean picture.

Tidal currents, varying in maximum magnitude from one-half to three knots, occur in the estuaries of the Chesapeake Bay system. Although the Coast and Geodetic Survey (1930) has made extensive measurements of the surface currents because of their importance to navigation, no previous attempt has been made to obtain sufficient

current data for an analysis of the net nontidal velocity distribution with depth. Most of the C and GS current observations were made at a depth of seven feet, with only a few short period measurements at greater depths.

An analysis of the few usable sets of observations from the C and GS shows that within the estuary there is an upper layer in which the

Figure 7. Mean salinity-depth curve at three stations in the James River estuary.

net current is directed toward the ocean and a deeper layer in which it is directed towards the fresh water. Although these data indicate that the deeper the water the lower the location of the boundary between the two layers, this suggestion cannot be verified. The mean depths in the James River, where extensive measurements are available, do not vary sufficiently to show such a relationship.

During the study of the James River oyster seed bed area in the summer of 1950, serial current measurements were obtained at five-foot depth intervals at some 12 stations. Only three of these stations were located in the relatively deep water of the channel, the others being located over the oyster bars on either side. The current data from these three stations showed that there is an upper layer with a net motion toward the mouth of the estuary and a deeper layer with a net motion toward the head of the estuary.

Continuous observations were obtained for three periods between 18 June and 21 July 1950. Mean current data for each of the three periods at one of the stations are shown in Figs. 8 and 9. In Fig. 8 the mean ebb-velocity and mean flood-velocity are plotted against depth. The ebb velocities are relatively large on the surface and decrease with depth, while the flood velocities are relatively small on the

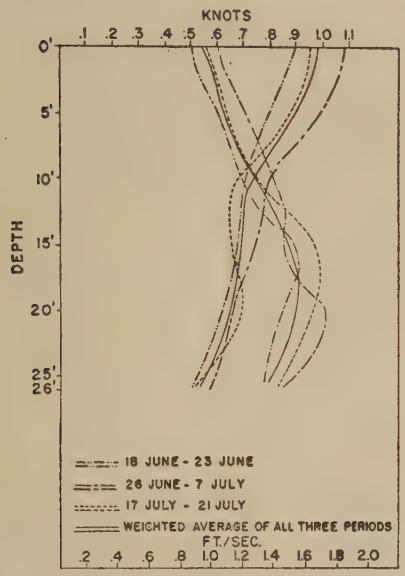


**Figure 8.** Mean ebb velocities (heavy lines) and mean flood velocities (light lines) for three periods in the James River estuary.

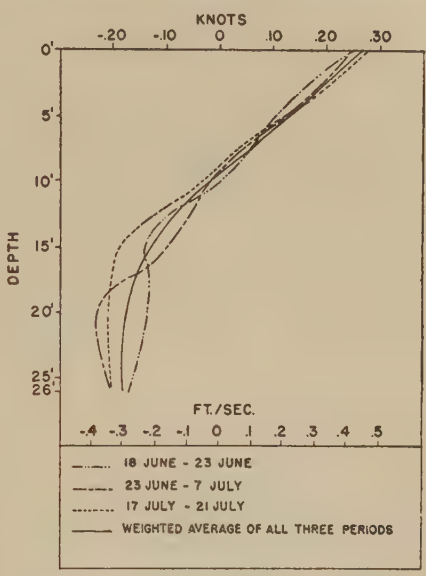


**Figure 9.** Mean velocities (nontidal) for three periods in the James River estuary.

surface, increase to a depth of about 17 feet, and then slowly decrease towards the bottom. The two sets of curves cross at about 10 feet, where the magnitude of the mean ebb current is the same as the magnitude of the mean flood current.

The net velocity-depth curve for each period is shown in Fig. 9. Above ten feet the current is directed down the estuary and is designated as positive; below ten feet the current is directed up the estuary and is designated as negative.

All of the current data produced similar curves. Although the shallow water stations gave only the upper portion of the curve, they served to reveal the cross-sectional structure. Fig. 10 gives the variations in depth of the boundary between the upper and lower layers in a section across the James River. This boundary, which is designated

as the surface of no net motion, appears to slope upwards from the right of the estuary to the left. This results in a thicker layer with positive flow on the right (low mean salinity) than on the left (high mean salinity).

This slight slope in the surface of no net motion, as well as the lateral salinity gradient, suggests the influence of the earth's rotation.

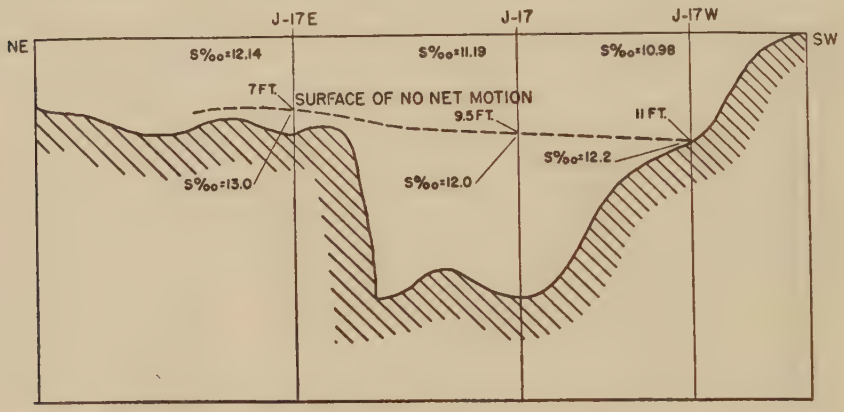


**Figure 10.** Cross section in James River estuary showing slope of surface of no net motion.

There is some indication that in certain estuaries the slope and depth of this surface of no net motion is such that it actually intersects the water surface, resulting in a net up-estuary flow at all depths on the left side of the estuary.

## SUMMARY OF THE OBSERVED PHYSICAL STRUCTURE AND CIRCULATION PATTERN

The observed distributions, as discussed, can be fitted into a consistent picture which describes the physical structure and the circulation pattern in a coastal plain estuary in the midlatitudes. As an aid in the presentation, a geographically simplified model estuary will be discussed. This estuary is elongated and a river brings in fresh water at the head. The smooth straight shore lines diverge from each other toward the mouth of the estuary. The bottom slopes smoothly upward from the sea towards the head.

Consider a coordinate axis with its origin in the fresh water at the head of the estuary. The $x_1$ axis is directed horizontally down the central axis of the estuary toward the mouth. The $x_2$ axis points vertically downward. The lateral coordinate is $x_3$ and is directed from the center of the estuary toward the right-hand shore.

The distribution of salinity governs the dynamic structure. The salinity increases from zero at the head of the estuary to nearly that of sea water at the mouth. The isohalines are not perpendicular to the $x_1$ axis but run rather obliquely across the estuary, the salinities on the right side being slightly lower than those on the left.

The vertical salinity profile has the general shape of an inverse tangent curve. Close to the bottom and to a lesser extent near the surface the curve departs from a typical tangent shape due to boundary effects.

From the standpoint of physical structure and circulation the estuary may be considered as having two layers. In the upper layer there is a net horizontal flow down the estuary, in the lower a net horizontal flow up the estuary. The boundary between the two layers has a slight lateral slope, with the right side deeper than the left.

The net-velocity-depth curve is exponential in character. In the upper layer it decreases from a maximum on the surface to zero at the boundary between the two layers. In the lower layer the horizontal component of velocity is directed in the negative $x_1$ direction, its magnitude increasing with depth until the frictional layer at the bottom is reached.

The boundary between the two layers occurs close to but does not necessarily coincide with the inflection point on the salinity-depth curve. Thus the upper layer is of lower salinity than the lower layer. The volume of flow in the upper layer must exceed the volume of flow in the lower layer by an amount equal to the inflow of fresh water from the river.

Though the salinity distribution shows a seasonal variation, it may be considered to be in steady state during any particular season. Since the upper layer is transporting seaward a net amount of fresh water equal to the inflow, there must be a flow of salt water into the upper layer to maintain the salinity distribution. This is accomplished by a net transfer of water of relatively higher salinity from the lower to the upper layer. Hence there must be a negative vertical velocity across the boundary between the two layers. The volume of flow in the upper layer increases toward the mouth and that in the lower layer decreases toward the head. A schematic presentation of the volume transport in a longitudinal section down the central axis of the estuary is shown in Fig. 11.

Though the tidal currents constitute the most obvious water movements, they are considered here as being primarily responsible for supplying the energy needed for the vertical and horizontal mixing. The tidal currents in the estuary are of the reversing type, directed up and down its longitudinal axis. The observed net horizontal current

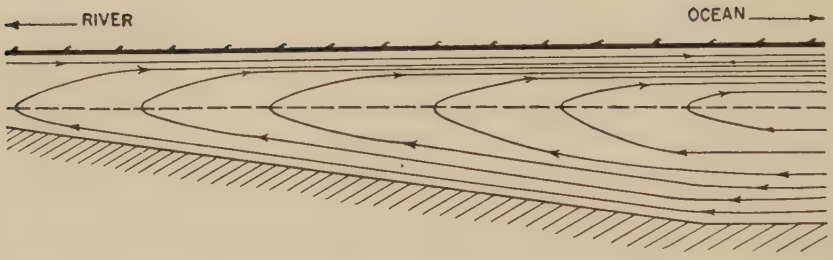


Figure 11. Schematic presentation of streamlines in a longitudinal section down central axis of the estuary.

is obtained by averaging the total current observations over one or more complete tidal cycles.

## PRELIMINARY INVESTIGATION OF THE SALT BALANCE

The studies in the James River are sufficient to evaluate certain features of the salt balance. Though a detailed analysis of the processes which control the salinity distribution is now in preparation, some preliminary results are reported here.

Neglecting molecular diffusion, the instantaneous local rate of change of salt concentration, $s$, is given by

$$(1) \qquad \partial s/\partial t = -\frac{\partial (v_i s)}{\partial x_i}. \qquad (i = 1, 2 \text{ and } 3)$$

Consider a segment of the estuary bounded at either end by a cross section. Designating the total salt content within the segment by $S = \int\int\int_V s dV$, where $V$ is the volume of the segment, we have from (1)

$$(2) \quad \partial S/\partial t = \frac{\partial}{\partial t}\left\{\iiint_V s dV\right\} = -\iiint_V \frac{\partial}{\partial x_i}(v_i s) dV$$

$$= -\iint_\sigma v_i s d\sigma_i,$$

where $\int\int_\sigma f d\sigma_i$ represents the integral over the bounding surfaces of the segment. Now taking the time mean of equation (2), and introducing sums of a mean term and a random term for both the instantaneous velocity and salinity, (2) becomes

$$(3) \qquad <\partial S/\partial t> = -\iint_\sigma <v_i s> d\sigma_i = -\iint_\sigma \bar{v}_i \bar{s} d\sigma_i$$

$$- \iint_\sigma <v_i' s'> d\sigma_i.$$

For steady state, $<\partial S/\partial t> = 0$, and hence

$$4) \qquad \iint_\sigma \bar{v}_i \bar{s} d\sigma_i + \iint_\sigma <v_i' s'> d\sigma_i = 0.$$

The first term of equation (4) represents the net flux of salt into the segment due to advection through the boundaries. The second term represents the net flux of salt due to random motion through the boundaries. Oceanographers have called this latter term "diffusion" and have replaced the terms of the type $<v_i's'>$ by terms of the type $A_i\partial\bar{s}/\partial x_i$, where $A_i$ is the eddy diffusivity.

If the segment under study is bounded by the surface, bottom, and sides of the estuary, then only the horizontal terms in equation (4) need be considered, since there can be no motion through the upper and lower boundaries. Equation (4) then becomes

$$\int\int_\sigma \bar{v}_1\bar{s}d\sigma_1 + \int\int_\sigma <v_1's'>d\sigma_1 = 0\,. \tag{5}$$

Observations of mean salinity and velocity are available for ten separate cases, such that for each case the first term in equation (5) can be evaluated. It is convenient, both for the present discussion and for later analysis, to consider this first integral in two parts: one term involving the upper layer where the velocity is positive, the other term involving the lower layer where the velocity is negative. The value of the integral $\int\int_\sigma <v_1's'>d\sigma_1$, as determined from equation (5), was in all cases less than 5% and in seven of the ten cases less than 1% of either of the two parts of the first term in equation (5).

This analysis is important in that the salinity balance within a segment bounded by the surface and the bottom is maintained primarily by horizontal advection, the horizontal diffusion being of only slight importance.

The fact that the horizontal diffusion term appears small suggests that the concepts employed to determine the net flow across the sill of certain basins (Sverdrup, Johnson and Fleming, 1946: 146–150) may be used in computing the net flow in both the upper and lower layers of this coastal plain estuary. Neglecting horizontal diffusion, equation (5) becomes

$$\int\int_\sigma \bar{v}_1\bar{s}d\sigma_1 = 0\,. \tag{6}$$

For nondivergent flow, $\partial\bar{v}_i/\partial x_i = 0$. Taking the integral over the volume $V$, and applying Green's formulae, we have

$$\int\int_\sigma \bar{v}_i d\sigma_i = 0\,, \tag{7}$$

which, when applied to a segment of the estuary bounded by the surface, by the bottom and sides, and by two cross sections, becomes

$$\int\int_\sigma \bar{v}_1 d\sigma_1 = 0\,. \tag{8}$$

Equations (6) and (8) represent surface integrals taken over the two cross sections that bound the segment. At the uppermost section, in

fresh water, the value of the integral in equation (8) is simply the river flow. At the lower section, within the estuarine region, the surface integrals in both of the above equations may be considered in two parts: one term involving integration over the upper layer, where the net velocity is in the positive $x_1$ direction, and the second integral involving integration over the lower layer, where the net velocity is in the negative $x_1$ direction. Equations (7) and (8) may then be solved simultaneously for the mean value of the velocity in each layer.

River-flow data from gaging stations of the U. S. Geological Survey are available for the James River at Richmond and for the two tributary streams, the Appomatox and the Chickahominy, which enter the James below Richmond. If the reported river flow is used directly in the computation of mean velocities, slightly high results are obtained. By correcting the river-flow data for an estimated evaporation excess of 0.01 foot per day, computed current velocities correspond closely to the observed ones.

Table I gives the results of such determinations at three stations on the James River estuary for four different periods of observations. In each of the ten cases presented, careful observations of velocity were made at each five feet of depth. Average velocities for the upper and lower layer were determined from these observed values; these are also given in Table I. Positive values designate down-estuary flow; negative values designate up-estuary flow.

TABLE I. Computed Mean Velocities and Observed Mean Velocities for a Series of Stations in the James River Estuary (ft/sec)

| | | *Computed Velocities* | | *Observed Velocities* | | *River* |
|---|---|---|---|---|---|---|
| *Station* | *Date (1950)* | *Upper Layer* | *Lower Layer* | *Upper Layer* | *Lower Layer* | *Flow* $ft^3\ sec^{-1}$ |
| J-24A | 18 to 23 June | .33 | −.23 | .31 | −.20 | 4357 |
| | 26 June to 7 July | .33 | −.24 | .32 | −.22 | 3685 |
| | 17 to 21 July | .39 | −.27 | .35 | −.25 | 4610 |
| J-17 | 18 to 23 June | .23 | −.24 | .21 | −.20 | 4357 |
| | 26 June to 7 July | .22 | −.23 | .22 | −.24 | 3685 |
| | 17 to 21 July | .22 | −.22 | .22 | −.22 | 4610 |
| | 30 August to 3 Sept | .19 | −.22 | .19 | −.18 | 2823 |
| J-11 | 18 to 23 June | .29 | −.23 | .30 | −.24 | 4357 |
| | 26 June to 7 July | .34 | −.28 | .34 | −.28 | 3685 |
| | 17 to 21 July | .35 | −.29 | .33 | −.27 | 4610 |

The computed velocities exceeded the observed by an average difference of 4.8%. The individual differences varied from −5 to 20%. This error of approximately 5% is only slightly larger than that to be

expected from neglecting the small term involving the random horizontal transfer of salt.

The standard deviation between the observed and computed velocities was less than 0.02 ft/sec, which is certainly close to the limits of accuracy of the observations. Thus it appears that, within the accuracy of the observations of the various parameters, it is possible to determine the mean down-estuary flow in the upper layer and the mean up-estuary flow in the lower layer from the river flow, the salinity distribution, and the cross-sectional dimensions.

## REFERENCES

Pritchard, D. W. and W. V. Burt

1951. An inexpensive and rapid technique for obtaining current profiles in estuarine waters. J. Mar. Res., *10:* 180–189.

Sverdrup, H. U., M. W. Johnson and R. H. Fleming

1946. The Oceans. Their Physics, Chemistry, and General Biology. Prentice-Hall, Inc., New York. 1087 pp.

U. S. Coast and Geodetic Survey

1930. Tides and currents in Chesapeake Bay and tributaries. By F. J. Haight and others. Spec. Publ. U. S. Dept. of Commerce, No. 162.

# THE DETERMINATION AND DISTRIBUTION OF COPPER IN SEA WATER

## PART I. THE SPECTROPHOTOMETRIC DETERMINATION OF COPPER IN SEA WATER

By

TSAIHWA J. CHOW AND THOMAS G. THOMPSON

*Oceanographic Laboratories*
*University of Washington, Seattle*

## ABSTRACT

The spectrophotometric determination of copper in sea water has been studied with sodium diethyldithiocarbamate as the color forming reagent. This reagent, compared with the frequently used dithizone, affords simpler operation, less interference from other metallic ions, higher sensitivity, and greater accuracy. Xylene has been found to be most desirable for extracting the copper diethyldithiocarbamate. Factors studied in some detail include the effects of varying the extracting time, concentration as it affects the coefficient of extraction, amount of reagent, hydrogen ion concentration, salinity, concentration of oxidizing and reducing agents, and the stabilities of the diethyldithiocarbamate reagent and the colored copper diethyldithiocarbamate. The composition of the color complex has been determined by the continuous variation method. Procedures for minimizing the effects of interfering substances have also been discussed. Samples of coastal sea water have been analyzed for copper content by this method.

## INTRODUCTION

Copper occurs in sea water in an extremely small concentration, but, similar to the nutrient salts, it plays an important role for certain marine organisms. Some invertebrates, oysters in particular, concentrate copper to a considerable extent. It appears in the blood of some invertebrates in the pigmented respiratory compound, hemocyanin, and serves as an oxygen carrier in a role somewhat analogous to that of iron in hemoglobin in the blood of mammals. It is present in the proteins hemocuprein and hepatocuprein in mammalian liver. It occurs in marine plants, and appreciable quantities are found in certain enzymes where it acts as an oxidation catalyst.

The lack of a convenient and accurate method for the determination of small amounts of copper has retarded a true understanding of its role in the sea, in sediments and in marine organisms. The primary purpose of this investigation was to develop such a method. The secondary objective was to determine the copper concentration and its variation in the waters of Puget Sound and the San Juan Archipelago,

paying attention to season, tide, location, depth, and other physical or biological changes.

## DISCUSSION OF LITERATURE

In Table I is given a summary of the copper determination obtained by previous investigators and of the methods used by them for analyses. Some of the results may be questioned because of the analytical technique employed and because of the apparent lack of precautions to prevent contamination of samples.

The results of Atkins (1932, 1933) and of Kalle and Wattenberg (1938) indicated that the copper content tended to increase at the greater depths. Prytherch (1934) found that the highest concentration of copper in coastal waters existed during low water periods. This was attributed to river discharge, because copper concentrations increased in the proximity of river mouths. He studied the role of copper in the setting of oysters and found correlations between the vertical and horizontal distribution of oysters and of dissolved copper in different coastal regions. Riley (1937) showed that the greatest concentration of copper in the Gulf of Mexico occurred in low salinity coastal waters, with some indication of concentrations decreasing seaward; he also showed that copper is not a limiting factor in the open sea to those organisms which require it for the synthesis of hemocyanin. Noddack and Noddack (1939) determined the extent to which the heavy metals, including copper, are accumulated by several marine organisms. Galtsoff (1943) reported on trace metals in sea water, describing seasonal variation, physiological roles, and accumulations by marine organisms. No systematic fluctuation of copper was found within one-half a period of tidal cycles. Black and Mitchell (1952) found that no change in the trace metal concentration resulted from diatoms adhering to the glassware or from surface adsorption of trace elements on the glass. In a recent paper Morita (1950) concluded that the copper content of sea water is probably less than 0.015 μg-at/l, and he attributed higher values hitherto reported to defective analytical procedures.

## CHEMICALS AND EQUIPMENT

All chemicals used in this investigation were analytical grade and were tested for traces of copper. The distilled water employed in the preparation of solutions was redistilled from an all-glass still.

In the preparation of all reagents, special care was necessary to avoid contamination. A 1% (w/v) sodium diethyldithiocarbamate reagent was prepared every few weeks by using pure sodium diethyl-

TABLE I. Copper Content of Sea Water Found by Various Investigators

| *Date* | *Investigators* | *Source of Water* | *No. of Samples* | *μg-at Cu/l* |
|---|---|---|---|---|
| 1879 | Dieulafait (a) | Mediterranean Sea | 1 | 0.16–0.19 |
| 1919 | Hiltner and Wichmann (l) | West Sayville, N. Y. and Keyport, N. J. | 2 | trace |
| 1920 | Rose and Bodansky (b) | Galveston, Texas | 1 | 2.20 |
| 1923 | Severy (b) | Pacific Ocean | | no trace |
| 1923 | Orton (h) | English Channel | 1 | 3.15 |
| 1931 | Meulen (b) | Roscoff (Brittany) | 1 | 0.95 |
| 1932 | Atkins (d) | English Channel | 1 | 0.16 |
| 1933 | Atkins (e) | Rivers entering English Channel | 6 | 0–0.60 |
| 1934 | Prytherch (c) | New Haven, Black Rock and Southport harbors, Connecticut | | 3.15–9.50 |
| 1937 | Riley (e) | Gulf of Mexico (surface) | 20 | 0.016–0.24 |
| 1938 | Bardet, et al. (j) | Roscoff (Brittany) | 1 | 1.42 |
| 1938 | Meyer (g) | Baltic Sea and North Sea | 16 | 0.095–0.41 |
| 1938 | Kalle and Wattenberg (g) | North Atlantic (surface) | 10 | 0.047–0.19 |
| | | Ditto (great depth) | * | 0.16–0.47 |
| 1939 | Noddack and Noddack (a) | Zoology Station Kristineberg, Sweden | 1 | 0.063 |
| 1940 | Isibasi, et al. (f) | Japan Sea | 1 | 0.47 |
| 1943 | Galtsoff (d) | Woods Hole, Mass. | 9 | 0.13–0.54 |
| 1943 | Galtsoff (e) | Bahamas | 6 | 0.016–0.13 |
| 1943 | Galtsoff (e) | Long Island Sound, N. Y. | 18 | 0–1.50 |
| 1944 | Buch (i) | Baltic Sea | | 0.032–0.13 |
| 1950 | Barnes and Rothschild (e) | Millport Marine Station, Scotland (surface) | 3 | 0.095 |
| 1950 | Morita (i) | Tokyo Bay, Japan | 21 | 0.016–0.095 |
| 1952 | Black and Mitchell (j) | Plymouth, England | 4 | 0–47.0 |
| 1952 | Thompson and Chow (k)† | Friday Harbor and Seattle, Wash. (surface) | 100 | 0.012–0.030 |

* One series

† Unpublished data

Legend: (a) Spectroscopic
(b) Ammonia colorimetric
(c) Hydrogen sulfide precipitation and carbamate
(d) Electrolysis and carbamate
(e) Extraction as carbamate
(f) Hydrogen sulfide precipitation and benzoin oxime
(g) Direct estimation as carbamate
(h) Turbidimetric
(i) Dithizone colorimetric
(j) Spectrographic
(k) Direct spectrophotometric
(l) Hydrogen sulfide precipitation

dithiocarbamate (Eastman Kodak Co.). This solution was stored at a pH of 10.

The sodium chloride solution was prepared by dissolving 30.24 g of the salt in redistilled water and diluting to one liter. The chlorinity of this solution, 18 °/₀₀, is approximately equal to that of coastal sea water.

A stock solution containing 10 μg-at Cu/ml was prepared by dissolving 2.505 g of analytical grade $CuSO_4$–$5H_2O$ in redistilled water and diluting to one liter. A solution containing 0.25 μg-at Cu/ml was made by forty-fold dilution with redistilled water. Other standard metallic ion solutions were prepared by a similar method.

Polyethylene containers were used whenever possible in order to minimize contamination from glassware. The extraction was carried out in polyethylene bottles thoroughly washed with xylene, since new polyethylene bottles sometimes gave an emulsion with xylene during the extraction. A wrist action Burrell mechanical shaker was employed for uniform agitation during the extraction process. In order to avoid contamination from metal sampling bottles, surface sea water was collected by immersion of a well-seasoned Pyrex glass bottle below the water surface by means of a weighted rope, and it was transferred immediately to polyethylene storage bottles. The absorbancy[1] (optical density) readings were measured with a Beckman DU spectrophotometer using Corex glass cells of 1 cm optical path.

## ANALYTICAL PROCEDURE

If the sea water sample contained much plankton, an emulsion would form with the xylene during the extraction. The plankton should be removed by filtration through a sintered glass plate before extraction of the sample.

500 ml of sea water were measured into a polyethylene bottle and 2 ml of 1% diethyldithiocarbamate reagent were added. The sample was then extracted with 5 ml of distilled xylene for one hour by means of a Burrell shaker. The xylene layer was pipetted out with a medicine dropper and transferred to the absorption cell. The absorbancy of the xylene extract was read in the Beckman DU spectrophotometer at the wave length of 436 mμ with a 0.05 mm slit width. Distilled xylene was used as a reference.

The copper concentration in the sea water sample was then obtained by reference to a calibration graph based on known amounts of copper. A corrected absorbancy reading of 0.005 was found to correspond to 0.0030 μg-at Cu/l of sea water. The molar absorbancy index (molar

[1] According to the National Bureau of Standards, Letter Circular LC-857 (1947).

extinction coefficient) of the copper complex in xylene was calculated to be 16,800 l/mole/cm.

## EXPERIMENTAL

*Selection of Reagent and Extracting Solvent.* Dithizone (diphenylthiocarbazone) has long been considered as a sensitive reagent for copper. It is a violet-black crystalline material which yields characteristic colors with a number of heavy metallic ions. Separation of these colored complexes has been achieved by regulating the pH of the solution to be extracted, by adding masking agents that form complexes with interfering ions, and by varying the extracting solvents.

Since dithizone is a sensitive but not specific reagent, it is difficult to avoid contamination that leads to errors in the determination of copper. The reagent itself is very unstable and is easily oxidized to form an inactive yellow product. The process involves two colors with uncertain reproducibility. Furthermore, the equilibrium point of the extraction is dependent upon the hydrogen ion concentration, and complete extraction is sometimes difficult to obtain.

Sodium diethyldithiocarbamate was introduced by Delépine (1908) as a reagent for detecting traces of copper. In order to increase the sensitivity of the determination, the colored copper complex is concentrated by extraction. Factors to be considered in the selection of the extracting solvent are its extractibility, solubility in water, volatility, and specific gravity. Amyl alcohol, iso-amyl alcohol, iso-amyl acetate, amyl acetate and chloroform are sufficiently soluble in water to give a serious error in the determination because of the large volume of sample required. Carbon tetrachloride and bromobenzene, which are less soluble in water, have been used as extracting solvents. Xylene, however, was found by the authors to be much more satisfactory. The colored complex in xylene did not show any change in the maximum absorption wave length. Xylene in water is quite insoluble, nonpolar, comparatively nonvolatile, and it is readily separated from water because of its lower specific gravity.

*Optical Absorption Spectrum of Copper Diethyldithiocarbamate.* 0.25 μg-at Cu was extracted as diethyldithiocarbamate with xylene from a solution having a chlorinity of 18 ‰ and a pH value of 8. The absorbancies of the colored xylene solution were measured at different wave lengths, the results of which are shown in Fig. 1. Maximum absorption was observed in the curve at the wave length of 436 mμ. Absorption decreased sharply when the peak was passed and it reached the minimum at 370 mμ. The increased absorption shown toward the ultraviolet region was due to the excess reagent.

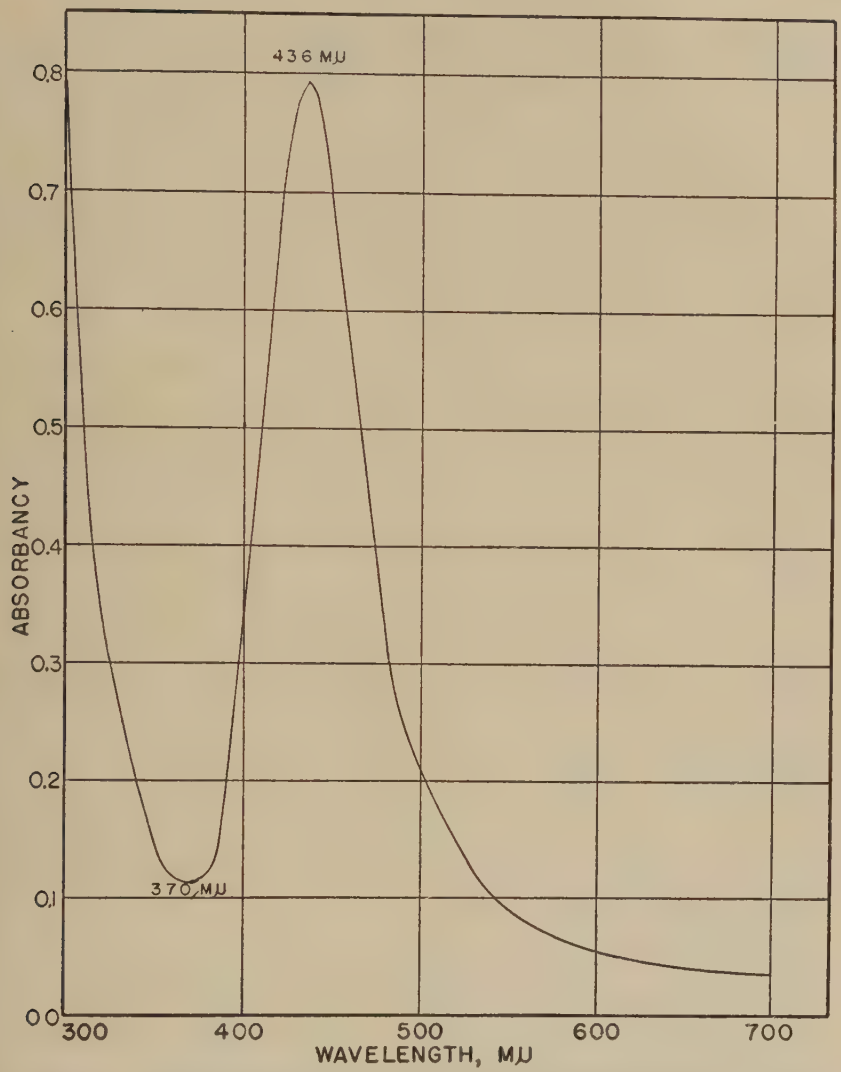


**Figure 1.** General absorption spectrum of copper diethyldithiocarbamate in xylene. 0.25 μg-at Cu extracted from pH 8, 18°/₀₀ Cl solution.

The absorption of various copper concentrations at the wave length of 436 mμ with a 0.05 mm slit width was reproducible and followed Beer's law. It was chosen as the working wave length.

*Stabilities of Sodium and Copper Diethyldithiocarbamates.* Sodium diethyldithiocarbamate reagent in solution decomposes slowly with the formation of carbon disulfide. Murakami (1950) suggested various methods for stabilizing the reagent by adding chloroform or hydroxylamine on the assumption that the instability was due to oxidation and bacterial action. In this investigation it was observed that the pH value is the main factor that influences the stability. The reagent solution decomposed immediately if it was stored at pH values of less than 7. The stability increased with increase in the pH value. At a pH of 10, about 30% of the reagent (original concentration 0.5 μg-at/ml) decomposed in 45 days.

The stability of copper diethyldithiocarbamate in xylene was examined by treating samples containing 0.25 μg-at Cu with a slight excess of diethyldithiocarbamate and by extracting the colored copper complex with 5 ml of xylene as described in the procedure. After this sample stood for 48 hours in darkness, the absorbancy reading at the wave length of 436 mμ showed no change. The color intensity, however, showed fading if the xylene extract was exposed to strong light. Also, fading was manifested if an excess of the reagent was not used.

The molar ratio between copper and diethyldithiocarbamate was determined by the continuous variation method to measure the absorbancies for mixtures of varying proportions of copper and the reagent. The proportion giving maximum absorption indicates the composition of the complex, if only one product is formed. If more than one product is formed, measurement at various wave lengths give different results. From the spectrophotometric study of copper diethyldithiocarbamate, it is concluded that the complex has a definite composition and that only one compound is formed with a molar ratio of copper to diethyldithiocarbamate of one to two, regardless of whether it is formed from equivalent amounts of copper and diethyldithiocarbamate or with one in excess.

*Influencing Factors on Color Intensity of the Copper Complex.* The effect of excess reagent on the color intensity was studied, and it was found that the color intensity in xylene is not affected even by a thirty-fold increase in excess of reagent.

Since the hydrogen ion concentration varies in sea water, the effect of the change of pH value on the color intensity of the copper complex in xylene was examined. The results showed that the color intensity is a linear function of the copper concentration at given pH values. The deviation in slope of the lines due to the change of pH value was about 2% per unit pH.

The effect of salinity on the determination was also studied. A

linear relationship was found between absorbancy and copper concentration, with slopes deviating about 1% for a change of 10 °/₀₀ Cl. The seasonal fluctuations of salinity, therefore, would not affect the determination.

The reducing and oxidizing substances in sea water have been shown to have no interference in the copper determination.

*Distribution Coefficient of Extraction.* The shaking time of extraction played an important role in the determination. Solutions, each containing 0.25 μg-at Cu, were shaken for varying time intervals,

TABLE II. Coefficient of Extraction

| *Copper Added* | *Absorbancies* | | *Coefficient of* |
|---|---|---|---|
| μg-at | *1st Extraction* | *2nd Extraction* | *Extraction* |
| 0.00 | 0.048 | 0.026 | — |
| 0.10 | 0.325 | 0.031 | 0.98 |
| 0.20 | 0.667 | 0.042 | 0.97 |
| 0.30 | 0.928 | 0.058 | 0.97 |
| 0.40 | 1.202 | 0.068 | 0.96 |
| 0.50 | 1.528 | 0.067 | 0.97 |

after which the absorbancies were determined. The absorbancy increased linearly in the first ten minutes of shaking and then leveled off and reached an equilibrium after 40 minutes.

The completeness of extraction at equilibrium was also studied at various copper concentrations. The colored copper complex formed in 18 °/₀₀ Cl solution with a pH of 8 was extracted with xylene by the normal procedure. The aqueous solution was separated from xylene by using a separatory funnel and it was again extracted with another 5 ml of xylene. The absorbancies of these two portions of xylene, measured separately at the wave length of 436 mμ, are shown in Table II. The completeness of extraction at equilibrium was calculated from the absorbancy readings. An average value of 97% completion was achieved after the first extraction.

*Effect of Possible Interfering Substances.* Individual solutions of various metallic ions, equivalent to 0.25 μg-at/ml, were prepared ($Ni^{+2}$, $Co^{+2}$, $Bi^{+3}$, $Mn^{+2}$, $UO_2^{+2}$, $Fe^{+3}$ and $Fe^{+2}$) in order to test the reaction of the diethyldithiocarbamate at various pH values from 5 to 10.

Throughout the range from pH 5 to 10, copper ion formed a brown precipitate with the reagent. Ferric and ferrous ions gave purple precipitates from pH 5 to 7, but no precipitate or color occurred in more basic ranges which include that of the sea water. The uranyl

group produced a yellow color from pH 5 to 8, but no coloration was observed in more basic solutions. The uranyl diethyldithiocarbamate was insoluble in xylene. Manganese diethyldithiocarbamate, which precipitated in solutions of pH less than 9, dissolved readily in xylene and gave a purple color which faded rapidly to a colorless solution. None of these substances interfered with the determination of copper, no increase in absorbancy readings being noted at the wave length of 436 mμ.

Nickel, cobalt, and bismuth gave pale green precipitates with the reagent. The concentration of these substances in sea water is so minute that no interference with the copper determination occurred. For analyses of marine products and of bottom sediments, these elements may be present in sufficient quantities to interfere, and therefore their effects on the copper determination were examined. The optical absorption spectra of the respective complexes of these three elements formed at various pH conditions were studied. The nickel complex shows maxima at wave lengths of 325 and 390 mμ and was not affected by changes in pH value. The complexes show a maximum absorption at 325 mμ for cobalt and at 305 and 365 mμ for bismuth. The wave lengths of maximum absorption of cobalt and bismuth complexes did not change with pH value, but their magnitudes were depressed considerably with increasing pH. A series of standard calibration graphs of bismuth, cobalt and nickel complexes at the wave length of 436 mμ are shown in Fig. 2. From the graphs in Fig. 2 the appropriate corrections to be applied to the absorbancy at the wave length of 436 mμ are calculated as follows:

| *Wave length* | *Element* | *Corresponding to Cu* |
|---|---|---|
| *mμ* | 1 μg-at | μg-at *at 436* mμ |
| 436 | Bi | 0.16 |
| 436 | Co | 0.21 |
| 436 | Ni | 0.14 |
| 365 | Bi | 0.77 |
| 325 | Co | 1.85 |
| 325 | Ni | 2.32 |

Since cobalt and nickel showed serious interferences if appreciable amounts were present, methods for eliminating the interference of these substances with dimethylglyoxime were studied. Diethyldithiocarbamate reagent was added to the solution containing 0.25 μg-at Ni in the presence of dimethylglyoxime. Absorbancy of the xylene extract was measured by the normal procedure. Nickel dimethylglyoxime was sparingly soluble in xylene, showing a pink

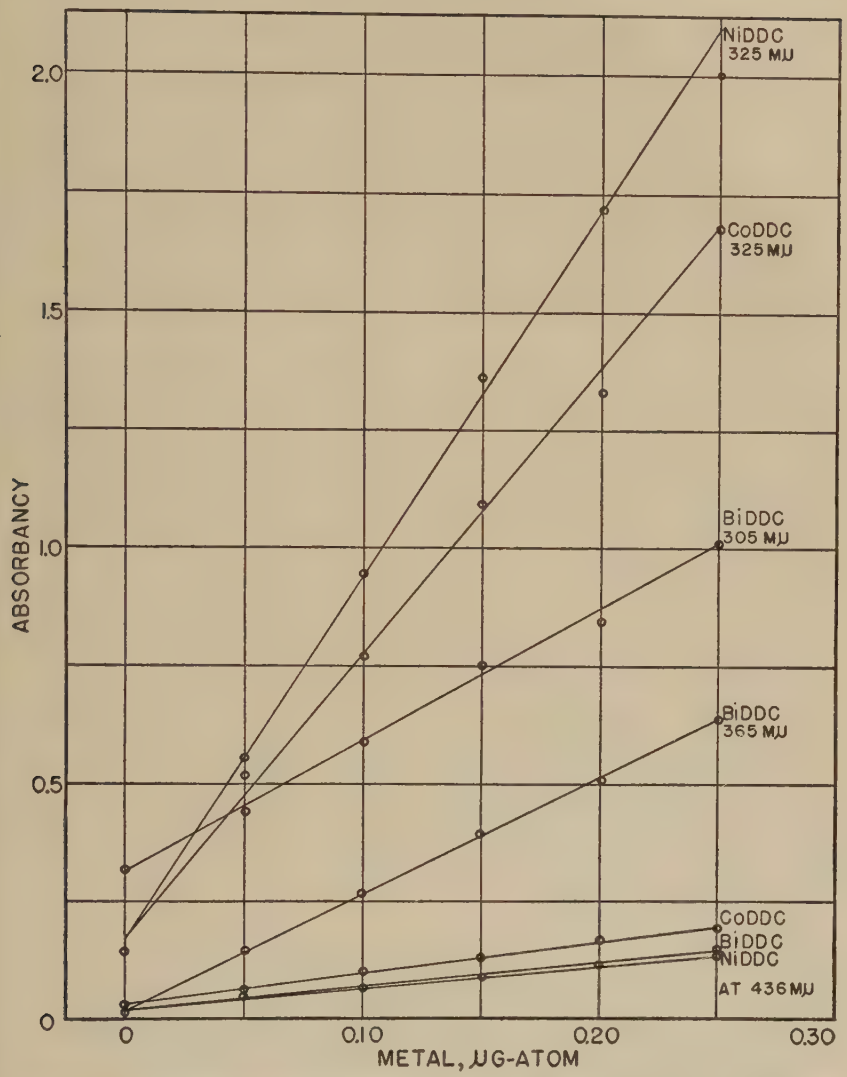


Figure 2. Calibration graphs for bismuth, cobalt and nickel diethyldithiocarbamates. Extracted from pH 8, 18°/₀₀ Cl solutions. Slopes: At 436 mμ, BiDDC = 0.52, CoDDC = 0.70, NiDDC = 0.47; at 325 mμ, CoDDC = 6.17, NiDDC = 7.74; at 365 mμ, BiDDC = 2.44; at 305 mμ, BiDDC = 2.78 units absorbancy/μg-at.

color. The absorbancy of the saturated solution at the wave length of 436 mμ corresponded to 0.05 μg-at Cu.

The solubility of the yellowish cobalt dimethylglyoxime was far less than that of nickel. The increase in absorbancy at the wave length of 436 mμ was obtained with 10 μg-at Co which corresponded to 0.03 μg-at Cu. The validity of the method of correcting for interfering elements was tested on known solutions containing 0.25 μg-at Cu and equal amounts of bismuth, cobalt, and nickel in 100 ml of pH 8, 18°/₀₀ Cl solutions. The resulting absorbancies of the xylene extract were measured by the normal procedure. The results obtained were very satisfactory.

*Calibration Graph for Sea Water.* A standard calibration graph was prepared by adding various quantities of a copper solution ranging from 0.0 to 0.20 μg-at to 500 ml of sea water. The absorbancy readings, measured as described in the procedure with an absorption cell of 1 cm optical path, are plotted against copper concentrations in Fig. 3. The slope[2] of the line was found to be 3.35 units absorbancy reading per one μg-at Cu. A corrected absorbancy reading of 0.005 was found to correspond to 0.0015 μg-at Cu in a 500 ml sea water sample. The blank varied with the particular sea water used and a corresponding correction should be made when reading the copper content directly from the calibration graph.

In studying the possible presence of elements which would interfere in the determination of copper in sea water, a sample was extracted by the normal procedure and the absorption spectrum was measured at different wave lengths over the range from 300 to 700 mμ. The absorption spectrum has shown maximum absorptions at the wave length of 436 mμ and approximately 300 mμ due respectively to copper and excess of the reagent. The spectrum showed no evidence of bismuth, cobalt or nickel.

An examination has been made of more than 100 samples of surface sea water collected periodically near Friday Harbor and Seattle, Wahington. The average concentration of copper in these waters, expressed in μg-at/l, was found to be 0.020, with a range of 0.012 to 0.030. Several fresh water lakes showed about 0.070 μg-at/l.

The authors are now investigating the copper concentration in lakes and rivers of Washington State, as well as that in sea sediments and marine organisms; they are also investigating its seasonal fluctuation at different depths in the sea, both in coastal and offshore localities. The findings obtained will be given in Part II of this investigation.

[2] The molar absorbancy index is calculated to be 16,800.

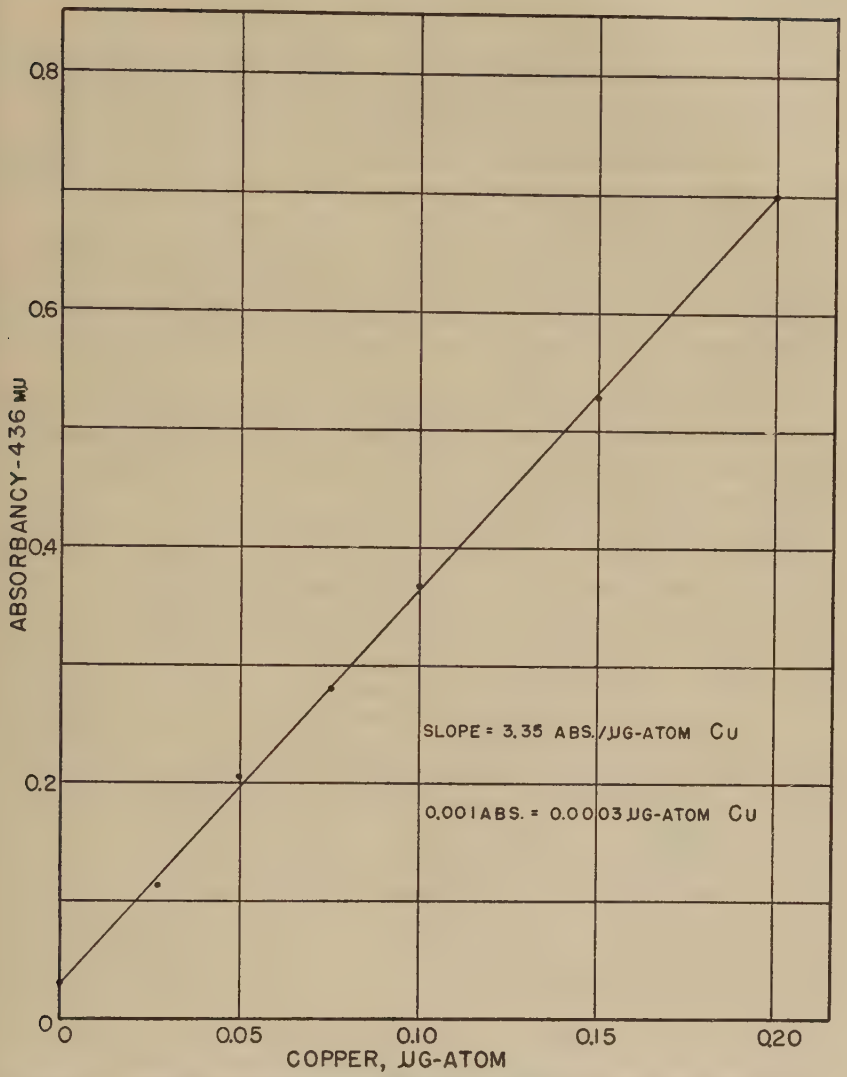


Figure 3. Copper calibration graph for sea water. July 19, 1951 High Tide, pH 7.8, 17.1‰ Cl. Slope = 3.35 absorbancy/μg-at Cu; 0.005 absorbancy = 0.0015 μg-at Cu in 500 ml sea water sample.

## SUMMARY AND CONCLUSIONS

1. Sodium diethyldithiocarbamate has been studied spectrophotometrically as a reagent to determine copper in sea water, and it has been found to be preferable to diphenylthiocarbazone (dithizone).

2. Increased sensitivity has been attained by extracting the colored copper complex with xylene. The useful lower limit of this method is approximately 0.002 μg-at Cu.

3. The effects of the amount of reagent, the hydrogen ion concentration, the salinity, and the oxidizing and reducing agents on the color system have been examined; it has been shown that they have no influence on the accuracy of the determination. The coefficient of extraction has also been studied.

4. The diethyldithiocarbamate reagent has been found stable in ammoniacal solution. The colored copper complex in xylene shows no change after standing in diffused light for 48 hours; it is far more stable than the color produced with dithizone.

5. The composition of the copper complex has been determined by the continuous variation method. It is a definite compound with a molar ratio of copper to diethyldithiocarbamate of one to two.

6. The general absorption spectrum of sea water extract with the reagent in xylene has been examined; it has been demonstrated that no interfering metals are present.

7. It has been shown that bismuth, cobalt, iron, manganese, nickel, uranium, and cyanide interfere in the copper determination but not at the concentration of these substances found in sea water. Procedures have been devised for minimizing the interference of these elements, should the method be applied to the analyses of marine organisms, bottom sediments, or other materials.

8. A calibration graph for sea water has been prepared. A corrected absorbancy reading of 0.005 has been found to correspond to 0.0030 μg-at/l of sea water. The molar absorbancy index of the copper complex in xylene at the wave length of 436 mμ has been calculated to be 16,800 l/mole/cm.

## ACKNOWLEDGMENT

This investigation was supported by the Office of Naval Research, under the terms of a research contract with the University of Washington. The authors wish to express their appreciation to Dr. Emery F. Swan for collecting sea water samples at Friday Harbor, Washington and to Dr. Rex J. Robinson for his valuable suggestions.

## LITERATURE CITED


Atkins, W. R. G.

1932. The copper content of sea-water. J. Mar. biol. Ass. U. K., *18:* 193–197.

1933. The rapid estimation of the copper content of sea-water. J. Mar. biol. Ass. U. K., *19:* 63–66.

Bardet, Jacques, Arakel Tchakirian and Raymonde Lagrange

1938. Recherche spectrographique des éléments existant à l'état de traces dans l'eau de mer. C. R. Acad. Sci., Paris, *206:* 450–452.

Barnes, H. and Lord Rothschild

1950. A note on the copper content of sea-urchin semen and sea water. J. exp. Biol., *27* (2): 123–125.

Black, W. A. P. and R. L. Mitchell

1952. Trace elements in the common brown algae and in sea water. J. Mar. biol. Ass. U. K., *30:* 575–584.

Buch, Kurt

1944. Dithizonmetoden för bestämning av zink och koppar i naturliga vatten. Finska Kemistsamfundets Medd., *53* (1–2): 25–37.

Delépine, Marcel

1908. Composés sulfurés et azotés dérivés du sulfure de carbone. XII. Thiosulfocarbamates métalliques. Bull. Soc. chim., France, (4) *3:* 643–652.

Dieulafait, M. L.

1879. Le cuivre. 2ième parte, chapitre 1. Cuivre dans les eaux des mers de tous les ages, et concentration de ce métal dans certains de leurs dépot. Ann. Chim. (Phys.), (5) *18:* 359–364.

Galtsoff, P. S.

1943. Copper content of sea water. Ecology, *24:* 263–265.

Hiltner, R. S. and H. I. Wichmann

1919. Zinz in oysters. J. biol. Chem., *38:* 205–221.

Isibasi, Masayosi, Kozo Kurata and Tugio Hirobe

1940. Chemical studies of the ocean. VII. Quantitative determination of copper in sea water and bittern. J. chem. Soc. Japan, *61:* 726–728.

Kalle, Kurt and Hermann Wattenberg

1938. Über den Kupfergehalt des Ozeanwassers. Naturwissenschaften, *26:* 630–631.

Meulen, H. ter

1931. Sur la répartition du molybdène dans la nature. Rec. Trav. chim., Pays-Bas, *50:* 491–504.

Meyer, Helga

1938. Die photometrische Bestimmung des Kupfers in Seewasser. Ann. Hydrogr., Berl., *49:* 325–330.

Morita, Yoshimi

1950. Distribution of copper and zinc. IV. Copper and zinc contents of sea water. J. chem. Soc. Japan, *71:* 246–248.

Murakami, Yukio

1950. Modified colorimetric determination of copper with sodium diethyldithiocarbamate in the presence of hydroxylamine. Bull. chem. Soc., Japan, *23:* 3–7.

Noddack, Ida and Walter Noddack
1939. Die Häufigkeiten der Schwermetalle in Meerestieren. Ark. Zool., 32A (4): 1–35.
Orton, J. H.
1923. An account of investigation into the cause or causes of the unusual mortality among oysters in English oyster beds during 1920 and 1921. Fish. Invest., London, (2) *6* (3): 166.
Prytherch, H. F.
1934. The role of copper in the setting, metamorphosis, and distribution of the American oyster, *Ostrea virginica*. Ecol. Monogr., *4:* 47–107.
Riley, G. A.
1937. The significance of the Mississippi River drainage for biological conditions in the northern Gulf of Mexico. J. Mar. Res., *1* (1): 60–74.
Rose, W. C. and Meyer Bodansky
1920. Biochemical studies on marine organisms. I. The occurrence of copper. J. biol. Chem., *44:* 99–112.
Severy, H. W.
1923. The occurrence of copper and zinc in certain marine animals. J. biol. Chem., *55:* 79–92.

# NOTE ON THE MERIDIONAL TRANSPORT OF ENERGY BY THE OCEANS[1]

By

GLENN H. JUNG

*Massachusetts Institute of Technology, Cambridge, Massachusetts*[2]

## ABSTRACT

The role of the oceans in providing poleward energy flux within the earth's fluid envelope is re-examined in regard to effective transport mechanisms. A hypothetical model near 30 degrees north latitude is found to produce a sizeable poleward energy transport when effects of closed vertical circulations operating in meridional planes are considered. Available data for the Atlantic do not conflict with this result. It is suggested that the importance of such meridional circulations should not be disregarded in computations of the global energy balance.

## INTRODUCTION

As is well known, in polar regions there is a net radiation of energy into space from the earth and from its fluid envelope, the oceans and atmosphere. In tropical regions these receive a net excess of solar radiation. However, temperatures show neither a corresponding progressive cooling in the polar cap nor a progressive warming in the more tropical regions. There must exist, therefore, a poleward transport of energy through the earth's fluid envelope in order to maintain the observed temperature equilibrium, since conduction through the earth proper is of negligible importance.

From qualitative considerations the poleward energy flux through the oceans has been assumed small compared with the transport through the atmosphere (see von Bezold, 1906; Bjerknes, 1933). Sverdrup (1942) made a quantitative estimate for ocean energy transported by the Gulf Stream System in the North Atlantic Ocean. This estimate gives a small percentage of the radiation requirements, suggesting that ocean currents transport no more than 10% of the total poleward energy flux. It is to be noted that this estimate, necessarily, did not include energy transported by means other than the standing horizontal eddy comprised of the Gulf Stream System and associated return currents.

[1] The research resulting in this work has been sponsored by the Geophysics Research Division of the Air Force Cambridge Research Center under contract No. AF 19-122-153.

[2] Present address: Department of Oceanography, Texas A. and M. College, College Station, Texas.

Let us consider first some possible energy transport mechanisms within the ocean which may be important. As Sverdrup has noted, standing horizontal eddies provide one such mechanism. In addition, it is conceivable that closed vertical mean circulations in meridional planes might transport large amounts of energy, even though the average velocities involved are extremely small.

Since it would seem improper to neglect this second possibility *a priori*, some estimate of the possible order of magnitude of the transport produced by it should be made. Furthermore, if this result is significant, then the actual presence of mean meridional circulations should be investigated from oceanographic data in so far as this is possible. It is hoped that the material which follows may serve as a beginning in the study of these two questions.

## HYPOTHETICAL VERTICAL CIRCULATION

Let us consider the energy transported by a simple closed vertical circulation that operates within a hypothetical model. The model used is illustrated in Fig. 1. As shown in *B* of Fig. 1, a northward velocity of about 0.51 cm $sec^{-1}$ is assumed to be present from the surface to a depth of 950 m. Mass continuity then gives a southward flow of about 0.14 cm $sec^{-1}$ in the layer below 950 m which extends to an assumed bottom depth of 4,250 m.

Reasonable values of the vertical distribution for temperature ($T$), salinity ($S$), and density ($\rho$), as given by Fuglister (1947), were employed in the hypothetical model. These values are for approximately 30 degrees north latitude. The temperature distribution is given in C of Fig. 1. The width of the model (extent of ocean in the west-east direction) was chosen to be 5,000 km, i. e., comparable to the width of the Atlantic at 30 degrees north latitude.

Within the earth's fluid envelope, the total energy flux across a latitude wall can be represented by the following expression used by Starr (1951):

$$F = \int_A (P + \rho c_v T + \rho g Z + \rho C^2/2) v_n \, dA \, . \qquad (1)$$

$P$ is pressure and $T$ is temperature. Applied only to the ocean, $Z$ is vertical distance counted upward, $\rho$ is the density, and $c_v$ is the specific heat of the ocean water. $C$ is the ocean current speed and $v_n$ is the northward component of velocity. $dA$ represents an element of area of the latitude wall within the ocean.

The term containing $P$ may be regarded as the rate at which pressure forces do work across the boundary surface. It is reasonable to assume that the term containing $T$ is a close approximation to the internal

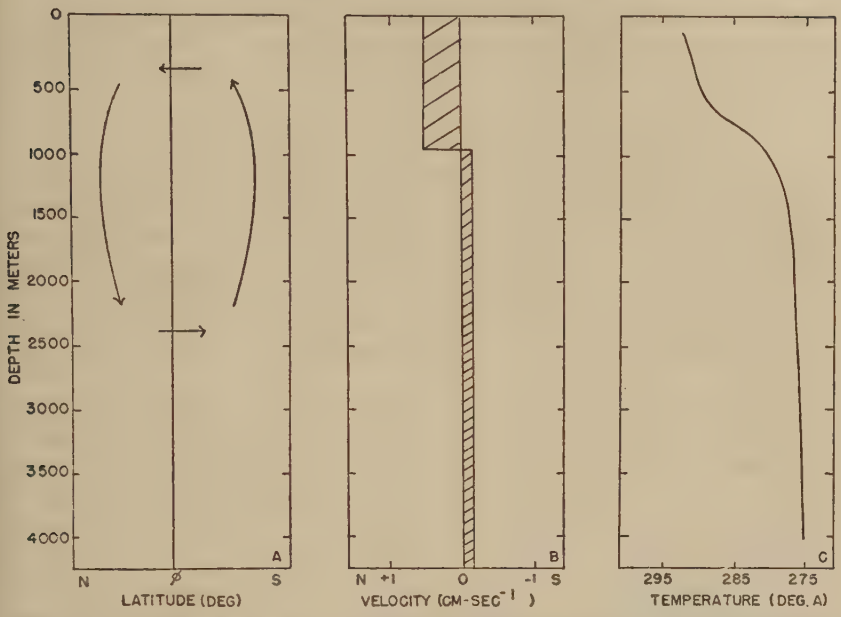


Figure 1. Hypothetical model of a closed vertical circulation in a meridional plane. *A*. Schematic representation. *B*. Assumed velocity distribution used for computations. *C*. Temperature distribution in vicinity of 30 degrees north latitude in the North Atlantic Ocean after Fuglister (1947).

energy transport. The terms containing $Z$ and $C^2/2$ represent transports of potential and kinetic energy, respectively.

Under conditions of hydrostatic equilibrium the term in (1) involving pressure nearly cancels the term involving potential energy, so that the sum gives a negligible contribution. This cancellation would become exact in the case of uniform density.

Using any reasonable assumed values for the magnitude of $C$, it can be shown easily that the advection of kinetic energy is several orders of magnitude smaller than the transport of internal energy.

The transport of internal energy thus determines the order of magnitude of the total energy flux across the latitude wall. For the model, this transport is of the order of $3 \times 10^{14}$ gm-cal sec$^{-1}$. In order to include the effects of all oceans in the northern hemisphere, this figure should be multiplied by a factor of 3.

The result is of the same order of magnitude as the total poleward energy transport required by radiation data for the entire fluid envelope. The latter figure is about $10^{15}$ gm-cal sec$^{-1}$ at 30 degrees north latitude according to estimates discussed below. It appears extremely

important, therefore, to determine whether or not such net meridional circulations do actually exist within the oceans. If so, their effect cannot be neglected in any complete study of the energy balance of the globe.

## COMPUTATIONS FROM ACTUAL DATA

From the model discussed, it is evident that measurements of velocity entering into ocean energy flux computations of the present type must be extremely accurate. Moreover, direct ocean velocity measurements are not sufficiently plentiful for this purpose. However, it is possible that new methods for measuring velocities, such as the one developed by von Arx (1950), may ultimately provide a solution to this problem after a large enough volume of data has been obtained.

It is interesting to note that a vertical meridional cell within an ocean differs essentially from a corresponding cell in the atmosphere. The latter must be nongeostrophic in order to effect a net meridional mass transfer at a given level, and thus it represents a motion in which the Coriolis forces are not balanced by pressure forces. In the ocean, on the other hand, due to the presence of continental barriers, this is not necessarily true. A net meridional transfer at a given level in an ocean may be associated with motion in which pressure forces balance Coriolis forces.

With appropriate reservations about possible motions other than those given by dynamic velocity measurements, we may use data compiled by Riley (1951) for the North Atlantic Ocean. At present these data represent the most comprehensive estimation of ocean volume transport available and results derived from them are at least of some interest.

The distribution with depth of the average meridional velocities so obtained across 27 degrees north latitude is shown in Fig. 2. Since Riley points out that his estimates do not account for Gulf Stream transport adequately, additional data from Sverdrup, et al. (1942) were obtained for this region and are incorporated into the averages shown in Fig. 2[3].

This velocity distribution gives a small net mass flow northward across the latitude section of the Atlantic Ocean. It is possible that a compensating outflow occurs on the opposite side of the hemisphere. Such an outflow would have to take place through the narrow and shallow Bering Strait into the Pacific Ocean with a velocity of about 100 cm $sec^{-1}$. However, such large ocean current velocities are im-

[3] The velocity at 4,000 m estimated from Riley's data agrees reasonably well with preliminary results of a carbon 14 dating technique reported by Kulp (1951).

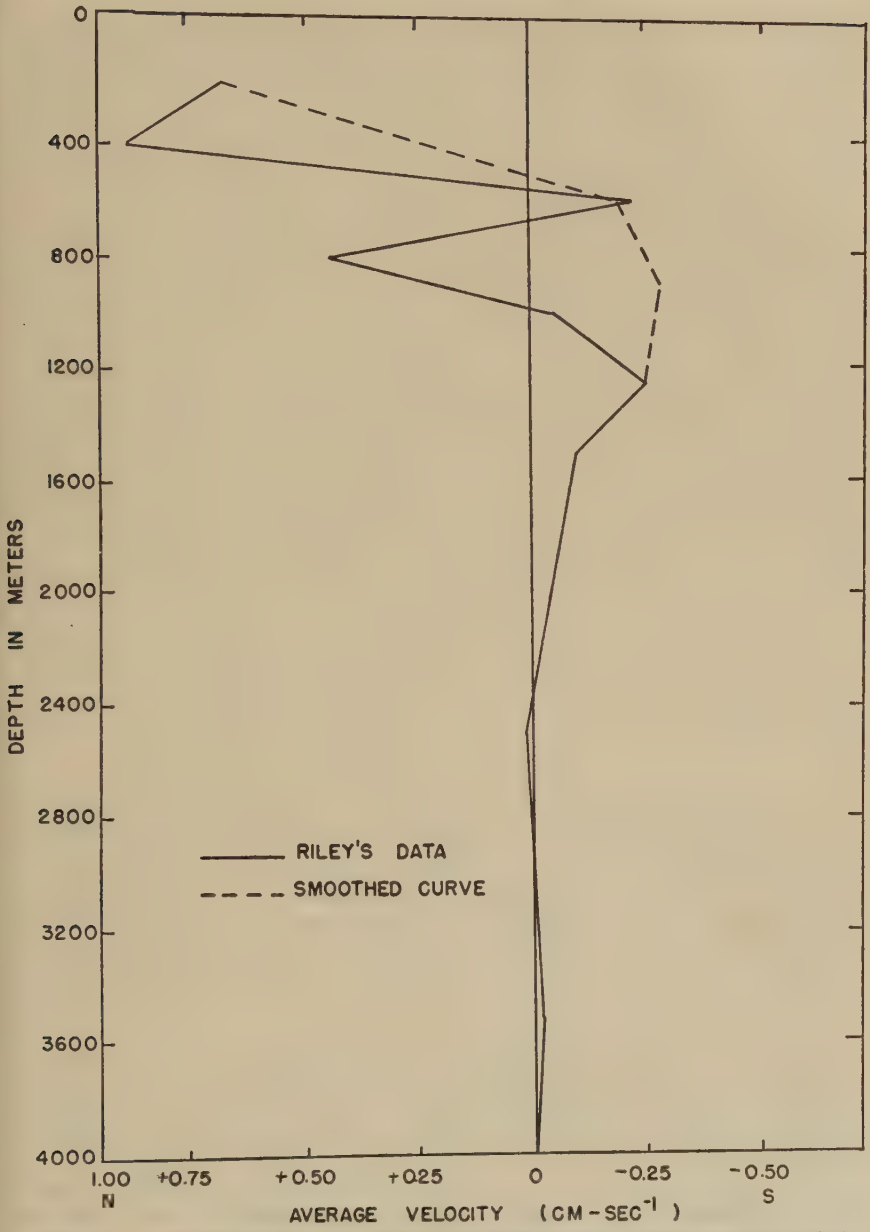


Figure 2. Vertical distribution of average velocities across 27 degrees north latitude in the North Atlantic Ocean. Solid curve is from data of Riley (1951). Dashed velocities give zero resultant net mass transport across this latitude.

probable in this region. In the event that such a mass outflow actually does exist, negative heat transport across 27 degrees north latitude in the Pacific Ocean must occur. This would bring about a cancellation of the heat energy transported northward by the net mass flow in the Atlantic Ocean, when the hemisphere as a whole is considered. Thus, whether or not this effect is real, it is perhaps best to eliminate it. This may be accomplished by one of several procedures.

The velocity profile may be shifted so that no net mass flux occurs. This may be accomplished by moving the profile a small amount in the negative velocity direction. As an alternate method, the ragged upper portion of the velocity profile may be appropriately smoothed, i. e., as shown in Fig. 2.

Each of these procedures was used together with an average sounding of oceanographic variables from the METEOR Atlas (Wüst and Defant, 1936) to obtain estimates of internal energy transport by meridional cells within the Atlantic Ocean. The METEOR sounding, representing averages over the entire Atlantic section, is quite similar to the Fuglister sounding used in the hypothetical model derived from a small region of the Atlantic Ocean. The Fuglister temperature curve is about 4° C warmer than the METEOR curve at 500 m depth, the level of the greatest difference between the two.

The estimate of the magnitude of the internal energy transported is about $3 \times 10^{14}$ gm-cal $sec^{-1}$ in each of these cases. This value is almost the same as that obtained from the hypothetical model discussed above.

## COMMENTS

Baur and Phillips (1935) gave radiation values which can be used to obtain net radiation excess or deficit values for the earth averaged over latitude belts for the northern hemisphere (see Haurwitz and Austin, 1944: 18). From these, estimates may be made of the energy required for poleward transport in order to maintain the observed temperature equilibrium. The amount required for transport by the entire fluid envelope across 30 degrees north latitude is approximately $10^{15}$ gm-cal $sec^{-1}$.

In this latitude, oceans occupy approximately three times the horizontal extent assumed in our hypothetical model or occupied by the Atlantic Ocean. Assuming that the results may be considered typical of all oceans in the northern hemisphere, the hypothetical model ocean could account for $9 \times 10^{14}$ gm-cal $sec^{-1}$, while from actual data the oceans could account for $9 - 10 \times 10^{14}$ gm-cal $sec^{-1}$. Of course these results depend upon dynamic velocity measurements, and therefore they must be treated with caution.

However, if such small vertical meridional cells in the ocean are capable of transporting energy in the amounts estimated here, then this possibility should not be neglected in energy balance relationships of the fluid envelope.

According to Wexler (1944), the atmospheric layer from the surface to 10,000 feet gains a maximum of heat energy in the region off the New England coast in the vicinity of 48 degrees north latitude for the month of February. This is located in a region of net radiation deficit (see Baur and Phillips' data), and hence such heating must depend on sources other than radiation. Wexler proposes that these sources may be adiabatic heating from subsidence in polar air masses over Canada as well as heat conducted upward from the ocean surface. The present estimates indicate that the ocean could indeed act as such a heat source for the atmosphere within this region, giving up the large amounts of energy transported across latitudes farther south.

## ACKNOWLEDGMENTS

Sincere thanks are expressed to Professor Victor P. Starr and Dr. Robert M. White for reading this manuscript and offering valuable comments. The assistance of Miss I. Kole, who prepared the diagrams, is gratefully acknowledged.

## REFERENCES

Baur, Franz and H. Phillips

1935. Die Wärmehaushalt der Lufthülle der Nordehalbkugel im Januar und Juli und zur Zeit der Äquinoktien und Solstitien. 2. Mitteilung: Ausstrahlung, Gegenstrahlung und meridionaler Wärmetransport bei normaler Solarkonstante. (Gerland's) Beitr. Geophys., *45* (82): 82–132.

Bjerknes, V. F. K., Jakob Bjerknes, H. S. Solberg and Tor Bergeron

1933. Physicalische Hydrodynamik. Julius Springer, Berlin. 797 pp.

Fuglister, F. C.

1947. Completion Report No. 4 on the hydrography of the western Atlantic; the hydrography of the northwestern Sargasso Sea. Woods Hole Oceanographic Institution. 13 pp. +

Haurwitz, Bernhard and James M. Austin

1944. Climatology. McGraw-Hill, New York and London. 410 pp.

Kulp, J. L.

1951. Age of deep ocean water. Tech. Rep. No. 4, Lamont Geological Observatory (Columbia University). 12 pp.

Riley, G. A.

1951. Oxygen, phosphate, and nitrate in the Atlantic Ocean. Bull. Bingham oceanogr. Coll., *13* (1): 1–126.

Starr, V. P.

1951. Applications of energy principles to the general circulation. Compendium of Meteorology, American Meteorological Society, Boston. pp. 568–574.

Sverdrup, H. U.
1942. Oceanography for Meteorologists. Prentice-Hall, New York. 246 pp.
Sverdrup, H. U., M. W. Johnson and R. H. Fleming
1942. The Oceans. Prentice-Hall, New York. 1087 pp.
von Arx, W. S.
1950. An electromagnetic method for measuring the velocities of ocean currents from a ship under way. Pap. phys. Oceanogr., *11* (3): 1–61.
von Bezold, Wm.
1906. The interchange of heat at the surface of the earth and in the atmosphere. Translation by Cleveland Abbé in The Mechanics of the Earth's Atmosphere, Smithson. misc. Coll., *51* (4): 376–415, 1910.
Wexler, Harry
1944. Determination of the normal regions of heating and cooling in the atmosphere by means of aerological data. J. Meteorology, *1* (1 & 2): 23–28.
Wüst, Georg and Albert Defant
1936. Atlas zur Zirculation des Atlantischen Ozeans, *VI*. Walter de Gruyter and Co., Berlin and Leipzig. 7 + 5 + 103 pp.

# THE ESTIMATION AND CHARACTERIZATION OF PLANKTON POPULATIONS BY PIGMENT ANALYSES

## I. THE ABSORPTION SPECTRA OF SOME PIGMENTS OCCURRING IN DIATOMS, DINOFLAGELLATES, AND BROWN ALGAE[1]

By

FRANCIS A. RICHARDS[2]

*Oceanographic Laboratories,*
*University of Washington, Seattle, Washington*

## ABSTRACT

The spectra of chlorophyll c, beta carotene, neofucoxanthin A, neofucoxanthin B, fucoxanthin, diadinoxanthin and diatoxanthin in 90% acetone solutions are reported. These constants are necessary for the simultaneous spectrophotometric determination of the major plankton pigments described.

## INTRODUCTION

There are reported herein the absorption spectra of 90% acetone solutions of a number of the pigments found in diatoms, dinoflagellates, and brown algae. These constants were determined as a necessary preliminary in the development of a spectrophotometric method for the simultaneous determination of several pigments found in acetone extracts of plant and animal materials. Solvent partition and chromatographic adsorption were used to prepare the compounds. The methods have been reported by Strain and his co-workers (4, 5, 6, 7), by Pace (3), and others. Spectral data reported by previous workers and chromatographic and chemical behavior were used as criteria of the purity and identity of the compounds. After the absorption spectrum of a compound was determined in a solvent as reported in the literature, that solvent was removed by evaporation *in vacuo* at room temperature, and the spectrum was then determined in 90% acetone solution. If specific absorption coefficients were available from the literature, they were used to calculate concentrations and specific absorption coefficients; otherwise, relative absorption coeffi-

[1] Part of a thesis submitted in partial fulfillment of the requirements for the degree of Doctor of Philosophy, University of Washington. The author wishes to acknowledge financial aid from the Office of Naval Research, under provisions of contract N8onr/520/III between the Office of Naval Research and the University of Washington.

[2] Present address: Woods Hole Oceanographic Institution, Woods Hole, Massachusetts.

cients were determined and are reported here. Ninety per cent acetone was chosen because of its greater effectiveness than 80% or absolute acetone in the extraction of pigments from plant cells.

## EXPERIMENTAL

Absorbencies were measured in a Beckman Model DU Spectrophotometer, using one centimeter glass-stoppered Corex cells and a tungsten filament light source. The slit and band widths used are shown in Table I. Tube and filter selections were in accordance with the manufacturer's recommendations.

*Chlorophylls.* To prepare chlorophyll *a*, fresh fronds of the brown alga *Nereocystis leutkeana* were extracted with absolute methanol in the presence of magnesium carbonate. After dilution with water, most of the pigments were transferred to petroleum ether; they were then washed first with methanol (to remove xanthophylls) and finally with water (to remove alcohol), after which they were dried over anhydrous sodium sulfate. The pigments in the petroleum ether solution were separated by chromatographic adsorption on a powdered sugar column, developing the chromatogram with petroleum ether containing small amounts (1 − 2.5%) of methanol.

The spectrum of chlorophyll *a* prepared by the above method agreed well with that of chlorophyll *a* prepared by Harris and Zscheile (2, 9) with a more elaborate method.

Chlorophyll *c* was prepared by the chromatographic method of Strain, *et. al.* (5, 6) from the diatom *Navicula araneosum.* The first formation and early development of the chromatograms always left a mixture of chlorophylls *a* and *c* in the top band. Spectrophotometric examination of the eluted pigments showed that chlorophyll *a* was removed from this band only upon extensive washing with petroleum ether containing up to 4% methanol. This apparent coadsorption of chlorophylls *a* and *c*, not described by Strain and his co-workers, was always observed by the writer.

The spectrum of the mixture eluted from the top green band of a chromatogram prepared by the method of Pace (3) showed that it was also chlorophylls *a* and *c*, not chlorophyll *b* as Pace assumed. Since the spectra of chlorophylls *b* and *c* are quite different, the results of his analyses of the chlorophylls of the diatom *Nitzschia Closterium* are probably in error as to the identity and amount of the second chlorophyll component.

It should be noted that Strain and Manning (5) found somewhat different spectra for methanol solutions of chlorophyll *c* prepared by solvent partition and by chromatographic adsorption. Acetone solu-

TABLE I. Slit and Nominal Band Widths Used in Making Absorption Measurements on the Beckman Spectrophotometer

| *Wave Length Range* mμ | *Slit (mm)* | *Nominal Band Width* mμ | |
|---|---|---|---|
| | *90% Acetone Solutions* | | |
| 320–322.4 | 1.8 | 9.0 | 9.4 |
| 322.5–324 | 1.3 | 6.76 | 6.89 |
| 325–329 | 0.8 | 4.24 | 4.52 |
| 330–334 | 0.3 | 1.69 | 1.75 |
| 335–339 | 0.2 | 1.17 | 1.22 |
| 340–359 | 0.15 | .92 | 1.12 |
| 360–399 | 0.10 | .75 | 1.05 |
| 400–700 | 0.04 | .42 | 2.00 |
| | *Methanol Solutions* | | |
| 320–324 | 0.3 | 1.50 | 1.69 |
| 325–334 | 0.2 | 1.06 | 1.17 |
| 335–354 | 0.15 | .88 | 1.06 |
| 355–399 | 0.10 | .71 | 1.05 |
| 400–409 | 0.05 | .52 | .56 |
| 410–599 | 0.04 | .45 | 1.36 |
| 600–619 | 0.07 | 2.38 | 2.80 |
| 620–700 | 0.04 | 1.60 | 2.00 |
| | *Hexane Solutions* | | |
| 320–324 | 0.3 | 1.50 | 1.59 |
| 325–334 | 0.2 | 1.06 | 1.17 |
| 335–349 | 0.15 | .88 | .96 |
| 350–399 | 0.10 | .64 | 1.05 |
| 400–599 | 0.04 | .42 | 1.36 |
| 600–700 | 0.07 | 2.38 | 3.50 |
| | *Ethanol Solutions* | | |
| 320–322.4 | 0.3 | 1.50 | 1.56 |
| 322.5–334 | 0.2 | 1.04 | 1.17 |
| 335–349 | 0.15 | .88 | .96 |
| 350–399 | 0.10 | .64 | 1.05 |
| 400–409 | 0.05 | .52 | .56 |
| 410–700 | 0.04 | .45 | 2.00 |

tions of chlorophyll *c* prepared by solvent partition have not been studied.

*Beta Carotene.* A commercial preparation of beta carotene (Eimer and Amend) was used to determine the 90% acetone spectrum of this compound. Although it was described by the manufacturers as xanthophyll, chlorophyll, oil and fat free, the commercial preparation

TABLE II. Absorption Spectra of Chlorophylls *a* and *c*

| *Wave Length* mμ | *Chlorophyll* a *in 90% Acetone* | *Chlorophyll* c *in 90% acetone. Corrected for chlorophyll* a *content* | | *Chlorophyll* c *in Methanol. Corrected for chlorophyll* a *content* | |
|---|---|---|---|---|---|
| | Log $E$ $\frac{1\text{ gm}}{1\text{ cm}}$ | *Soln.* 1 Log $E$ 1 cm | *Soln.* 2 Log $E$ 1 cm | *Soln.* 1 Log $E$ 1 cm | *Soln.* 2 Log $E$ 1 cm |
| 320 | 1.449 | 1.449 | 1.528 | — | — |
| 325 | 1.453 | 1.448 | 1.526 | — | — |
| 330 | 1.399 | 1.362 | 1.394 | — | — |
| 335 | 1.419 | 1.305 | 1.281 | — | — |
| 340 | 1.403 | 1.283 | 1.279 | — | — |
| 345 | — | 1.264 | 1.257 | — | — |
| 350 | 1.464 | 1.241 | 1.245 | — | — |
| 355 | 1.499 | 1.221 | 1.233 | — | — |
| 360 | 1.552 | 1.236 | 1.233 | — | — |
| 365 | 1.599 | — | — | — | — |
| 370 | 1.648 | 1.262 | 1.257 | — | — |
| 375 | 1.685 | — | — | — | — |
| 380 | 1.697 | 1.307 | 1.302 | — | — |
| 385 | 1.701 | — | — | — | — |
| 390 | 1.701 | 1.361 | 1.352 | — | — |
| 395 | 1.714 | — | — | — | — |
| 400 | 1.764 | 1.378 | 1.373 | 1.299 | 1.271 |
| 405 | 1.829 | — | — | — | — |
| 410 | 1.859 | 1.441 | 1.436 | 1.362 | 1.331 |
| 415 | 1.854 | — | — | — | — |
| 420 | 1.849 | 1.572 | 1.573 | 1.461 | 1.434 |
| 425 | 1.894 | — | — | — | — |
| 430 | 1.940 | 1.730 | 1.733 | 1.626 | 1.605 |
| 440 | 1.696 | 1.883 | 1.889 | 1.748 | 1.718 |
| 445 | 1.347 | 1.922 | 1.922 | 1.764 | 1.764 |
| 450 | .949 | 1.895 | 1.899 | 1.763 | 1.751 |
| 455 | .625 | — | — | — | — |
| 460 | .405 | 1.677 | 1.674 | 1.635 | 1.622 |
| 465 | .313 | — | — | — | — |
| 470 | .276 | 1.216 | 1.202 | 1.342 | 1.317 |
| 480 | .278 | .732 | .718 | .929 | .910 |
| 490 | .368 | .468 | .441 | .452 | .442 |
| 500 | .410 | .368 | .344 | .237 | .216 |
| 505 | .414 | — | — | — | — |
| 510 | .412 | .329 | .295 | .201 | .113 |
| 515 | — | .325 | .286 | — | — |
| 520 | .417 | .353 | .320 | .220 | .192 |
| 530 | — | .437 | .415 | — | .238 |
| 540 | .591 | .519 | .499 | .384 | .352 |

TABLE II—(*continued*)

| Wave Length mμ | *Chlorophyll a in 90% Acetone* Log $E\frac{1\text{ gm}}{1\text{ cm}}$ | *Chlorophyll c in 90% acetone. Corrected for chlorophyll a content* Soln. 1 Log $E$ 1 cm | Soln. 2 Log $E$ 1 cm | *Chlorophyll c in Methanol. Corrected for chlorophyll a content* Soln. 1 Log $E$ 1 cm | Soln. 2 Log $E$ 1 cm |
|---|---|---|---|---|---|
| 550 | .567 | .545 | .529 | .442 | .414 |
| 560 | .706 | .654 | .645 | .502 | .493 |
| 570 | .855 | .763 | .736 | .580 | .539 |
| 580 | .942 | .867 | .857 | .703 | .685 |
| 585 | — | .843 | .834 | .720 | .693 |
| 590 | .915 | .757 | .748 | .684 | .560 |
| 600 | .986 | .583 | .560 | .555 | .560 |
| 605 | — | .554 | .541 | .492 | .456 |
| 610 | 1.144 | .573 | .563 | .483 | .442 |
| 615 | 1.179 | .646 | .637 | .538 | .539 |
| 620 | 1.172 | .760 | .760 | .638 | .618 |
| 625 | 1.138 | .931 | .914 | .779 | .776 |
| 630 | 1.076 | 1.015 | 1.024 | .856 | .846 |
| 631 | — | 1.021 | — | — | — |
| 634 | — | — | — | .869 | — |
| 635 | 1.035 | .985 | .983 | .868 | .851 |
| 640 | 1.074 | .841 | .837 | .821 | .794 |
| 645 | 1.215 | .642 | .621 | .720 | .700 |
| 650 | 1.417 | .444 | .441 | .547 | .493 |
| 655 | 1.730 | .268 | .268 | — | — |
| 660 | 1.838 | .036 | .043 | −.383 | −.461 |
| 663 | 1.851 | — | — | — | — |
| 665 | 1.824 | .020 | .043 | — | — |
| 670 | 1.534 | — | — | — | — |
| 675 | 1.378 | — | — | — | — |
| 680 | .972 | — | — | — | — |
| 685 | .548 | — | — | — | — |

Concentrations of chlorophyll *a* solutions computed from specific absorption coefficients reported by Zscheile (10).

The relative absorption coefficients of the acetone solutions of chlorophyll *c* at 445 mμ are arbitrarily given the value 1.922 at 430 mμ. Values for chlorophyll *a* are *specific* absorption coefficients, those for chlorophyll *c* are relative absorption coefficients.

gave a blue color, characteristic of the xanthophylls (1) when shaken (in hexane solution) with 85% phosphoric acid. In 90% acetone solution it showed a sudden rise in absorbency in the range 320 to 350 mμ. To purify the preparation it was dissolved in hexane, shaken with 90% methanol, washed with water, and dried over anhydrous

TABLE III. Specific Absorption Coefficients of Beta Carotene in 90% Acetone

| *Wave Length* | Log $E\,\frac{1\text{ gm}}{1\text{ cm}}$ | *Wave Length* | Log $E\,\frac{1\text{ gm}}{1\text{ cm}}$ |
|---|---|---|---|
| 320 | 1.216 | 455 | 2.400 |
| 322.5 | 1.163 | 456 | 2.400 |
| 325 | 1.181 | 460 | 2.385 |
| 330 | 1.205 | 465 | 2.351 |
| 335 | 1.227 | 470 | 2.332 |
| 340 | 1.248 | 475 | 2.339 |
| 345 | 1.238 | 480 | 2.349 |
| 350 | 1.248 | 485 | 2.337 |
| 355 | 1.227 | 490 | 2.285 |
| 360 | 1.253 | 500 | 2.042 |
| 370 | 1.377 | 510 | 1.658 |
| 380 | 1.554 | 520 | 1.181 |
| 390 | 1.725 | 530 | 0.771 |
| 400 | 1.906 | 540 | 0.570 |
| 410 | 2.033 | | |
| 420 | 2.170 | | |
| 425 | 2.212 | | |
| 430 | 2.251 | | |
| 440 | 2.309 | | |
| 445 | 2.355 | | |
| 450 | 2.388 | | |
| 452 | 2.400 | | |
| 453 | 2.400 | | |

Concentrations of solutions determined from aliquot samples in hexane, using specific absorption coefficients reported by Zechmeister and Polgar (8). In 90% acetone the maximum is a little lower (cf. 2.410) and displaced slightly toward the longer wave lengths (cf. 450 $m\mu$) than in hexane solutions.

sodium sulfate. Hexane solutions of beta carotene thus treated also showed unusually high absorbencies in the range 320–370 mμ, but if the solvent were removed and the carotene exhaustively dried under reduced pressure at room temperature, the absorbencies in this range showed no great increases. These observations suggest the formation of methanol solvates which persist in hexane and acetone solution but which can be broken down by drying *in vacuo*. Similar observations were made on fresh xanthophyll preparations.

*Xanthophylls.* Neofucoxanthin A and B, fucoxanthin, diadinoxanthin and diatoxanthin were prepared by the methods of Strain, *et al.* (7) from mixed diatoms. Their spectra in ethanol and 90% acetone solutions over the range 350 to 560 mμ are reported in Table IV. In the range 320 to 350 mμ, the spectra were found to be inconsistent and to vary with the treatment of the material, as was the case with beta carotene (see above).

TABLE IV. Absorption Spectra of Diatom Xanthophylls in Ethanol and 90% Acetone Solution. Values of Log $E_{1cm}$ Given.

| Wave Length $m\mu$ | *Neofucoxanthin A* | | *Neofucoxanthin B* | | *Fucoxanthin* | | *Diadinoxanthin* | | *Diatoxanthin* | |
|---|---|---|---|---|---|---|---|---|---|---|
| | *Ethanol* | *90% Acetone* | *Ethanol* | *90% Acetone* | *Ethanol* | *90% Acetone* | *Ethanol* | *90% Acetone* | *Ethanol* | *90% Acetone* |
| 350 | 1.657 | 1.667 | 1.581 | 1.553 | 1.328 | 1.312 | 1.494 | 1.521 | 1.808 | 1.805 |
| 355 | — | 1.675 | — | 1.568 | 1.336 | 1.340 | 1.464 | 1.472 | 1.757 | 1.765 |
| 360 | 1.688 | 1.706 | 1.620 | 1.608 | 1.402 | 1.400 | 1.494 | 1.480 | 1.729 | 1.734 |
| 365 | — | — | — | — | 1.465 | — | 1.552 | 1.537 | 1.731 | 1.734 |
| 370 | 1.761 | 1.789 | 1.714 | 1.721 | 1.550 | 1.567 | 1.622 | 1.610 | 1.771 | 1.756 |
| 375 | — | — | — | — | 1.621 | — | 1.687 | — | 1.808 | — |
| 380 | 1.868 | 1.892 | 1.833 | 1.846 | 1.700 | 1.726 | 1.753 | 1.748 | 1.879 | 1.846 |
| 390 | 1.966 | 1.996 | 1.950 | 1.974 | 1.854 | 1.885 | 1.913 | 1.907 | 1.957 | 1.946 |
| 400 | 2.081 | 2.110 | 2.070 | 2.099 | 1.994 | 2.027 | 2.022 | 2.027 | 2.070 | 2.066 |
| 410 | 2.166 | 2.196 | 2.178 | 2.206 | 2.114 | 2.148 | 2.157 | 2.157 | 2.171 | 2.162 |
| 420 | 2.244 | 2.279 | 2.251 | 2.283 | 2.216 | 2.252 | 2.239 | 2.258 | 2.266 | 2.264 |
| 430 | 2.302 | 2.330 | 2.316 | 2.343 | 2.283 | 2.316 | 2.272 | 2.282 | 2.297 | 2.314 |
| 440 | 2.352 | 2.381 | 2.359 | 2.392 | 2.346 | 2.377 | 2.365 | 2.376 | 2.354 | 2.353 |
| 444 | — | — | — | 2.398 | 2.368 | — | 2.375 | 2.400 | 2.371 | — |
| 445 | 2.367 | 2.397 | 2.373 | 2.398 | 2.369 | 2.394 | 2.372 | 2.400 | 2.373 | 2.381 |
| 446 | 2.369 | 2.398 | 2.374 | 2.400 | 2.368 | 2.398 | 2.365 | 2.399 | 2.373 | 2.384 |
| 448 | 2.370 | 2.400 | 2.375 | 2.400 | 2.374 | 2.400 | 2.354 | — | 2.375 | 2.392 |
| 449 | 2.374 | 2.399 | 2.373 | 2.395 | — | 2.400 | — | — | — | — |
| 450 | 2.375 | 2.397 | — | — | 2.374 | 2.398 | 2.336 | 2.379 | 2.371 | 2.396 |
| 451 | 2.374 | — | — | — | 2.374 | — | — | — | — | 2.400 |
| 452 | 2.373 | — | 2.371 | — | 2.375 | — | 2.317 | — | 2.363 | 2.396 |
| 455 | 2.369 | 2.379 | 2.367 | 2.385 | 2.373 | 2.387 | 2.285 | 2.330 | 2.343 | 2.388 |
| 460 | 2.360 | 2.374 | 2.358 | 2.374 | 2.364 | 2.373 | 2.258 | 2.389 | 2.308 | 2.360 |
| 465 | — | 2.366 | — | 2.361 | 2.358 | 2.366 | 2.272 | 2.389 | 2.288 | 2.329 |
| 470 | 2.346 | 2.359 | 2.336 | 2.351 | 2.352 | 2.362 | 2.299 | 2.320 | 2.293 | 2.314 |
| 472 | — | — | — | — | — | — | 2.300 | 2.328 | 2.317 | — |
| 475 | — | — | — | — | 2.337 | — | 2.287 | 2.327 | 2.318 | 2.318 |
| 476 | — | — | — | — | — | — | — | 2.321 | 2.317 | 2.322 |
| 478 | — | — | — | — | — | — | — | — | — | 2.324 |
| 480 | 2.304 | 2.312 | 2.277 | 2.278 | 2.305 | 2.308 | 2.201 | 2.269 | 2.275 | 2.322 |
| 485 | — | 2.257 | — | 2.213 | 2.259 | 2.246 | 2.037 | 2.139 | 2.211 | 2.294 |
| 490 | 2.206 | 2.184 | 2.160 | 2.135 | 2.201 | 2.171 | 1.793 | 1.933 | 2.091 | 2.198 |
| 500 | 2.056 | 1.998 | 1.993 | 1.931 | 2.043 | 1.969 | 1.229 | 1.362 | 1.715 | 1.905 |
| 510 | 1.890 | 1.792 | 1.808 | 1.710 | 1.866 | 1.753 | 0.871 | 0.953 | 1.322 | 1.527 |
| 520 | 1.673 | 1.583 | 1.598 | 1.448 | 1.645 | 1.494 | 0.649 | 0.706 | 1.021 | 1.187 |
| 530 | 1.442 | 1.306 | 1.346 | 1.192 | 1.409 | 1.222 | 0.514 | 0.417 | 0.817 | 0.960 |
| 540 | 1.211 | 1.049 | 1.101 | 0.939 | 1.152 | 0.960 | 0.376 | 0.379 | 0.662 | 0.797 |
| 560 | 0.734 | 0.634 | 0.592 | 0.448 | 0.637 | 0.358 | 0.251 | 0.254 | 0.516 | 0.659 |

Values of Log $E_{1cm}$ computed by arbitrarily assigning the value 2.375 to the maxima of ethanol solutions and 2.400 in 90% acetone. The former value is close to the value found by Strain (4) for eight leaf xanthophylls in ethanol; the latter is an average observed for aliquot samples in acetone solution.

## RESULTS

The absorption spectra of the compounds discussed above are tabulated in Tables II to IV. Except for chlorophyll *a* and beta carotene, logarithms of the relative absorption coefficients, computed from observed absorbencies, arbitrarily assigning the value 2.400 to the yellow maximum, are given. Logarithms of specific absorption coefficients of chlorophyll *a* and beta carotene were calculated from concentration values that were determined as indicated in the tables. The Beer-Bouquer law was used in the form

$$\log E = \log D - (\log L + \log c) ,$$

which, for a one cm light path ($L = 1$), reduces to

$$\log E = \log D - \log c .$$

$D$ is the absorbency, $\log I_0/I$. Logarithms are reported, following the practice of Strain, because the shape of the plot of $\log E$ against wave length is independent of the concentration.

The coefficients given in Table IV were determined on compounds prepared in the presence of dimethyl aniline, and therefore the data extend only to 350 mμ.

## DISCUSSION

The absorption spectra presented herein represent comparable data for the major pigments found in the diatoms, a group of plants which is responsible for a very large proportion of the world's photosynthetic production of organic compounds. These data have been used for the spectrophotometric estimation of the components of 90% acetone extracts of mixed plankton by a method published in a paper by Richards with Thompson which appears earlier in this issue.

It should be of interest to the evolutionist that chlorophyll *c* absorbs relatively much more blue than red light as compared with chlorophylls *a* and *b*. Thus, the diatoms, dinoflagellates, and brown algae possess a pigment admirably suited to the absorption of light of the wave lengths which penetrate deepest into the sea. Because chlorophyll *c* is not intensely green, its amount is apt to be underestimated; for this reason it has been generally ignored by oceanographers and limnologists in studies of photosynthesis, although Strain, Manning and Hardin (6) have come to the conclusion that "chlorofucine (Chlorophyll *c*) may be an important pigment in the carbon economy of nature."

## SUMMARY

Chlorophylls *a* and *c*, neofucoxanthin A and B, fucoxanthin, diadinoxanthin and diatoxanthin have been prepared, and their absorption spectra, as well as that of beta carotene, in 90% acetone solution

have been determined and reported. Previously reported spectra of the diatom xanthophylls in ethanol have been extended into the near ultra-violet.

## REFERENCES CITED

1. Haagen-Smit, A. J., C. E. P. Jeffreys and J. G. Kirchner
   1943. Separation of carotenes from xanthophylls. Industr. Engng. Chem., Anal. Ed., *15:* 179–180.
2. Harris, D. G. and F. P. Zscheile
   1943. Effects of solvent upon absorption spectra of chlorophylls *a* and *b*, their untraviolet absorption spectra in ether solutions. Bot. Gaz., *104:* 515–527.
3. Pace, N. J.
   1941. Pigments of the marine diatom Nitzschia Closterium. J. biol. Chem., *140:* 483–489.
4. Strain, H. H.
   1938. Leaf xanthophylls. Carneg. Instn. Wash., Publ. No. 490.
5. Strain, H. H. and W. M. Manning
   1942. Chlorofucine (chlorophyll *c*), a green pigment of diatoms and brown algae. J. biol. Chem., *144:* 625–636.
6. Strain, H. H., W. M. Manning and G. Hardin
   1943. Chlorophyll *c* (chlorofucine) of diatoms and dinoflagellates. J. biol. Chem., *148:* 655–668.
7. Strain, H. H., W. M. Manning and G. Hardin
   1944. Xanthophylls and carotenes of diatoms, brown algae, dinoflagellates, and sea anemones. Biol. Bull. Woods Hole, *86:* 169–191.
8. Zechmeister, L. and A. Polgar
   1943. Cis-trans isomerization and spectral characteristics of carotenoids and some related compounds. J. Amer. chem. Soc., *65:* 1522–1528.
9. Zscheile, F. P., Jr.
   1934. An improved method for the purification of chlorophylls *a* and *b;* quantitative measurement of their absorption spectra; evidence for the existence of a third component of chlorophyll. Bot. Gaz., *95:* 529–562.
10. Zscheile, F. P., Jr.
   1934. A quantitative spectro-photoelectric analytical method applied to solutions of chlorophylls *a* and *b*. J. phys. Chem., *38:* 95–102.

# THE ESTIMATION AND CHARACTERIZATION OF PLANKTON POPULATIONS BY PIGMENT ANALYSES

## II. A SPECTROPHOTOMETRIC METHOD FOR THE ESTIMATION OF PLANKTON PIGMENTS[1]

By

FRANCIS A. RICHARDS[2] with THOMAS G. THOMPSON

*Oceanographic Laboratories*
*University of Washington, Seattle, Washington*

## ABSTRACT

A semimicro spectrophotometric method is described for the estimation of chlorophyll *a*, *b*, and *c* and of astacin and nonastacin type carotenoids in acetone extracts of plant and animal material. Developed specifically for use in estimating and characterizing plankton populations, the method is highly sensitive and practical for shipboard use. Methods of collecting, preparing and extracting plankton samples, spectrophotometric measurements, computation of results, and errors are discussed.

## INTRODUCTION

A semimicro method has been developed for the simultaneous spectrophotometric determination of chlorophylls *a*, *b*, and *c* and of two types of carotenoids in 90% acetone extracts of plant and animal material. This method, which avoids the separation and individual determination of the several components, results in minimum manipulation, loss and contamination of the sample.

The method was developed specifically for the examination of plankton, since pigment analyses, extended to include the various chlorophylls and carotenoids, should give: (a) a measure of the potential of the plankton for absorbing radiant energy for photosynthesis, (b) some measure of the extent and stage of development of the phytoplankton, and (c) a possible measure of the presence of animals grazing on the crop. The method can be considered as a logical development of "pigment unit" determinations by Harvey (5) and of chlorophyll determinations by Graham, Kozminski, Krey, Riley, Tucker, and others (4, 7, 8, 14, 15, 20).

The method meets the practical requirements necessary for the

[1] The authors wish to acknowledge financial aid from the Office of Naval Research, under provisions of contract N8onr/520/III between the Office of Naval Research and the University of Washington.

[2] Present address: Woods Hole Oceanographic Institution, Woods Hole, Massachusetts.

determination of pigments in plankton on shipboard. It permits the use of relatively small water samples rather than net catches; it also enhances the value of surface samples and microplankton, and it aids in definitely fixing the origin of the sample. One to two liters of sea water provide an adequate sample except in cases of very sparse plankton. Net tows readily give sufficient material for analysis.

## METHOD OF ESTIMATION OF PLANKTON PIGMENTS

*Reagents.* 90% Acetone: Reagent grade acetone is distilled over aqueous $Na_2CO_3$ and $Na_2SO_3$ solution through an 18 inch fractionating column. 100 ml of water are pipetted into a one liter flask and made up to the mark with acetone, B.p. 56.5° C.

Magnesium carbonate: Reagent grade powdered magnesium carbonate.

*Procedure.* About 0.1 g of powdered magnesium carbonate (to prevent acidity and subsequent pheophytin formation) is added to a one to two liter water sample. After shaking, the sample is poured into an aspirator bottle[3] from which a rubber tube fitted with a stopcock leads to the intake of a Foerst Plankton Centrifuge (Foerst Mechanical & Specialties Co.). The stopcock is adjusted so that one liter flows through the centrifuge in about seven minutes. The centrifuge is turned on before the flow is started and is left on until the aspirator bottle is completely rinsed and the centrifuge drained. When the last of the sample has flowed through, the bottle is rinsed three times with a strong stream of distilled water. The centrifuge is then stopped and the cup is removed.

The particulate matter in the cup is scrubbed down with a rubber policeman and is rinsed into a 16 or 20 by 125 mm screw-cap test tube; the cup is then rerinsed. The material is then centrifuged at high speed in a clinical centrifuge for three minutes, the water is poured off, and the particulate matter is allowed to drain in the tube. The tube is placed in a vacuum desiccator and dried.

When the tube is dry, a definite volume of 90% acetone is pipetted into it and is stirred with the particulate matter and magnesium carbonate. The volume of acetone depends on the amount of plankton present; 5 ml has been used in most cases. The tube, tightly capped, is then placed in the dark for 18–24 hours, after which time the material is again mixed; the tube is then recapped and the material is centrifuged in the clinical centrifuge for three minutes at high speed.

The extract is decanted into a 1 cm properly calibrated glass-stoppered Corex absorption cell, and the absorbencies at 665, 645, 630,

[3] A large leveling bulb has been found more convenient than an aspirator bottle.

510, and 480 mμ are determined on a Beckman Model DU quartz spectrophotometer (2, 3). The red-sensitive tube is used for readings at 665, 645, 630 mμ, the blue-sensitive tube at 510 and 480 mμ. The tungsten filament light source is used at these wave lengths.

*Calculation of Results.* The equations for the calculation of chlorophylls *a*, *b*, and *c* are:

$$D_{665} = .0667\ C_a + .0065\ C_b + .0011\ C_c\ ;$$
$$D_{645} = .0164\ C_a + .0456\ C_b + .0044\ C_c\ ;$$
$$D_{630} = .0119\ C_a + .0127\ C_b + .0104\ C_c\ .$$

$D_{665}$, $D_{645}$ and $D_{630}$ are the observed absorbencies (log $I_0/I$) at 665, 645 and 630 mμ respectively and are determined directly with the spectrophotometer. $C_a$, $C_b$ and $C_c$ are concentrations of chlorophylls *a*, *b*, and *c* in milligrams per liter. Solving these equations:

$$C_a(\text{mg/L}) = 15.6\ D_{665} - 2.0\ D_{645} - 0.8\ D_{630}\ ;$$
$$C_b(\text{mg/L}) = 25.4\ D_{645} - 4.4\ D_{665} - 10.3\ D_{630}\ ;$$
$$C_c(\text{MSPU/L})^4 = 109\ D_{630} - 12.5\ D_{665} - 28.7\ D_{645}\ .$$

It is evident from their spectra that the carotenoids make no contribution to the absorbencies at these wave lengths.

The concentrations of two carotenoid components are calculated from absorbencies at 510 and 480 mμ. The contributions of the chlorophylls to these absorbencies are computed and subtracted, leaving residual absorbencies ($D_{res}$) which are the result of carotenoid absorption. The equations for these calculations are:

$$D_{res,\ 510} = D_{510} - .0026\ C_a - .0035\ C_b - .0021\ C_c = .045\ C_{nac} + .169\ C_{ac}\ ,$$
$$D_{res,\ 480} = D_{480} - .0019\ C_a - .0136\ C_b - .0054\ C_c = .203\ C_{nac} + .249\ C_{ac}\ ,$$

where $C_{nac}$ and $C_{ac}$ are the respective concentrations of nonastacin type and astacin type carotenoids.

Solving:

$$\text{Astacin type carotenoids (MSPU/L)} = 2(4.45\ D_{res,510} - D_{res,\ 480})\ ;$$
$$\text{Nonastacin type carotenoids (MSPU/L)} = 7.6(D_{res,480} - 1.49\ D_{res,510}).$$

To illustrate these computations, the pigment concentrations in a plankton extract were calculated from the observed absorbencies:

$D_{665} = .068$, $D_{645} = .020$, $D_{630} = .018_5$, $D_{510} = .127$ and $D_{480} = .325$ ;

$$\text{Chlorophyll } a, \text{ mg/L} = 15.6 \times .068 - 2 \times .020 - 0.8 \times .0185 = 1.01 \text{ mg/L}\ ;$$
$$\text{Chlorophyll } b, \text{ mg/L} = 25.4 \times .020 - 4.4 \times .068 - 10.3 \times .018_5 = 0.02 \text{ mg/L}\ ;$$
$$\text{Chlorophyll } c, \text{ (MSPU/L)} = 109 \times .018 - 12.5 \times .068 - 28.7 \times .020 = 0.59 \text{ MSPU/L}\ ;$$

[4] For definition and explanation of MSPU, see page 160.

$D_{res,510} = .127 - 2.6 \times .00101 - 3.5 \times .00002 - 2.1 \times .00059$
$= .123$ ;
$D_{res,480} = .325 - 1.9 \times .00101 - 13.6 \times .00002 - 5.4 \times .00059$
$= .320$ ;
Astacin type carotenoids, MSPU/L $= 2(4.45 \times .123 = .320)$
$= 0.45$ MSPU/L ;
Nonastacin carotenoids, MSPU/L $= 7.6\ (.320 - 1.49 \times .123)$
$= 1.04$ MSPU/L .

The concentrations in a known volume of the extract can be converted to concentrations of pigments in the original sea water by multiplying by the appropriate factor according to the volume of sea water used, the final extraction volume, and the units in which the concentrations are expressed. For example, if 1.50 l of sea water were used and if the final volume of the acetone extract prior to spectrophotometric analysis were 5.0 ml, multiplying by the factor 5.0/1.50 would give the concentration in mg/M³ for chlorophylls *a* and *b* or MSPU/M³ in the case of chlorophyll *c*, astacin and nonastacin carotenoids.

The concentrations of the pigments in the extracts in the example above can be converted to concentrations in sea water as follows:
Chlorophyll *a* $= 1.01 \times 5.0/1.50 = 3.37$ mg/M³ ;
Chlorophyll *b* $= 0.02 \times 5.0/1.50 = 0.07$ mg/M³ ;
Chlorophyll *c* $= 0.59 \times 5.0/1.50 = 1.97$ MSPU/M³ ;
Astacin type carotenoids $= 0.45 \times 5.0/1.50 = 1.50$ MSPU/M³ ;
Nonastacin type carotenoids $= 1.04 \times 5.0/1.50 = 3.47$ MSPU/M³ .

The individual calculations of the several components of the carotenoid mixture were found impracticable, because in such calculations it is necessary to solve a number of simultaneous equations equal to the number of components present and to make measurements at an equal number of wave lengths. Errors in such calculations are cumulative, and small errors in density measurements become magnified. Furthermore, the exact number of components, which depends on the phylogenetic groups represented in the plankton (17) is unknown.

## DISCUSSION OF PROCEDURE AND CALCULATIONS

*Removal of Plankton from Water Samples.* The most satisfactory apparatus for the removal of plankton from water samples is the Foerst plankton centrifuge. Various filters—paper, sintered glass, and Caldwell type, were used both with and without freshly precipitated barium sulfate, but they were rejected because of inadequate speed or retention and because of the presence of extraneous matter in the

separated plankton. With the Foerst centrifuge, the plankton can be collected from one liter of water in about seven minutes.

*Extraction Methods.* Less than nine hours of steeping was found to be inadequate, although other workers have used much shorter periods (4, 5, 7, 14). After 24 hours there was no spectrophotometric evidence of decomposition of pigments. Neither grinding nor re-extracting the cells with fresh portions of solvent materially increased the amount of pigment extracted; evidently the excess of solvent was so great that the equilibrium distribution of pigment was greatly in favor of the solution instead of the particulate phase.

*Beer's Law.* Dilution experiments showed that, at the wave lengths used for calculating pigment concentrations, absorbencies below 0.8 were directly proportional to concentrations, conforming to Beer's Law. It was necessary to dilute extracts having absorbencies over 0.8.

*Calculation of Results.* Absorbencies of some of the mixtures of pigments obtained by acetone extractions of plankton samples were determined over the spectral range 320–700 m$\mu$ (Fig. 1A, B). The concentrations of the pigments can be computed from these spectra, since the absorbency is directly proportional to concentration. However, the computations require knowledge of the absorption coefficients of each component at various wave lengths. The number of wave lengths must equal the number of components to be computed, and each should be chosen where the absorption of one of the compounds is large. In the spectral range 320–430 m$\mu$, substances other than the chlorophylls and carotenoids frequently give high absorbencies, eliminating this range from the useful portion of the spectrum.

*Specific absorption coefficients* of 90% acetone solutions of chlorophylls *a* and *b* and beta carotene are reported in the literature (13, 21), but they are unknown for chlorophyll *c* and for the xanthophylls expected in the plankton. In order to express relative concentrations of the latter compounds, *Specified Pigment Units* (*SPU*) *are used. These units are defined so that one such unit in a liter of 90% acetone has, at the wave length of maximum absorption, the absorbency shown in Table I. These absorbencies were chosen equal (or nearly so) to the specific absorption coefficients of corresponding maxima in the spectra of related compounds, and thus the SPU represents a specific but undetermined weight of the pigment which should be about one gram.* For those pigments whose *Specific* Absorption Coefficients are unknown, the SPU is used instead of the gram in calculating *Specified* Absorption Coefficients. These are symbolized by $E\frac{lgm}{lcm}$ and $E\frac{SPU}{lcm}$ respectively.

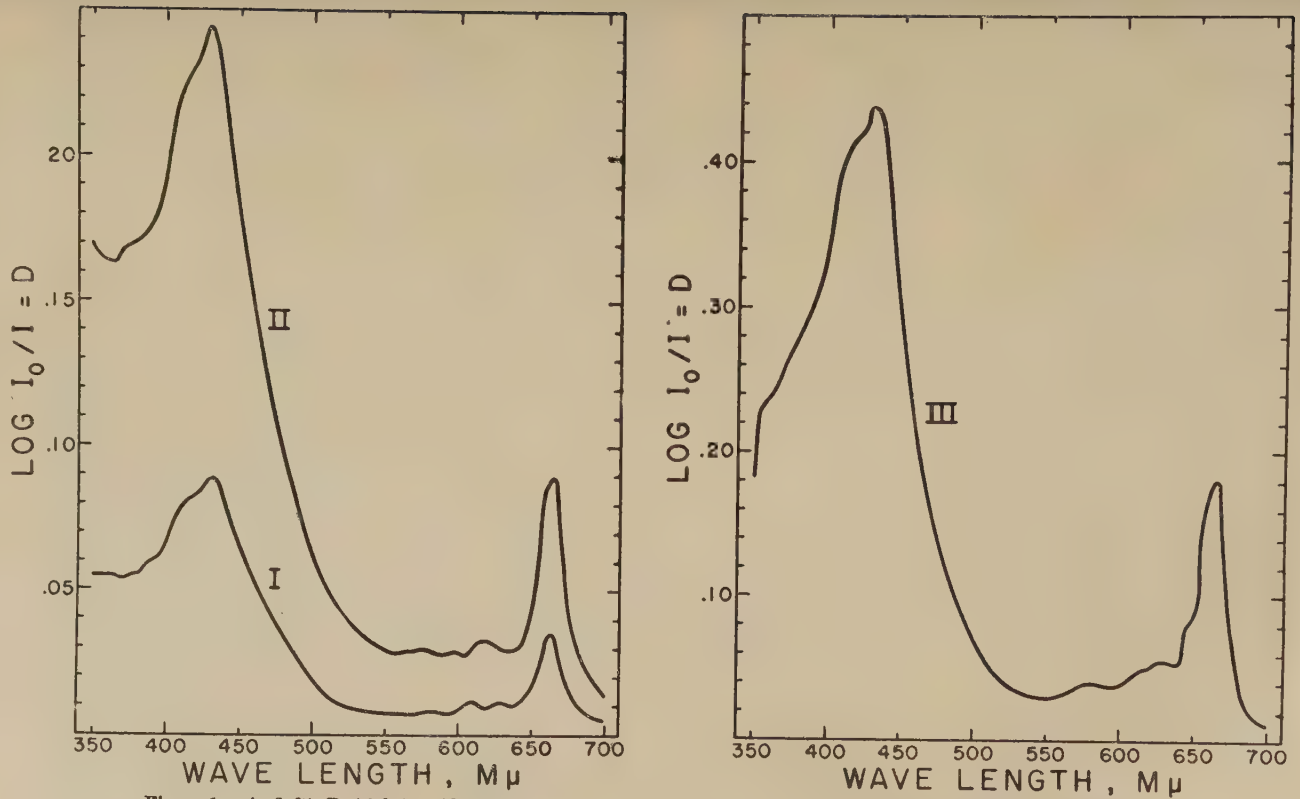


Figure 1. A (left) B (right). Absorption spectra of 90% acetone extracts of natural plankton collections.

Concentrations of chlorophyll *c* and the xanthophylls in Table I can thus be expressed in terms of SPU or in thousandths thereof (MSPU).

Table II shows specific and specified absorption coefficients for a group of pigments to be found in plankton. These were calculated from absorption spectra (13) and according to the definition of Specified Pigment Units given above. Using them, the concentrations in grams or SPU of the pigments in a mixture can be calculated from the total absorption at these wave lengths. In practice it has been found

TABLE I. Absorbencies of Solutions Containing One Specified Pigment Unit per Liter of 90% Acetone at Wave Length of Absorption Maximum

| *Compound* | *Wave Length of Absorption Maximum, mμ* | *Specified Absorbency* $\left(E \frac{SPU}{1cm}\right)$ *of a one cm layer* |
|---|---|---|
| Chlorophyll c | 445 | 83.5 |
| Neofucoxanthin A | 447–8 | 251 |
| Neofucoxanthin B | 446–8 | 251 |
| Fucoxanthin | 448–9 | 251 |
| Diatoxanthin | 451 | 251 |
| Diadinoxanthin | 444–5 | 251 |
| Astacin-type pigment | 475 | 251 |

necessary to group together those carotenoids with absorption maxima close to 450 mμ and to calculate the concentration of this group as a whole.

Simplifications tacit in the above calculation of the two types of carotenoids follow. The principal carotenoids of diatoms and dinoflagellates are beta carotene, fucoxanthin, neofucoxanthin A and B, diatoxanthin, diadinoxanthin, and pigments of very similar absorption spectra. These were found by Strain, Manning and Hardin (19) and by Richards (13) in a variety of diatomaceous and brown algal materials examined by chromatographic and spectrophotometric methods. The absorption spectra of peridinin, reported by Strain, et al., as the principal carotenoids of dinoflagellates, and of neoperidinin are similar to that of fucoxanthin, although chromatographically they are separable. If the above carotenoids occur in a fixed ratio in the plankton, then they can be grouped together, and absorption coefficients for the average mixture can be calculated.

Pace (11) has reported quantitative analyses of the pigments that occur in cultures of the marine diatom *Nitzschia Closterium*, and these ratios can be used to compute average absorption coefficients. He found five xanthophyll fractions which, on the basis of recent work by

TABLE II. SPECIFIC AND SPECIFIED ABSORPTION COEFFICIENTS OF SOME PLANKTON PIGMENTS IN 90% ACETONE SOLUTION*

| *Wave Length* $M\mu$ | *Chlorophyll a* $E$ *1gm 1cm* | *Chlorophyll b* $E$ *1gm 1cm* | *Chlorophyll c* $E$ *SPU 1cm* | *Beta Carotene* $E$ *1gm 1cm* | *Neofucoxanthin A* $E$ *SPU 1cm* | *Neofucoxanthin B* $E$ *SPU 1cm* | *Fucoxanthin* $E$ *SPU 1cm* | *Diadinoxanthin* $E$ *SPU 1cm* | *Diatoxanthin* $E$ *SPU 1cm* | *Astacin-type pigment* $E$ *SPU 1cm* | *Nonastacin type Carotenoids in average mixture (p. 158)* $E$ *SPU 1cm* |
|---|---|---|---|---|---|---|---|---|---|---|---|
| 665 | 66.7 | 6.5 | 1.1 | 0 | 0 | 0 | 0 | 0 | 0 | 0 | 0 |
| 645 | 16.4 | 45.6 | 4.4 | 0 | 0 | 0 | 0 | 0 | 0 | 0 | 0 |
| 630 | 11.9 | 12.7 | 10.4 | 0 | 0 | 0 | 0 | 0 | 0 | 0 | 0 |
| 510 | 2.6 | 3.5† | 2.1 | 45.5 | 62.0 | 51.3 | 56.6 | 9.0 | 33.7 | 169 | 45 |
| 480 | 1.9 | 13.6 | 5.4 | 223 | 205 | 190 | 203 | 186 | 210 | 249 | 203 |
| 450 | 8.9 | 54.0 | 78.5 | 244 | 249 | 248 | 249 | 239 | 250 | 221 | 246 |
| 420 | 70.7 | 26.8 | 37.3 | 148 | 190 | 192 | 169 | 181 | 184 | 147 | 171 |

* Values from Richards (13), except chlorophyll *b* values, which are from Zscheile, Comar, and Mackinney (21).

† Estimated.

Strain, et al. (19) and by Richards (13), are assumed to be neofucoxanthin *A* and *B*, fucoxanthin, diadinoxanthin, and diatoxanthin. Revising Pace's identifications in the light of the more recent work, he found that these pigments occur in the following averaged ratios:

| *Pace's Identification* | *mg*/100 *gm Dry Weight* | *Fraction of Total* | *Revised Identification* |
|---|---|---|---|
| Beta carotene | 65.9 | .107 | |
| Cryptoxanthin | 11.1 | .018 | Neofucoxanthin A or B |
| Lutein | 87.9 | .142 | Diadino- or Diatoxanthin |
| Isolutein | 22.2 | .036 | Neofucoxanthin A or B |
| Fraction Y | 339.1 | .549 | Fucoxanthin |
| Fraction Z | 90.2 | .146 | Diadino- or Diatoxanthin |
| | 616.4 | | |

Fraction Y (fucoxanthin) is by far the most important contributor to the mixture.[5] The other less abundant pigments probably occur in a more or less fixed ratio to fucoxanthin.

From the foregoing ratios as well as from the absorption coefficients of the individual carotenoids, average specified absorption coefficients for these carotenoids were calculated. These coefficients are the sum of the products of the ratios of the pigments found by Pace and the absorption coefficients shown in Table I. Averaged coefficients were used for neofucoxanthin *A* plus *B* and for diatoxanthin plus diadinoxanthin.

$$\text{At } 420\ m\mu\ \mathrm{E}\frac{\text{SPU}}{1\text{cm}}\text{, total nonastacin carotenoids} = 171\ ;$$

$$450\ m\mu\ \mathrm{E}\frac{\text{SPU}}{1\text{cm}}\text{, total nonastacin carotenoids} = 246\ ;$$

$$480\ m\mu\ \mathrm{E}\frac{\text{SPU}}{1\text{cm}}\text{, total nonastacin carotenoids} = 203\ ;$$

$$510\ m\mu\ \mathrm{E}\frac{\text{SPU}}{1\text{cm}}\text{, total nonastacin carotenoids} = 45\ .$$

These are the coefficients used in the equations on page 158 for the calculation of carotenoid concentrations.

Carotenoids of the astacin[6] type (Kuhn and Lederer, 9), presumably

[5] Strain, et al. and the present writers have found this to be the case in other diatoms as well as brown algae. Strain (16) also reports that in leaf plants the ratio in which the xanthophylls occur is rather constant until autumnal yellowing begins.

[6] The absorption maxima of carotenoids having 11 conjugated double bonds occur around 450 $m\mu$ in acetone solution, whereas the maxima in the spectra of those carotenoids having 13 conjugated double bonds (e. g., astacin) should occur at 25–30 $m\mu$ closer to the red.

TABLE III. Relative Absorption Spectrum of a 90% Acetone Solution of Astacin-type Pigment Extracted from Crustaceans, Corrected for Chlorophyll *a* Absorption

| *Wave Length* $M\mu$ | $E_{1cm}$ | *Wave Length* $M\mu$ | $E_{1cm}$ | *Wave Length* $M\mu$ | $E_{1cm}$ | *Wave Length* $M\mu$ | $E_{1cm}$ |
|---|---|---|---|---|---|---|---|
| 350 | 47.2 | 400 | 84.3 | 450 | 220.9 | 500 | 204.2 |
| 355 | 48.9 | 405 | 92.7 | 455 | 236.0 | 510 | 168.7 |
| 360 | 47.2 | 410 | 106.2 | 460 | 236.0 | 520 | 126.5 |
| 365 | 50.6 | 415 | 121.3 | 465 | 246.0 | 530 | 86.1 |
| 370 | 52.2 | 420 | 134.9 | 470 | 251.2 | 540 | 50.5 |
| 380 | 59.0 | 425 | 146.9 | 475 | 251.2 | 550 | 28.6 |
| 390 | 69.0 | 430 | 161.8 | 480 | 249.5 | 560 | 16.9 |
| | | 435 | 177.0 | 490 | 227.5 | | |
| | | 440 | 195.4 | | | | |
| | | 445 | 208.9 | | | | |

characteristic of the crustaceans, can also be estimated when they become an important part of the plankton pigments. Samples of this pigment were obtained from two plankton tows consisting mainly of crustaceans (copepods, other crustaceans, crustacean larvae) and a few diatoms. The spectra of 90% acetone extracts of this material showed that one contained very small amounts of chlorophylls, the other appreciable concentrations. Absorption spectra of these extracts, corrected for the chlorophyll content, are shown in Fig. 2 and Table III. These spectra, very similar to those of pigment extracts from shrimp (Brown, 1) and a chloroform extract from lobster blood (Redfield, 12), can be tentatively identified as astacin, which Kuhn and Lederer (9) prepared from the Norwegian lobster, *Astacus gammarus*. Since the absorption maximum of astacin in carbon disulfide and pyridine occurs at 500 $m\mu$, and since the absorption maximum of astacin in acetone solution should occur at wave lengths 25–30 $m\mu$ nearer the blue (16), it is concluded that the spectra represent a pigment (or pigments) of the astacin type which occurs in naturally growing crustaceans. Following the practice established on page 160, a specified pigment unit of the astacin-type carotenoid was defined so that the absorbency, as in Table I, is 251 at 474 $m\mu$. Specified absorption coefficients computed on this basis are shown in Table II.

*Instrument Errors.* At low absorbencies, errors in reading the spectrophotometer might become important, but at these densities the scale divisions are large and readings are reproducible within $\pm$ .0015 absorbency (log $I_0/I$ units). The concentrations of the five components at which these instrumental errors cause 5, 10 and 20% errors in concentrations are shown in Table IV. An absorption cell, such as

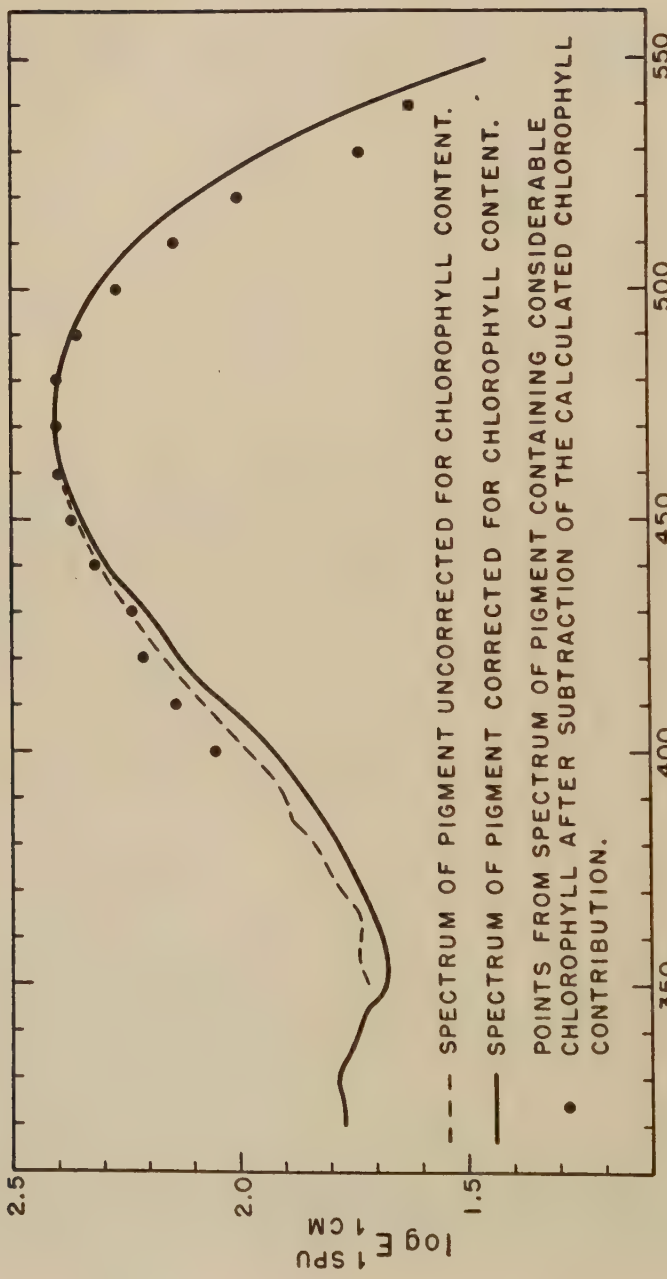


Figure 2. Specified absorption spectrum of astacin-type carotenoids.

that described by Kirk, et al. (6), in which the length to volume ratio is increased, should permit greater precision in the determination of the absorbencies of the more dilute solutions.

In plankton extracts, chlorophyll *b* concentrations have been found to be very small or absent; calculations frequently lead to small negative values which are within the instrumental error.

TABLE IV. Concentrations of Pigments and Corresponding Instrumental Errors

| *Compound* | ±20% *or over* | ±10% | ±5% |
|---|---|---|---|
| Chlorophyll *a*, mg/L | .16 | .32 | .64 to 12.8* |
| Chlorophyll *b*, mg/L | .25 | .50 | 1.00 to 20.0* |
| Chlorophyll *c*, MSPU/L | 1.09 | 2.18 | 4.36 to 87.2* |
| Nonastacin Carotenoids MSPU/L | .105 | .210 | .420 to 7.12* |
| Astacin-type Carotenoids MSPU/L | .190 | .380 | .760 to 6.08* |

* At higher concentrations there is a deviation from Beer's Law and extracts should be diluted.

*Chlorophyll c.* Large errors in the determination of chlorophyll *c* might be expected because of its small absorption in the red spectral range. In general these errors are difficult to estimate, particularly in view of the difficulty in preparing the pure material for study.

At concentrations of chlorophyll *c* frequently found in collections of natural plankton, the instrumental error (Table IV) would frequently be very large. However, both chlorophyll *c* and carotenoid concentrations can be checked by computing them from the absorbencies at 450 $m\mu$, where the nonchlorophyll absorption is represented by

$$D_{res,450} = D_{450} - .0089\ C_a - .054\ C_b - .0785\ C_c\ .$$

From the large chlorophyll *c* coefficient (this is within 5 $m\mu$ of its absorption maximum), it can be seen that errors in its estimation would result in inordinately large errors in $D_{res,450}$. The good checks (± 5%), which were found between carotenoid values calculated from absorbencies at this wave length and at 480 $m\mu$, afford verification of both chlorophyll *c* and carotenoid concentrations.

The chlorophyll *c* values shown in Fig. 3 may appear high (even considering the errors discussed above) for a pigment which so many workers in the field have disregarded as unimportant. A search has failed to reveal reports of other determinations of chlorophyll *c* in phytoplankton. However, Pace determined chlorophyll *a* and *b* in extracts of *Nitzschia Closterium* (mg/100 g dry weight) as follows:

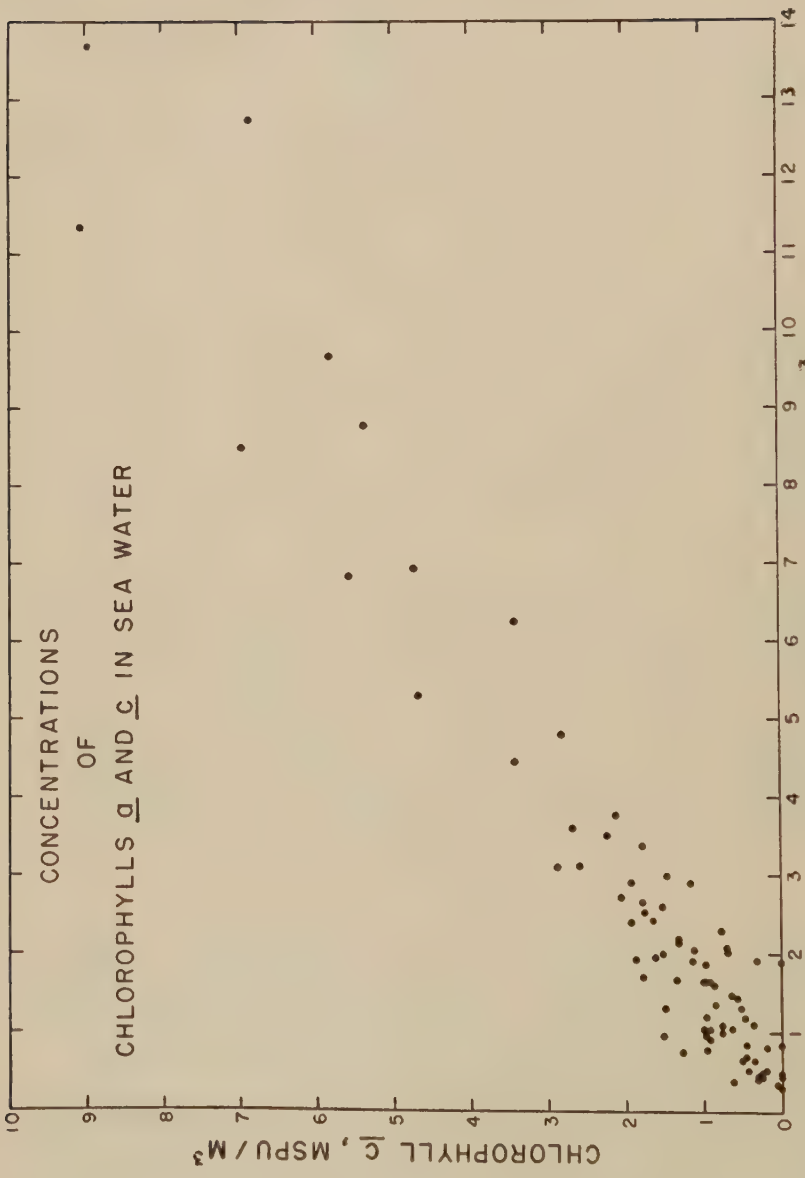


Figure 3. Chlorophyll *a* and *c* concentrations found in sea water samples.

| *a* | *b* |
|---|---|
| 2310 | + |
| 2000 | 95 |
| 1850 | 130 |
| 2530 | 240 |

If *N. Closterium* contains chlorophyll *c* instead of *b*, as is true of other diatoms (13, 18), then Pace's values (assuming chlorophyll *b*) should be recalculated. His determinations were based on a calibration curve prepared with a chlorophyll *b* standard, which would have a much greater absorbency in the region measured than would an equal concentration of chlorophyll *c*. This difference would be greater than the ratio of the spectral maxima, because both peaks are broad for their height, and since a filter photometer with a relatively wide transmission was used, the area *under* the absorption curve was involved. His filter would eliminate about half of the chlorophyll *c* absorption, but it includes most of the peak of the chlorophyll *b* used for the construction of the calibration curve. It is estimated that the values given by Pace for the second (nonchlorophyll *a*) chlorophyll component are too low, perhaps by a factor of 10 to 20. Therefore, Pace's small chlorophyll *b* values would represent rather large amounts of chlorophyll *c*.

Perhaps a more important factor in the apparent concentration of chlorophyll *c* is the method used to prepare the material from which the coefficients in Table II were determined. Strain and Manning (18) observed that at 630 m$\mu$ the characteristic absorption coefficient of chlorophyll *c* (in methanol solution) prepared by solvent partition is about 0.1 unit larger than that prepared by chromatographic absorption. This would make the specified absorption coefficient at this wave length about 25% greater than that of chromatographed material. If this is also true of acetone solutions, the specified adsorption coefficient of unchromatographed material should be, at 630 $m\mu$, 13.1 instead of 10.4 as shown in Table II, and the equations for computing the chlorophyll concentrations would be:

$$C_a \text{ (mg/L)} = 15.7\ D_{665} - 2.07\ D_{645} - 0.64\ D_{630}\ ;$$
$$C_b \text{ (mg/L)} = 25.1\ D_{645} - 4.75\ D_{665} - 8.02\ D_{630}\ ;$$
$$C_c \text{ (MSPU/L)} = 85.6\ D_{630} - 9.80\ D_{665} - 2.25\ D_{645}\ .$$

*Carotenoids.* Calculations of nonastacin carotenoid concentrations from independent measurements at 450 and 480 $m\mu$ gave good checks ($\pm$ 5%). Values calculated from absorbencies at 420 $m\mu$,

$$(D_{res,420} = D_{420} - .0707 \times C_a - .0268 \times C_b - .0373 \times C_c),$$

were found to be high because of invisible impurities, as expected.[7] Density readings at 510 $m\mu$ are generally low; when astacin-type carotenoids are less than 8–10% of the total pigments, the calculated concentrations are probably unreliable.

*Over-all Errors.* A series of analyses made on as nearly identical samples as could be prepared showed good reproducibility of results. The over-all errors would include errors in preparing identical samples, in the operation of the centrifuge, measuring of extractant, etc. They are shown in Table V; reproducibility of the same order has been achieved by students using the method in classroom and field work. Experience in using the method should afford increased reproducibility.

TABLE V. Instrumental and Other Errors Found in Over-all Analytical Procedure

| *Pigment and Concentration* | *Maximum Deviation* | *Expected Instrumental Error* | *Other Errors* |
|---|---|---|---|
| Chlorophyll *a* 1.0 mg/L | 14% | ±5% | 9% |
| Chlorophyll *c* .75 MSPU/L | 43% | Ca. ±30% | Ca. ±13% |
| Astacin-type Carotenoids 1.17 MSPU/L | 20% | ±5% | 15% |
| .40 MSPU/L | 10% | 10% | —— |
| Nonastacin-type Carotenoids 1.0 MSPU/L | 6% | 5% | 1% |

## SUMMARY

A semimicro spectrophotometric method is presented for the estimation of chlorophylls *a*, *b* and *c* as well as astacin and nonastacin type carotenoids in acetone extracts of plant and animal material. Developed specifically for use in estimating and characterizing plankton populations, the method is highly sensitive and practical for shipboard use. Methods of collecting, preparing and extracting plankton samples, spectrophotometric measurements, computation of results, and errors are discussed.

## REFERENCES CITED

1. Brown, F. A., Jr.
1934. The chemical nature of the pigments and the transformation responsible for color changes in Palaemonetes. Biol. Bull. Woods Hole, *67:* 365–380.

[7] This observation, and the frequently observed very high absorbencies in the spectral regions 320–400 $m\mu$, appears consistent with investigations by Lane (10) of a "plankton oil" extracted from zooplankton. The material Lane describes as a noncarotene provitamin A has a very high absorption maximum near 310 $m\mu$ and appreciable absorption at 400 and 450 $m\mu$, dropping to negligible values at 500 $m\mu$.

2. Cary, H. H. and A. O. Beckman
1941. A quartz photoelectric spectrophotometer. J. opt. Soc. Amer., *31:* 682.
3. Gibson, K. S. and M. M. Balcom
1947. Transmission measurements with the Beckman quartz spectrophotometer. J. Res. Nat. Bur. Stand., *38:* 601–616.
4. Graham, H. W.
1943. Chlorophyll-content of marine plankton. J. Mar. Res., *5:* 153–160.
5. Harvey, H. W.
1934. Measurement of phytoplankton population. J. Mar. biol. Ass. U. K., *19:* 761–773.
6. Kirk, P. L., R. S. Rosenfels and D. J. Hanahan
1947. Capillary absorption cells in spectrophotometry. Industr. Engng. Chem., Anal. Ed., *19:* 355–357.
7. Kozminski, Z.
1938. Amount and distribution of the chlorophyll in some lakes of northeastern Wisconsin. Trans. Wis. Acad. Sci., *31:* 411–438.
8. Krey, J.
1939. Die Bestimmung des chlorophylls in Meerwasser-Schöpfproben. J. Cons. int. Explor. Mer, *14:* 201–209.
9. Kuhn, R. and E. Lederer
1933. Über die Farbstoffe des Hummers (Astacus gammarus L.) und ihre Stannsubstanz, das Astacin. Ber. dtsch. chem. Ges., *66B:* 488–495.
10. Lane, C. E.
1950. A noncarotene provitamin A for fishes. Science, *111:* 471–472.
11. Pace, N. J.
1941. Pigments of the marine diatom Nitzschia closterium. J. biol. Chem., *140:* 483–489.
12. Redfield, A. C.
1930. The absorption spectra of some bloods and solutions containing hemocyanin. Biol. Bull. Woods Hole, *58:* 150–175.
13. Richards, F. A.
1952. The estimation and characterization of plankton populations by pigment analyses. I. The absorption spectra of some pigments occurring in diatoms, dinoflagellates, and brown algae. J. Mar. Res., *11* (2)*:* 147–155.
14. Riley, G. A.
1938. The measurement of phytoplankton. Int. Rev. Hydrobiol., *36:* 371.
15. Scripps Institution of Oceanography
1949. Marine Life Research Program, Progress Report for 1 Aug.–31 Oct., 1949.
16. Strain, H. H.
1938. Leaf xanthophylls. Carneg. Instn. Wash., Publ. No. 490.
17. Strain, H. H.
1949. Private communication.
18. Strain, H. H., and W. M. Manning
1942. Chlorofucine (chlorophyll *c*), a green pigment of diatoms and brown algae. J. biol. Chem., *144:* 625–636.

19. Strain, H. H., W. M. Manning and G. Hardin
1944. Xanthophylls and carotenes of diatoms, brown algae, dinoflagellates, and sea-anemones. Biol. Bull. Woods Hole, *86:* 169–191.
20. Tucker, A.
1949. Pigment extraction as a method of quantitative analysis of phytoplankton. Trans. Amer. micr. Soc., *68:* 21.
21. Zscheile, F. P., Jr., C. L. Comar and G. Mackinney
1942. Interlaboratory comparison of absorption spectra by the photoelectric spectrophotometric method.—Determinations on chlorophyll and Weigert's solution. Plant Physiol., *17:* 666–670.

# TITANIUM IN SEA WATER

By

JOHN V. GRIEL[1] AND REX J. ROBINSON

*Oceanographic and Chemical Laboratories*
*University of Washington, Seattle 5, Washington*

## ABSTRACT

Small amounts of titanium have been detected in sea water by a colorimetric procedure using a thymol reagent and also by a spectrographic method. Diatoms and sea muds were found to have larger amounts of titanium than sea water. Thus it would seem that titanium is concentrated by diatoms in their shell structures.

## INTRODUCTION

Silicon, an important constituent in the sea whose role is well established, is utilized by diatoms and various marine animals in the building of their shell structures. Titanium is very much like silicon chemically; thus it might be expected to be present in sea water as the titanate ion. Titanium is widespread in the earth's crust and ranks ninth in abundance, but information on the occurrence of titanium in the sea is very meager. Bardet, et al. (1938) reported the spectroscopic detection of titanium in the hydroxide precipitate from 60 l of sea water, and Webb and Fearon (1937) reported the presence of titanium in both land and sea organisms. To date there has been no confirmation of these findings.

In the present investigation an attempt has been made to explore, in a preliminary fashion, the titanium content of sea water. Various water samples, diatoms, and sea muds have been analyzed by a spectrophotometric method with thymol as the reagent. This method, reported by Griel and Robinson (1951), has greater sensitivity than the commonly used hydrogen peroxide method (Lenher and Crawford, 1913). A number of sea water samples have also been analyzed spectrographically for titanium.

## SPECTROPHOTOMETRIC INVESTIGATION

*Method of Analysis.* The method of analysis is essentially the same as that of Chuiko (1940) in which the titanium was concentrated by coprecipitation with aluminium hydroxide. Thirty mg of aluminium-ion as aluminium sulfate were added to 1 liter of filtered sea water; the pH was adjusted to 5.5–6.5. Regulation of the pH is essential, since aluminium hydroxide is known to coagulate at a pH of 4.1 or

[1] Present address: Centralia Junior College, Centralia, Washington.

greater and to begin dissolving at a pH of about 9. The mixture was allowed to stand for 12 hours at room temperature; aging on a steam plate made the precipitate easier to filter but it did not increase the recovery of titanium. Precipitation with magnesium hydroxide at pH 9 was also tried as a carrier for titanium in place of aluminium hydroxide. The results were perhaps as good but no better. The precipitate was filtered off by using Whatman paper No. 30, after which it was washed with distilled water and dissolved in about 50 ml of 10% sulfuric acid. The solution was evaporated to fumes of sulfur trioxide, cooled slightly, and then 0.25 ml of 30% hydrogen peroxide was added to remove color due to organic matter. The excess hydrogen peroxide was destroyed by fuming again for 5 minutes. After cooling, 0.25 ml of thymol reagent was added for each 8 ml of sulfuric acid solution. The optical density was obtained on a Beckman DU spectrophotometer at a wavelength of 440 mμ, using a 1 cm Corex cell and a 0.1 mm slit-width. The titanium concentration was obtained from a calibration chart in which concentration had been plotted against optical density.

*Reagents and Standard Solutions. Thymol.* A 1% solution of thymol was made by adding molten thymol slowly from a medicine dropper to ice-cold concentrated sulfuric acid that was stirred rapidly. *Standard Titanium Solutions.* 3.68 g of air-dried $K_2TiO(C_2O_4)_2.2H_2O$ were digested for 10 minutes with 100 ml of concentrated sulfuric acid and 8 g of ammonium sulfate. The resulting solution was diluted to 1 liter with concentrated sulfuric acid and standardized gravimetrically. The titanium was precipitated either with cupferron (Yoe and Sarver, 1941: 145) or ammonium hydroxide (Kolthoff and Sandell, 1943: 704) and ignited to $TiO_2$. This stock solution analyzed 10 μg-at Ti/ml of solution; a working standard solution containing 0.1 μg-at Ti/ml was prepared by dilution with concentrated sulfuric acid.

*Testing the Method.* To test the reliability of the method when applied to natural waters, analyses were made of various waters (shown in Table I) to which known amounts of titanium had been added. The recovery of titanium was satisfactory, particularly in the case of the natural sea water and distilled water media. The results in general were slightly low. It was felt, however, that the method possessed sufficient accuracy to furnish useful information, if titanium is present in sea water in appreciable amounts.

With this method the possibility of interference by fluoride in sea water was considered. Since slightly ionized complexes of the type $TiF_6''$ are known to be formed by titanium, and since appreciable amounts of fluorides occur in sea water (Thompson and Taylor, 1933),

TABLE I. Recovery of Titanium from Water Samples

| *Water Type* | *Titanium Content, μg-at Ti/L* | | |
|---|---|---|---|
| | *Added* | *Found* | *Deviation* |
| Distilled | 0.10 | 0.12 | +0.02 |
| | 0.15 | 0.13 | −0.02 |
| | 0.20 | 0.20 | 0.00 |
| | 0.40 | 0.30 | −0.10 |
| Artificial Sea Water | 0.20 | 0.14 | −0.06 |
| | 0.20 | 0.20 | 0.00 |
| S = 34.5 °/₀₀ | 0.30 | 0.20 | −0.10 |
| | 0.40 | 0.30 | −0.10 |
| Pacific Ocean | 0.10 | 0.07 | −0.03 |
| | 0.20 | 0.17 | −0.03 |
| Ocean City, Wash. | 0.20 | 0.23 | +0.03 |
| | 0.20 | 0.17 | −0.03 |
| Aug. 8, 1949 | 0.10 | 0.13 | +0.03 |
| S = 30.4 °/₀₀ | 0.20* | 0.17 | −0.03 |

* In addition to the titanium, 5 mg $NH_4F$ were added to 1 liter of the sea water.

there would seem to be a definite possibility that titanium might be held as the complex, in which case it would not be available for estimation by the present method. On the basis of the following evidence it was concluded that this is not the case. First, as shown in Table I, there was satisfactory estimation of titanium when known amounts were added to sea water samples. Second, when additional fluoride was added to sea water along with known amounts of titanium (Table I), satisfactory determination of titanium was still obtained. Third, no significant increase in titanium content was noted when a sea water sample (Table II) was fumed with concentrated sulfuric acid to destroy any possible titanifluoride complex and to expel HF before estimation of titanium. In this experiment, after fuming the sample with sulfuric acid, it was diluted to its original volume with distilled water, and the titanium content was then determined by the usual procedure.

*Analysis of Water Samples.* Seven surface samples from the Puget Sound area, plus one from the Pacific Ocean, were analyzed for titanium. Most samples showed only trace quantities, though one sample was found to have 0.02 μg-at Ti/l, which is the minimum concentration estimable by this method. Analysis of fresh water samples from three streams flowing into Puget Sound indicated the same minimum concentrations.

Analysis of the vertical series of samples from Point Jefferson, Puget Sound gave the results shown in Table II. These results con-

TABLE II. Titanium Content of Puget Sound Water at Various Depths

Location: Point Jefferson, Lat. 47° 44′ 30″ N, Log. 122° 25′ 30″ W

| *Date* | *Depth* | *Salinity* ‰ | *Titanium Content* μg-at *Ti/L* |
|---|---|---|---|
| June 14, 1951 | S | 27.5 | 0.04 |
| | 50 | 29.7 | Tr |
| | 100 | 29.9 | Tr |
| | 150 | 30.1 | 0.02 |
| | 200 | 30.1 | 0.02 |
| | 275 | 30.2 | 0.04 |
| Nov. 8, 1951 | S | 30.1 | Tr |
| | 50 | 30.7 | 0.02 |
| | 150 | 30.8 | Tr |
| | 250 | 30.9 | 0.02 |
| | 270 | 30.9 | Tr |
| Dec. 27, 1951 | S | 29.4 | 0.04 |
| | 100 | 30.1 | 0.02 |
| | 200 | 30.2 | 0.02 |
| | Composite | | 0.04 |
| | S* | 29.4 | 0.04 |

* Water sample fumed with $H_2SO_4$ to destroy any titanium fluoride complex.

firm previous results that the titanium content is in the neighborhood of the minimum sensitivity of the method. The data in Table II also indicate that there is no significant increase in the titanium content with depth.

*Analysis of Diatoms and Sea Muds.* From previous results on the analysis of sea water, it appears that titanium, while present in sea water, is found in amounts that are barely detectable by the present method of analysis. Further evidence for the presence of titanium in sea water was sought in the analysis of diatom and sea-bottom mud samples to ascertain whether or not titanium is utilized and concentrated by diatoms in their siliceous structures.

The diatom samples, taken with a No. 20 silk bolting cloth plankton net, were washed with distilled water to remove sea salts and then dried at 95°C. The mud samples, taken with a bottom sampler, were also dried at 95°C.

A 0.3 g sample was weighed into a platinum crucible and the ash content was determined. The ash was mixed with 1.5 g of anhydrous sodium carbonate and fused. The product was leached with water and filtered, and the residue was dissolved in 10% sulfuric acid. The sulfuric acid solution was evaporated to fumes of sulfur trioxide, diluted to three times its volume with water, cooled and filtered; the

filtrate was again evaporated to fumes of sulfur trioxide. The concentrated sulfuric acid was cooled, thymol indicator was added, and the color was measured in the spectrophotometer. Some of the samples gave a color to the sulfuric acid, so portions without indicator were used in the reference cell. Results are shown in Table III. Too few samples were analyzed to attach any significance to the variation in the results obtained; however, it is clear that titanium is present in all samples in appreciable amounts.

TABLE III. Titanium Content of Diatoms and Sea Muds

| *Location* | *Date* | *% Ash* | *% Titanium* | |
|---|---|---|---|---|
| | | | *On Dried Sample* | *On Ash* |
| | Diatoms | | | |
| Strait of Georgia | | | | |
| Dodd Narrows, B. C. | April 30, 1930 | 43 | 0.052 | 0.12 |
| San Juan Channel | | | | |
| Friday Harbor, Wash. | Aug. 19, 1937 | 58 | 0.048 | 0.083 |
| East Sound | | | | |
| Orcas Island, Wash. | Aug. 16, 1937 | 72 | 0.0021 | 0.0028 |
| Lake Washington | | | | |
| Seattle, Wash. | April 22, 1935 | 69 | 0.0036 | 0.0052 |
| | Sea Mud | | | |
| East Sound | | | | |
| Orcas Island, Wash. | Aug. 10, 1937 | 86 | 0.20 | 0.23 |
| Bering Strait | Aug. 1938 | 93 | 0.21 | 0.23 |
| Lat. 65° 22′ N. | | | | |
| Long. 165° 17′ W. | | | | |

## SPECTROGRAPHIC ANALYSIS OF SEA WATER

With the titanium concentration in sea water at the threshold value of the colorimetric method of analysis, confirmation of its presence in sea water was sought by spectrographic analysis. Mr. Boyd C. Mills made the analyses on a grating spectrograph at the College of Puget Sound, Tacoma, Washington. This instrument had a 3.5 m Perkin-Elmer grating in a modified Rowland mount. The dispersion was 3.58 Å/mm. The aluminium hydroxide coagulants from liter samples of sea water were air-dried and excited in a carbon arc. The electrodes were ¼″ carbon rods; a current of 14 amperes was passed through a 1 cm gap.

Spectrographic analyses were made of: four samples collected at Point Jefferson on December 27, 1951 (Table II); a surface sample collected at Hood Canal on December 19, 1951; a distilled water sample

containing 0.04 μg-at Ti/l; and a blank on the reagents. Positive titanium lines in the 3300 Å region, with the 3349 Å line being most prominent, were obtained for the surface samples from Point Jefferson and Hood Canal and for the distilled water containing 0.04 μg-at Ti/l; no titanium lines were obtained for the other samples. It is probable that titanium could have been detected spectrographically in all samples if it had been concentrated from larger volumes of sea water, as Bardet, et al. (1938) had done in their work. It should be noted also that these same sea water samples were analyzed colorimetrically for titanium and that minimum quantities were found (Table II). The authors believe that the spectrophotometric method with thymol is somewhat more sensitive than the spectrographic method.

## DISCUSSION

It would seem that titanium, though present in sea water samples, is found in extremely small concentrations. It has been detected both spectrographically and spectrophotometrically in certain sea water samples. Apparently it occurs to the extent of about 0.02 μg-at Ti/l, which is about the threshold value for the colorimetric thymol method used. The fact that titanium was found in considerable amounts in diatoms and sea-bottom mud samples substantiates the conclusion that titanium is present in sea water. An exact determination of the titanium content of sea water must await the development of a more sensitive method of estimation.

The finding of 0.0021 to 0.032% Ti in diatoms is only about 1/20 of the 0.05 to 1% range reported by Webb and Fearon (1937) for living organisms in general. Possibly this is due in part to the fact that diatoms grow in a medium low in titanium content, whereas land plants are able to extract titanium from the soil where it is present to the extent of about 0.62%.

### Literature Cited

Bardet, J., A. Tchakirian and R. Lagrange
1938. Determination of traces of titanium in natural waters. C. R. Acad. Sci. Paris, *206:* 450–452.

Chuiko, V. T.
1940. Spectrographic search for traces of elements in sea water. Chem. Abstr., *34:* 1783.

Griel, J. V. and R. J. Robinson
1951. The spectrophotometric determination of titanium with thymol. Anal. Chem., *23:* 1871–1873.

Kolthoff, I. M. and E. B. Sandell
1943. Textbook of Quantitative Inorganic Analysis. Macmillan Company, New York. 794 pp.

Lenher, V. and W. G. Crawford
1913. A new colorimetric method for titanium. J. Amer. chem. Soc., *35:* 138–145.
Thompson, T. G. and H. J. Taylor
1933. Determination and occurrence of fluorides in sea water. Industr. Engng. Chem., Anal. Ed., *5:* 87–89.
Webb, D. A. and W. R. Fearon
1937. Studies on the ultimate composition of biological material. I. Aims, scope and methods. Sci. Proc. R. Dublin Soc., N. S. *21:* 487–504.
Yoe, J. H. and L. A. Sarver
1941. Organic Chemical Reagents. John Wiley and Sons, New York. 339 pp.

# STUDIES ON THE PRODUCTION OF UNDERWATER SOUND BY NORTH ATLANTIC COASTAL FISHES[1]

By

MARIE POLAND FISH
*Narragansett Marine Laboratory*

ALTON S. KELSEY, JR.
*Brown University*

WILLIAM H. MOWBRAY
*Narragansett Marine Laboratory*

## ABSTRACT

Previous studies suggest that at least 42 families of Pacific Ocean fishes are potential sources of underwater sound. The present investigation has undertaken to ascertain experimentally which North Atlantic coastal species fit into that category and what stimuli are involved in sound production among fishes. Apparatus, test and analysis procedures are described. Recorded for 26 species are "biological" sound, the mechanism responsible for sound production, the frequency range, the principal frequency components, and a description of each sound. Relationship is noted between origin of sound and its frequency characteristics. The majority of species tested have principal frequencies between 75 and 300 cps; none exhibited sounds lower than 20 cps, and with three exceptions none produced sounds higher than 1600; stridulatory sounds of triggerfish, filefish, and burrfish reached the 2400–4800 cps octave. With the available filter system, nothing could be measured faithfully above that band. Noise of "mechanical" origin was recorded for 22 additional species. No sound was observed during routine testing of six species.

## PREVIOUS INVESTIGATIONS

Widespread use of underwater acoustical systems during World War II made exigent a knowledge of ambient noise conditions. Early background measurements indicated that in the absence of extraneous noises (as from shipping, shore activity, and animal life) a magnitude of one dyne/cm$^2$ in an octave band would seldom be exceeded (8), whereas biological sources might be responsible for sustained noise levels of 200 to 300 dynes/cm$^2$ (6).

So little was understood of the noisemaking propensities of marine animals, however, that "a list of all known (worldwide) forms of marine life producing subsurface sound," prepared by the United

[1] Contribution No. 1 from the Narragansett Marine Laboratory of the University of Rhode Island. This paper is based on research conducted under contract with the Office of Naval Research.

States National Museum for the Navy in 1942, included only 14 families of fishes and 17 families of crustaceans. Collected data on their sound production were fragmentary, often mere hearsay, and they seldom included more than a few descriptive terms like "loud grunt," "hoarse croak," or "nasal whine." No information was available on the actual magnitude or frequency spectra of the various sounds.

Accordingly, investigations were initiated in such areas as Chesapeake Bay, where croaker interference at times masked the propeller sounds of ships, and San Diego, where observations as early as 1933 had spotlighted a crackling noise of great magnitude, identified (5) in late 1942 as snapping shrimps (*Crangon* and *Synalpheus*). Observations on noisemaking crustaceans continued throughout the war. Monitoring and disc recording were undertaken on the southeastern and southwestern coasts of the United States and in the vicinity of Hawaii, Ellice Islands, Noumea, Guadalcanal, and the Russell Islands. Also, during this period, six species (representing five families) of Virginia coastal fishes (9) and members of five families in captivity at the Shedd Aquarium (7) were isolated for sound recording and analysis. The only other experimental work of this type was done by Dr. Yoshio Hiyama in Japanese waters between 1944 and 1945 (1).

In 1946 the senior author undertook a Navy assignment to "assemble, analyze, and where possible correlate with environmental factors, available information from the central and western Pacific" on underwater sound of biological origin. The resulting reports (3, 4) added 31 families of fishes to the existing list of soundmakers in that area, bringing the total to 42. Since most of these families are represented by many species, it became evident that the potential sonic species might number thousands. For each known or suspected sonic family, available data were presented on geographical, seasonal and vertical distribution, size of individuals, abundance, and especially on the type of sound mechanism involved and a description of the sound produced.

## PRESENT OBJECTIVE

Previous study (see REFERENCES) had thus indicated that noisemaking is common among many types of marine animals. It had shown which species are potential sources of underwater sound, what their characteristic sounds are, how produced, and when and where they may be expected. However, no attention had been given to the underlying causes of this ability. Thus the present investigation attempts to determine primarily the biological significance of soundmaking among fishes. From the physical viewpoint, the problems

emphasized are: 1) the sound intensity possible from an individual fish; 2) the frequency spectrum of sound made by each species; 3) the duration and repetition rate of the sound; 4) the maximum distance at which it can be detected.

## APPARATUS

Laboratory and vessel facilities were made available by the Narragansett Marine Laboratory, headquarters for the Project. Its location directly on Narragansett Bay, with no surf or industrial activity along shore and almost no ship traffic, provided an ideal low background level. A large wire enclosure and numerous live cars constructed in the Bay acted as storage space and test areas where specimens could be maintained under more normal conditions than those of indoor aquaria. Bay hydrophones were connected with recording instruments in the main laboratory, an arrangement which made possible protracted monitoring within a distance of 540 feet. Monitored also by hydrophone were many large glass aquaria inside the building as well as a concrete floor tank (19 x 3 x 2 feet), all with running seawater.

Marine sounds were recorded with a modified Naval Ordnance Laboratory Mk2 acoustic system. Type 1-A (Q4) quartz crystal hydrophones were used with the permanently installed equipment. These hydrophones have no significant temperature coefficient; they have a smooth, fairly flat frequency response from 10 to 5,000 cps and a rising characteristic from 5,000 to 10,000 cps. Sounds picked up by hydrophone were fed into an analyzer unit consisting of an audio amplifier with flat response from 40 to 20,000 cps, low and high pass filters, and power supply. The filter output was recorded by Esterline Angus Graphic Ammeters (EA) which indicated the root-mean-square pressure in the frequency bands below and above 500 cps. The response of the low pass EA is flat from 10 to 500 cps, while the high pass EA is flat from 500 to 30,000 cps.

During the earlier experiments, the putput of the audio amplifier was applied directly to a Presto 88A3S recording amplifier and Presto 6-N recording turntable, which made permanent disc recordings at 78 rpm. For playback, a Brush PL-20 pickup was used. Assembled thus, the response of the over-all recording system was from 20 to 5,000 cps, being flat within 4 db from 30 to 1,500 cps.

Later, a Webster Electric Model 111 tape recorder replaced the Presto equipment for direct recording. The tape recorder had not only the advantage of better frequency response, being $\pm$ 3 db from 35 to 7,500 cps, but it could be run continuously for long periods at

low expense and the results could be edited later to yield a short recording of selected sounds.

In addition to this fixed apparatus, a portable outfit was assembled for use in the field. This consisted of a Navy JO Underwater Sound Receiving Equipment set and either a converted office type disc recorder (Gray Audograph Electronic Soundwriter) or the tape recorder (Webster Ekotape).

For permanent filing, all tapes made in the Laboratory, as well as field recordings, were transcribed to Presto discs.

## ANALYSIS PROCEDURE

1. With Harmonic Wave Analyzer (Hewlett Packard, Model 300A).

Frequency spectra of the sounds were obtained by applying the output of the disc recordings directly to this instrument. The meter element in the analyzer was replaced by an Esterline-Angus Graphic Ammeter to obtain permanent records. A half band width of 30 cycles was used for each measurement; that is, the selectivity of the analyzer was such that voltages 30 cps off the measured frequency were attenuated 40 db. Readings were taken at intervals of 25 cps throughout the entire audible frequency spectrum, each sound being replayed into the analyzer for measurement at each frequency. Deflections obtained on the EA are proportional to the rms sound pressure in a narrow band centered at the measured frequency. These points were plotted for typical and extreme individual cases, and for average sets of readings for selected fish of each species.

The assumption is made here that the fish sounds have a uniform energy distribution over the band width of the analyzer. In such a case, the ordinate of the curve at a given frequency would be proportional to the rms pressure in a band one cycle wide centered at that frequency. The area under each curve would then be proportional to the over-all rms sound pressure.

To obtain the proportionality factor, the area under each curve was measured by a planimeter. The factor $K$ was then immediately given by the relation $P = \int_0^\infty p_f df = \int_0^\infty KD\, df$, where $P$ = over-all rms pressure measured, $p_f$ = pressure per cycle, $f$ = frequency, and $D$ = $EA$ deflection.

Typical curves were plotted, giving pressure per cycle vs. frequency. Since the area under the corrected curve represents the total sound pressure, the pressure in any frequency interval could be calculated by obtaining the area under the curve in that interval.

2. With Octave Filter (Western Electric Type RA-363).

The sounds to be analyzed were played back through this filter set, and the a-c voltage output was measured by an Esterline-Angus recording d-c milliameter with full-wave bridge rectifier.

Recordings were first played with the octave filter switches in the over-all position, allowing all frequencies to pass equally; the a-c voltage measured was proportional to the over-all sound pressure. The recordings were then played once for each of the 14 filter sections, each of which passed frequencies within a one octave band and produced voltages proportional to the sound pressure in the chosen octave.

The actual over-all sound pressure was determined by direct measurement of the system gain from the hydrophone to the filter output with reference to the hydrophone calibration curves. The combination of these data furnished the value of sound pressure corresponding to the measured output voltage.

The sound pressure in each octave was obtained by applying a proportionality factor to the output voltage measured in that range. This factor was determined by plotting the voltages against frequency and by mechanically integrating the curve to find the area subtended. Since the area is directly related to the over-all pressure and can be expressed in terms of pressure per octave, frequency, and a constant, these quantities can be equated and the expression can be solved for the constant.

## TEST PROCEDURE

Experimental material was obtained regularly from commercial traps in the vicinity of Pt. Judith and outer Narragansett Bay. Members of the staff who accompanied fishermen on their trap-hauling cruises, transported specimens as quickly as possible to the Laboratory, where they were tested immediately and again later after adjustment to captivity. Occasionally portable listening and recording equipment was taken out in the fishing boats in order to detect new noisemakers and to study the effect of crowding upon known sonic species. In some cases (e. g., *Opsanus tau*) recordings were made in the field in a natural environment, after which the captured noisemakers were delivered to the Laboratory for further observation.

Hydrophones permanently installed in the various test areas were valuable in picking up the general "chorus" of newly added specimens. Intensity levels were measured over 24-hour periods to investigate the diurnal cycle of sonic activity for mixed populations as well as for individual species.

There is always urgency in working with live specimens, and long periods of observation in captivity, which often decrease or even

prevent normal sonic behavior, may be impossible. Thus, as laboratory study progressed, it became evident that some quick means of sorting the potential soundmakers from the silent ones must be found. Accordingly, a simple electric stimulator, consisting of a conventional glass and wooden aquarium (lined with insulating layers of rubberized hair to prevent knocking of the fish against bottom and sides), screen electrodes, and a variable autotransformer, was rigged. Currents up to three amperes were passed into the water. To date every species which has had the necessary soundmaking apparatus has responded to this electric shock by emitting sound. Whenever such capability was shown, the fish was earmarked for continued study.

Each species was subjected to a routine set of conditions to determine, if possible, what stimuli induce sound production. In brief, reactions to the following situations were studied:

1) When the fish was introduced into new surroundings.
2) After it became accustomed to the tank. (According to the species, this period varied from 10 minutes to several days. In each case, specimens were undisturbed until they seemed to be swimming and behaving normally.)
3) When food was offered.
4) When other fishes were added to the tank.
   a. One or more of the same species.
   b. One or more of a different species known to live peaceably in the same natural habitat.
   c. One or more of a known or suspected enemy species.
   d. Enough other specimens to create crowding.
5) When subjected to artificial stimulation, which varied from the lightest touch to extreme duress. (Sometimes sudden movement of the experimenter outside a glass tank was sufficient to provoke sound, whereas in other cases aggravation of a closely imprisoned specimen was necessary to bring about the same reaction.)
6) When electrically stimulated.

## GENERAL RESULTS

Sound-recording apparatus was in operation between the following dates: 22 July to 1 September 1949; 22 to 25 March, and 19 June to 6 September 1950; 26 June to 11 September 1951. Sounds of biological origin were successfully recorded for 26 species, as indicated in Table I. The term "biological," used here to indicate sound, often purposeful, which originates in the body of the fish itself by action of either internal or external organs, is differentiated from "mechanical" noise, always accidental, which results from swimming, collision, feeding, or other activity of the fish.

TABLE I. Fishes Which Produced Sound of Apparent Biological Origin. In the Species Marked by an Asterisk (*), This Source Is Questionable

| Species | Number Tested |
|---|---|
| Common eel (*Anguilla rostrata*) | 10 |
| Thread herring (*Opisthonema oglinum*) | 5 |
| Sea horse (*Hippocampus hudsonius*) | 1 |
| Hardtail (*Caranx crysos*) | 29 |
| Rudderfish (*Seriola zonata*) | 13 |
| Butterfish (*Poronotus triacanthus*)* | 3 |
| Striped bass (*Roccus lineatus*) | 8 |
| Black sea bass (*Centropristes striatus*) | 22 |
| Scup (*Stenotomus chrysops*) | 75 |
| Squeteague (*Cynoscion regalis*) | 10 |
| Kingfish (*Menticirrhus saxatilis*) | 5 |
| Cunner (*Tautogolabrus adspersus*) | 7 |
| Tautog (*Tautoga onitis*) | 7 |
| Spadefish (*Chaetodipterus faber*) | 1 |
| Common triggerfish (*Balistes carolinensis*) | 1 |
| Foolfish (*Monacanthus hispidus*) | 6 |
| Orange filefish (*Alutera schoepfii*) | 12 |
| Puffer (*Spheroides maculatus*) | 45 |
| Burrfish (*Chilomycterus schoepfii*) | 21 |
| Giant sunfish (*Mola mola*) | 2 |
| Longhorn sculpin (*Myoxocephalus octodecimspinosus*) | 31 |
| Common searobin (*Prionotus carolinus*) | 55 |
| Redwinged searobin (*P. evolans*) | 69 |
| Toadfish (*Opsanus tau*) | 45 |
| Silver hake (*Merluccius bilinearis*) | 1 |
| Sand flounder (*Lophopsetta aquosa*)* | 3 |

The 22 species listed in Table II were responsible for noise of varying intensities attributable to accidental sources rather than to sound-making mechanisms within the body of the fish. In the case of large specimens, such as rays and scombroids, mechanical disturbance of the water caused by violent activity was audible, but it was easily distinguished from the air bladder knocking heard when striped bass, squeteague and others were agitated. Likewise, the frenzied rotation of a group of clupeoids could be detected by the hydrophone, but such swishing was quite unlike the pharyngeal rasping which hardtails produced under similar conditions. Sounds from collision against the tank or disturbance of gravelly bottom by swimming flatfish were commonly heard. Very small sounds made by sticklebacks might have been due to stridulation, but the evidence is not conclusive. Similarly with the scombroids and pilotfish, a suggestion of animal noise occurred, but, lacking verification, the record remains question-

able. Specimens were sometimes injured or too exhausted by capture and transportation to react normally, and some died before they were sufficiently adapted to captivity for the full routine of experiments. In certain forms, therefore, the fact that biological sound has not yet been noted does not mean, necessarily, that the species is silent.

TABLE II. Fishes Which Produced Mechanical Noise as a Result of Normal or Induced Activity within the Test Area. In Those Cases Where Biological Sound May Have Occurred as Well, though Records Are Not Conclusive, the Species Is Marked by an Asterisk (*). None Were Subjected to Electric Stimulation

| Species | Number Tested |
|---|---|
| Northern stingray (*Dasyatis centroura*) | 2 |
| Butterfly ray (*Gymnura micrura*) | 1 |
| Eagle ray (*Myliobatus freminvillii*) | 1 |
| Conger eel (*Conger conger*) | 1 |
| Bonefish (*Albula vulpes*) | 1 |
| Sea Herring (*Clupea harengus*) | 15 |
| Hickory Shad (*Pomolobus mediocris*) | 2 |
| Alewife (*P. pseudoharengus*) | 12 |
| Blueback (*P. aestivalis*) | 1 |
| Menhaden (*Brevoortia tyrannus*) | 5 |
| 2-spined stickleback (*Gasterosteus aculeatus*)* | 10 |
| 4-spined stickleback (*Apeltes quadracus*)* | 3 |
| Common mackerel (*Scomber scombrus*)* | 7 |
| Frigate mackerel (*Auxis thazard*)* | 14 |
| Spanish mackerel (*Scomberomorus maculatus*)* | 4 |
| Cero mackerel (*Scomberomorus regalis*)* | 1 |
| Pilotfish (*Naucrates ductor*)* | 7 |
| Barrelfish (*Palinurichthys perciformis*) | 13 |
| Shark sucker (*Echeneis naucrates*) | 12 |
| Sand dab (*Hippoglossoides platessoides*) | 5 |
| Northern fluke (*Paralichthys dentatus*) | 23 |
| Winter flounder (*Pseudopleuronectes americanus*) | 6 |

TABLE III. Fishes Which Produced No Measured Sound, either of Biological or Mechanical Origin, During Routine Testing. None Were Subjected to Electrical Stimulation

| Species | Number Tested |
|---|---|
| Pipefish (*Syngnathus fuscus*) | 4 |
| Silverside (*Menidia menidia notata*) | 50 |
| Waxen silverside (*M. beryllina*) | 3 |
| Mullet (*Mugil cephalus*) | 2 |
| Sand launce (*Ammodytes americanus*) | 5 |
| Mackerel scad (*Decapterus macarellus*) | 1 |

TABLE IV. Data on Species Which Produced Sufficient Biological Sound for Analysis and Study

| *Species* | *Origin of Sounds* | *Description of Sounds* | *Frequency Range (cps)* | *Principal Frequency (cps)* |
|---|---|---|---|---|
| Family Anguillidae | | | | |
| Common Eel<br>*Anguilla rostrata* | Air bladder.<br>Escape of air bladder gas through pneumatic duct and branchial aperture. | Dull thud; thump.<br>Clucking; bubbling "put-put." | <50–1200 | (75–150) or (150–300)* |
| Family Clupeidae | | | | |
| Thread Herring<br>*Opisthonema oglinum* | Air bladder. | Hollow knock of very low intensity. | <50–1200 | (75–150) or (150–300)* |
| Family Hippocampidae | | | | |
| Sea Horse<br>*Hippocampus hudsonius* | Stridulation of posterior margin of skull and coronet. | Loud click similar to snap of finger against thumb; single or 2–5 in series at c. 1 sec. intervals. | <50–1600 | (400–800) |
| Family Carangidae | | | | |
| Hardtail<br>*Caranx crysos* | Pharyngeal teeth and air bladder. | Low thumps with electric shock. | 20–850 | (150–300) and (75–150)† |
| | | Very loud rasps, as with a rough file, when netted. | 325–1100 | 500 |
| Family Seriolidae | | | | |
| Rudderfish<br>*Seriola zonata* | Pharyngeal teeth and air bladder. | Sharp knock. | <50–1200 | (150–300) |
| Family Serranidae | | | | |
| Striped Bass<br>*Roccus lineatus* | Air bladder region, possibly "drummed" by operculum. | Low "unk" with tom-tom quality, single or in bursts of 3 or 4. | <50–1200 | (75–150) or (150–300)* |
| Black Sea Bass<br>*Centropristes striatus* | Air bladder. | Single small grunts. | <50–1200 | 225 |
| Family Sparidae | | | | |
| Scup<br>*Stenotomus chrysops* | Air bladder.<br>Stridulation of upper and lower incisors.<br>Extrinsic feeding. | Single guttural thumps.<br>Scrape and rasp.<br>Loud crunching. | 20–1400<br>350–1150<br>350–700 | 200–225<br>700<br>350 |

TABLE IV—(*Continued*)

| *Species* | *Origin of Sounds* | *Description of Sounds* | *Frequency Range (cps)* | *Principal Frequency (cps)* |
|---|---|---|---|---|
| Family Sciaenidae | | | | |
| Squeteague<br>*Cynoscion regalis* | Air bladder and associated muscles. | Croaks; beats with deep, drum-like quality. | 20–1200 | (50–100) or 250* |
| | Pharyngeal teeth. | Clucks somewhat similar to above, but in bursts of higher pitch. | 100–550 | 325 |
| Kingfish<br>*Menticirrhus saxatilis* | Pharyngeal teeth. | Short rasp. | 175–1475 | 250 and 350† |
| Family Labridae | | | | |
| Cunner<br>*Tautogolabrus adspersus* | Air bladder. | Single low thump. | <50–800 | (150–300) |
| Tautog<br>*Tautoga onitis* | Air bladder. | Single deep thump similar to above but stronger. | <50–800 | (75–150) or 200–225* |
| Family Ephippidae | | | | |
| Spadefish<br>*Chaetodipterus faber* | Air bladder and intrinsic muscles. | Low-pitched, drum-like beats, single or as a short burst. | <50–800 | (75–150) |
| Family Balistidae | | | | |
| Common Triggerfish<br>*Balistes carolinensis* | Pharyngeal teeth and air bladder. | Metallic scratching and spitting. | <50–4800 | (2400–4800) |
| | Stridulation in pectoral arch. | Hissing and heavy humming. | | |
| | Pectoral flarays drumming against taut membrane above air bladder. | Humming | | |
| | First dorsal fin. | Clicking. | | |
| Family Monacanthidae | | | | |
| Foolfish<br>*Monacanthus hispidus* | Specially adapted incisor teeth and air bladder. | Sharp, whining swish-swish. | <50–800 | (150–300) |
| | First dorsal spine. | Low click. | | |
| | Extrinsic feeding. | Considerable "chirp." | | |

TABLE IV—(*Continued*)

| *Species* | *Origin of Sounds* | *Description of Sounds* | *Frequency Range (cps)* | *Principal Frequency (cps)* |
|---|---|---|---|---|
| Family Monacanthidae (cont.) | | | | |
| ORANGE FILEFISH<br>*Alutera schoepfii* | Specially adapted incisor teeth and air bladder.<br>Feeding on soft food. | Toothy scratching; wheezing; "ha-chu."<br>Very loud scratching similar to above. | <50–4800 | 700 |
| Family Tetraodontidae<br>PUFFER<br>*Spheroides maculatus* | Grating of incisor teeth. | Long burst of "erk-erk"s; nasal rasp, double like stroke and recovery of saw. | 200–1600 | 300<br>and<br>800 |
| Family Diodontidae<br>BURRFISH<br>*Chilomycterus schoepfii* | Grating of incisor teeth. | High-pitched whining scrape like puffer, but "erk" single, c. ½ sec. duration. | <50–4800 | (150–300)<br>or<br>(2400–4800)* |
| Family Cottidae<br>LONGHORN SCULPIN<br>*Myoxocephalus octodecim-spinosus* | Stridulation in pectoral arch. | Low drumming, like a generator hum. | 20–650 | 50–70 |
| Family Triglidae<br>COMMON SEBOBIN<br>*Prionotus carolinus* | Air bladder and intrinsic muscles. | Single squawk or series of rapid clucks, always with vibrant quality. | 40–1400 | 300<br>150<br>450<br>600† |
| REDWINGED SEAROBIN<br>*P. evolans* | Air bladder and intrinsic muscles. | Single grunt or burst of croaks, less staccato than above. | 40–800 | 200<br>100<br>300† |
| Family Batrachoididae<br>TOADFISH<br>*Opsansus tau* | Air bladder and intrinsic muscles. | Growl or coarse grunt, single, of c. ½ sec. duration. | 80–650 | 100<br>200<br>300<br>400† |
| | | Very loud, intermittent blast like a boat whistle; "boop"; c. ½ sec. duration. | 220–1000 | 330<br>625<br>950† |
| Family Gadidae<br>SILVER HAKE<br>*Merluccius bilinearis* | Air bladder. | Low knock or rap. | 80–875 | 300 |

* Indicates variation among specimens.

† Indicates more than one principal frequency in an individual sound (listed in order of magnitude).

## GENERAL CONCLUSIONS

The mechanism producing sound obviously determines its frequency range, and the principal frequencies involved may be a key to the origin of each sound. Thus species which use the air bladder for noisemaking exhibit a wide spread of frequency, extending very often from below 50 to 1,200 or 1,400 cps. Most of the sound energy, however, is concentrated toward the low end of the spectrum, with principal frequencies in the 75–150 cps octave band. Examples are the spadefish, squeteague, striped bass, tautog, common eel, thread herring, and toadfish (growl).

The size of the air bladder is roughly proportional to the over-all length of the fish. Thus, since the frequency increases as the size of the air bladder decreases, we may expect smaller specimens to exhibit higher frequency characteristics. Accordingly smaller fishes of the species listed above, as well as small sea bass, scup, cunner, common and redwinged searobins, have principal frequencies in the 150–300 cps octave band. Except for variations according to size, the frequency characteristics of most species are quite constant, and each individual maintains an almost identical sound pattern under repeated stimulation.

Often the curves are strikingly harmonic in nature. In the case of the common searobin, present records show a pronounced maximum at 300, with lesser signals at 150, 225, 450, and 600 cps. Harmonic content is apparent also in curves for toadfish grunts where the maximum is 100, with decreasingly strong components at 200, 300, 400, 500, and 600 cps. A second sound typical of toadfish during the spawning season, also produced by means of the air bladder and its intrinsic muscles, has a frequency range of 220 to 1,000 cps. Here there is a strong fundamental at about 330 in a very narrow band, with a second peak about one-ninth as high at 625, and a third peak at 950 cps one-twentieth as large as the fundamental.

Typically the air bladder sound has a hollow tom-tomish quality, which has been described as similar to the noise of a wet finger drawn across the surface of an inflated balloon. The words "thump," "knock," "thud," "grunt," "groan," "growl," "cluck," "bark," and "boop," used to define this type of sound, evidence its drum-like, vibrant, and often guttural property.

Where the sound is produced by stridulation, that is, by the scraping of some body part against another, the spread of frequency may be extremely wide, and the maximum energy is usually located higher in the spectrum than is the case for sounds originating in the air bladder. Typical are the seahorse clicks, where the principal frequency is in the

400–800 cps octave band, and the burrfish rasps, which reach the 2,400–4,800 cps band. In all cases of stridulatory origin, the sound is quite easily identified by its rasping, scratching, or whining characteristic.

In certain fishes more than one mechanism may function for sound production, but the frequency characteristics as well as the observed tonal qualities usually serve to differentiate between the various sounds. The hardtail, for instance, is capable of very noisy rasping when agitated, with its maximum at 500 cps. The loudness of the burst indicates that the stridulation of the upper and lower pharyngeal teeth may be amplified by air bladder reinforcement. When the same specimen is subjected to electrical stimulation, a typical air bladder thump concentrated in the 75–150 cps and 150–300 cps octave bands predominates. The knock produced by electrically stimulating the rudderfish also has the general frequency characteristics of an air bladder sound, but a sharp rather than a dull quality to this sound suggests pharyngeal teeth participation.

The scup is a notable example of a fish with the ability to produce more than one sound. Under certain conditions, single guttural thumps, spread between 20 and 1,400 cps with principal frequencies in the low 200's, indicate air bladder origin, whereas shrill rasping, limited to a narrower band between 350 and 1,150 cps with a maximum at 700, accompanied the observed scraping of upper and lower incisors.

Also the squeteague uses its air bladder for single, deep, drum-like croaks spread between 20 and 1,200 cps with a usual maximum in the 50–100 cps band; under different stimulation, by grating the pharyngeal teeth it emits bursts of higher-pitched clucking in a narrow frequency range of 100 to 550, the maximum peak being at 325 cps.

No fish of the North Atlantic coastal waters auditioned to date has exhibited a sound lower than 20 cps nor higher than the 2,400–4,800 cps octave band. The large majority of species has principal frequencies between 75 and 300 cps. The possibility of frequencies beyond the range indicated by present apparatus is to be explored.

A detailed analysis of sonic species, especially with reference to frequency pattern, amplitude and periodicity of the recorded sounds, mechanisms and stimuli necessary for sound production, and the general significance of each fish as a maker of underwater sound, will be presented in a separate paper (4).

## ACKNOWLEDGMENTS

We are greatly indebted to the Naval Ordnance Laboratory for loan of much equipment, to Professors R. Bruce Lindsay and Robert T. Beyer for advice on the analysis of the 1949 physical data, and to

John S. Kelly, Jr., Marilyn P. Fish, Joseph B. Munro, Jr., and Walter A. Sturm, summer student assistants.

## REFERENCES

(1) Fish, C. J.
1946. Oceanography in Japan. Navy. F2M–1007–46 (1) Oceanography. NTJ Ser. No. 112 (Index No. X–40N) (Jap) 409–900 MS7–10 Mar. 1946. 114 pp.

(2) Fish, Marie P.
1948. Sonic fishes of the Pacific. Pacif. Ocean. Biol. Project, Tech. Rept., *2:* 1–144 (Woods Hole Ocean. Inst.)

(3) 1949. Marine mammals of the Pacific with particular reference to the production of underwater sound. Pacif. Ocean. Biol. Project, Tech. Rept., *8:* 1–69 (Woods Hole Ocean. Inst.)

(4) Character and significance of sound production among the fishes of the North Atlantic. In preparation.

(5) Johnson, M. W., F. A. Everest and R. W. Young
1947. The role of snapping shrimp (Crangon and Synalpheus) in the production of underwater noise in the sea. Biol. Bull. Woods Hole, *93* (2): 122–138.

(6) Naval Ordnance Laboratory
1942. Measurement of background noise in the water at the Wolf Trap Range. NOL Rept., *691:* 1–6 (U. S. Navy Yard, 9 Nov. 1942).

(7) 1943. Acoustic measurements at the John G. Shedd Aquarium, Chicago, Ill. NOL Memorandum, *3416:* 1–10 (U. S. Navy Yard, 30 Mar. 1943).

(8) 1943. Analysis of available data on underwater background noise, in the region from 50 to 10,000 cps. NOL Memorandum, *2923:* 1–12 (U. S. Navy Yard, 21 Jun. 1943).

(9) 1944. Investigation of biological underwater background noises in vicinity of Beaufort, N. C. (10B1). NOL Rept., *880:* 1–22 (U. S. Navy Yard, Mar. 1944).

# MICROFILTRATION IN OCEANOGRAPHIC RESEARCH

## I. MARINE SAMPLING WITH THE MOLECULAR FILTER[1]

By

EDWARD D. GOLDBERG, MARJORIE BAKER, AND DENIS L. FOX

*Scripps Institution of Oceanography, University of California*
*La Jolla, California*

## ABSTRACT

Molecular filters, composed of cellulose acetate and nitrate membranes, may be used for the quantitative estimation of microplankton populations, for the determination of suspended organic and inorganic matter in natural waters, and in studies of photosynthetic productivity by phytoplankton cells in collected samples. Organisms retained by microfiltration are fixed, dehydrated, stained, estimated microscopically as to size and numbers, and preserved, all *in situ*, on each filter disc. Inorganic materials recovered on the membranes may be determined by microchemical analyses and by ashing. Photosynthetic productivity is measured in collected water samples by (1) addition thereto of dilute $NaHC^{14}O_3$, (2) exposure of the system for an interval to light, (3) subsequent quantitative collection of the organisms upon a filter disc, and (4) radioassay of the $C^{14}$ fixed by the plant cells. Microplankton and other suspended materials are inhomogeneously distributed in marine waters. Larger samples or integrative collecting devices are indicated for clarifying the true picture of the dispersed suspensions.

Natural waters contain two general classes of nongaseous suspended matter: (1) Organisms of the hydrosphere and their degradation products, and (2) solid particulate matter resulting from inorganic precipitation processes or from rock erosion. The quantitative separation of these suspended phases from their aqueous environment is of paramount importance in earth science and in certain biochemical investigations. Somewhat over 80% of the organic material produced by photosynthesis occurs in the oceans (Riley, 1944). The relative importance of the various categories of micro-organisms responsible for this production is yet undetermined. Studies of the biological standing crop in water masses have suffered from the fact that adequate samples for microscopic examination have not included all of the smaller organisms, since much of the nannoplankton readily passes through the sampling nets.

For similar reasons investigations on the physico-chemical processes of precipitation and resolution of solid phases, as well as the transport

[1] Contribution from the Scripps Institution of Oceanography, New Series No. 583.

of suspensions, have been hindered in their development. From both a biological and a hydrographical viewpoint, the concentration and character of particulate matter is interlinked with the chemical and physical properties of water masses.

The development of the molecular filter (hereafter referred to as MF) by Goetz, et al. (Goetz and Tsuneishi, 1951) has given impetus to a more intimate study of the particulate constituents of natural waters. These filter membranes are composed of incompletely cross-linked high polymer molecules of partially substituted cellulose acetate and cellulose nitrate. The MF has a uniform pore size whereby screening action retains all particles above a given size. Although the filters can be made with an effective pore size ranging from 1 to 5000 m$\mu$, those used in the following investigation retained all particles greater than approximately 0.5 $\mu$ (type HA, available from the Lovell Chemical Company, Watertown, Mass.). Another characteristic of the MF is the anisomorphism of the structure perpendicular to the membrane surface. The upper surface of the filter where the water enters has the uniformly graded small pore size, whereas the body of the filter which acts as a support for the upper portion is much more porous. Hence the filterable material is adsorptively and mechanically retained in the top surface, i. e. the MF acts chiefly as a two-dimensional screen in contrast to paper filters which accumulate material in the pores. The HA type MF discs are 50 mm in diameter. The material may be rendered transparent with a liquid of similar refractive index (1.49). The flow rates of sea water through the MF are more rapid in comparison with the finest grades of paper filters or adsorptive powders. Depending upon the amount and type of particulate matter, one liter will pass through the HA membrane in from 5 to 30 minutes. A filter for use with the MF is shown in Fig. 1.

*Standing Crop and Productivity Measurements with the MF.* A description of the distribution and photosynthetic activity of marine plankton in an area depends upon adequate sampling and quantitative assay. The first problem can not be dealt with until a satisfactory solution of the second problem is at hand. The analysis of plant populations has normally been accomplished by either "chlorphyll" measurements or visual counting of cells concentrated by either gravitational or centrifugational settling. Neither method is completely satisfactory, since the micro-organisms responsible for the pigment production are not thus differentiated, nor is there achieved complete recovery of the plankton cells from the water and from the walls of the glass or other hydrophilic vessels.

A filtering technique that utilizes the MF largely disposes of these

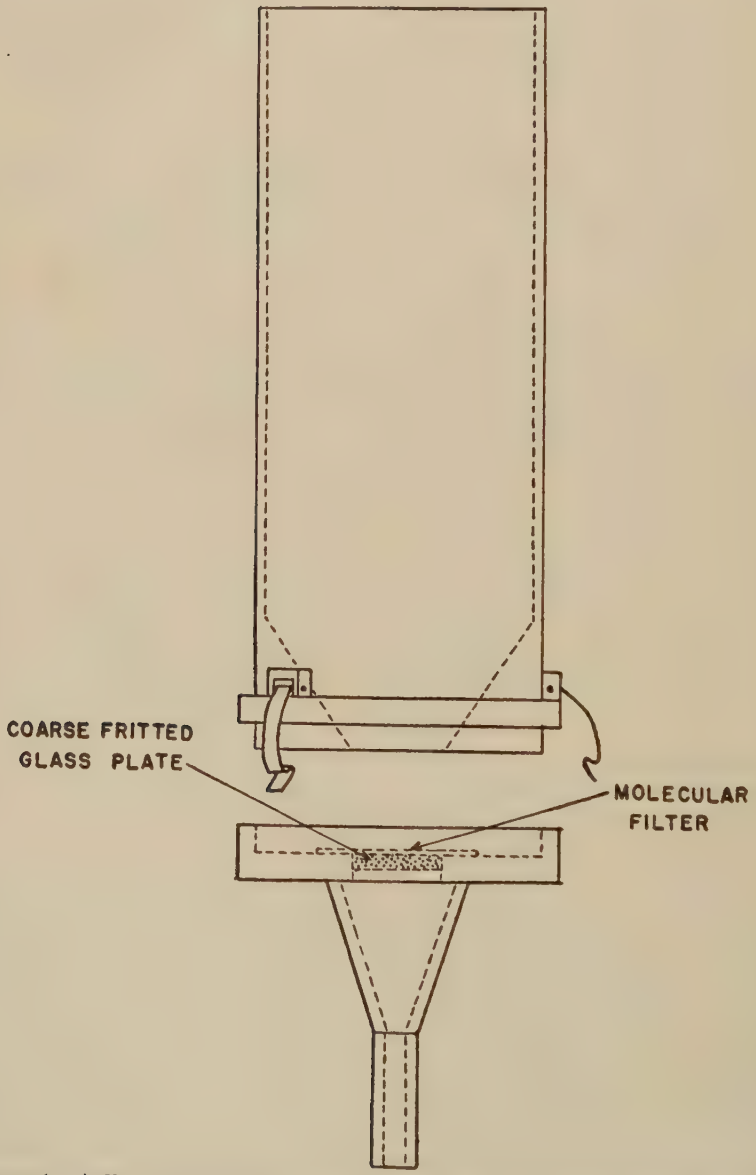


Figure 1. A filter apparatus constructed for use with the Molecular Filters. The unit may be fabricated from stainless steel or from plastics. The upper and lower unit are held together by means of distributor clips. The MF serves as a gasket to prevent water leakage from the apparatus.

difficulties. One or two liter samples of marine water, collected preferably in a hydrophobic plastic bottle, can be passed through the MF; thus all of the organisms with a maximum dimension larger than 0.5 $\mu$, as well as many smaller bodies, are retained by adsorption on the upper surface. With subsequent fixing, staining, and preservation, this defined plankton population can readily be assayed both for type and volume of organisms. Many phytoplankton cells, when stained with Fast Green, suffer few if any morphological changes and may be readily recognized.

The technique can be readily used in field operations. About three hours are required to prepare a single sample, but this time can be reduced by simultaneous preparation of many collected samples if more than one filtering apparatus is available.

*Sample Preparation.*

1. To a freshly collected liter of sea water add 40 ml of a saturated solution of $KI_3$ to kill and fix the organisms.
2. After the fixed solution has stood for one hour pass it through an MF. Replace the excess iodine fixative and the sea water retained on the filter disc with distilled water by serial washes with graduated dilutions; draw ten ml of 5, 10, 25, 50, 75, 90 and 100% dilutions with distilled water through the MF under vacuum.
3. Add 20 ml of a Fast Green dye solution (Johansen, 1940: 59) and leave in contact with the membrane for 30 minutes.
4. Draw the dye solution through the filter apparatus and pass distilled water through the membrane until the unadsorbed dye is thoroughly removed.
5. Dehydrate the organisms with a graded series of solutions of ethanol in distilled water; pass each of the washes of the series—5, 10, 25, 50, 75, 90 and 100% alcohol by volume—through as rapidly as possible to minimize dissolution of the membrane by the alcohol. Optional use may be made of higher alcohols, such as propanol or butanol, which are somewhat less destructive.
6. Render the water-free membrane transparent with cedar oil by drawing through it serial dilutions of 10, 25, and 50% cedar oil in alcohol, and finally 100% cedar oil. When the pure cedar oil has been drawn through, remove the cleared membrane from the filter, halve, and mount in balsam on a microscope slide.
7. For preservation, a small crystal of thymol may be dissolved in 100 ml of the cedar oil or balsam.

In order to remove any contaminating particles, all reagents and rinsing fluids are initially passed through an MF. These solutions are kept in covered containers to protect them from recontamination by

air-borne dust particles. Indigo-carmine picrate has been employed alternatively as the dye, although the organisms are not so strikingly stained with this as with Fast Green. Karo syrup can be substituted for the alcohol and cedar oil in the dehydration and clearing processes. Serial dilutions of the sugar solution in water passed through the MF, as in step 5 above, produces a cleared membrane suitable for mounting.

TABLE I. Size Distribution of Plankton as Measured on a MF

| *Size range of organisms (Average radius)* | *Number of organisms* | | *Volume* $\mu^3$ | |
|---|---|---|---|---|
| | *Sample A* | *Sample B* | *Sample A* | *Sample B* |
| $\mu$ | | | | |
| 1 | 199 | 491 | 834 | 2,476 |
| 4 | 101 | 160 | 27,078 | 42,895 |
| 6 | 89 | 105 | 80,529 | 95,007 |
| 8 | 44 | 50 | 94,370 | 107,238 |
| 10 | 29 | 21 | 121,481 | 87,969 |
| 12 | 10 | 12 | 72,368 | 86,863 |
| 16 | 15 | 20 | 257,370 | 343,160 |
| 18 | 5 | 1 | 122,151 | 24,430 |
| 20 | 5 | 3 | 100,536 | 167,560 |
| 24 | 7 | 9 | 405,363 | 521,181 |
| 32 | 2 | 7 | 65,536 | 229,376 |
| 40 | 2 | — | 536,192 | —— |
| 48 | 2 | 1 | 926,540 | 426,270 |
| 64 | 1 | — | 1,098,121 | —— |
| | TOTAL | | 3,908,469 | 2,171,425 |

Both surveys made on 28 March 1952. Samples 500 ml in volume. 50 microscopic fields studied out of 256 fields of filtered area.

Quantitative estimates can be made of the total volume of plankton contained upon an MF by ascertaining the total number of organisms and their respective average radii in a representative number of fields of the microscope. By assuming that the individual cells are approximate spheroids, the volume of the stained organic matter is determined. Where long chains of diatoms or plankton of known asymmetric shape are encountered, their volume may be calculated mathematically. Table I depicts a typical distribution of plankton with respect to size.

The static picture of the standing crop represents but a transitory condition in a dynamic process. The production of organic matter by a given standing crop has been investigated by the measurement of photosynthetic oxygen in a collected sample of sea water, or by the more recently developed method of the fixation of radioactive carbon dioxide (Nielsen, 1951). In waters where the planktonic populations

are low or where but little growth is encountered, the oxygen method is not satisfactory, whereas the newer technique is much more sensitive to the photosynthetic fixation of very small amounts of carbon dioxide.

In the radioassay of productivity, add a one ml aliquot containing one microcurie of radioactive carbon[2] as dissolved $NaHC^{14}O_3$ to a freshly drawn liter sample of sea water. The total inorganic carbon content of the water is directly propor-

TABLE II. Carbon Dioxide Fixation by Standing Crop of 28 March 1952

| *Net counts/minute of filtered plankton* | *Per cent of $CO_2$ of water removed by plankton/day* | *Micro-equivalents $CO_2$ of sea water removed by plankton/day* |
|---|---|---|
| Sample 1 304.5 | 0.85 | 16 |
| Sample 2 323.5 | 0.90 | 17 |

One liter samples taken. 1.91 milli-equivalents $CO_2$/L of water of chlorinity = 18.32. Specific activity of $C^{14}$ initially added = 36,000 counts/min/L.

tional to the initial activity of the radioactive carbon, since the quantity of carbonate introduced with the active tracer is negligible in relation to the amounts of carbonate normally present in sea water. After photosynthesis by the resident organisms has proceeded for a determined time under conditions comparable to those of the marine environment, the entire sample is collected on an MF. The filter is washed with inactive sea water, dehydrated in a desiccator, and assayed radiometrically for the carbon taken up by the organisms (Table II).

The organisms are retained on the top of the membrane, not penetrating into the lower portion, and hence any absorption by the filter disc of the weak beta rays emitted by the fixed radioactive carbon is minimized. Further, the complete retention of all plankton above a size of 0.5 $\mu$ gives a measure of productivity usable in the quantitative equations of Riley, Stommel, and Bumpus (1949).

*Estimation and Characterization of the Inorganic and Organic Suspended Matter.* The suspended material of marine waters has been investigated with regard to the over-all inorganic chemical composition (Armstrong and Atkins, 1950) by routine chemical analyses of the sediment collected from an average of 22 liters of sea water. Jerlov (1951) has studied the distribution of suspended particles in the sea by the intensity of light scattered from a Tyndall beam. Fox, Isaacs and Corcoran (1952) have determined the organic carbon and organic

[2] The radioactive $C^{14}$ used in this investigation was supplied by the Oak Ridge National Laboratory on allocation from the Isotopes Division, U. S. Atomic Energy Commission.

nitrogen in marine leptopel by wet combustion of the material retained on inert inorganic powder. Krey (1949, cited by Jerlov), by fractional filtration, has subjected the collected particles to microscopic analysis; he also studied the chemical constitution of the suspended organic matter. However, none of these methods can give size distributions and chemical constitution on the same sample.

The MF has been used to advantage in the study of the size distribution of particles containing suspended iron in coastal marine waters. Recent studies on the growth of marine diatoms have indicated that particulate or colloidal iron is utilized as a growth nutrient (Harvey, 1935; Goldberg, 1952) and may actually be a limiting factor in their multiplication. Thus, a semiquantitative technique has been developed to ascertain the number and size of particles containing iron in a water sample. It should be emphasized that the chemical combination of the iron has not actually been determined. In all probability it occurs chiefly as hydrous ferric oxides.

*Sample Preparation.*

1. One or two liters of sea water are passed through the MF. The collected residue and the MF are washed with distilled water to remove any salts which would otherwise inhibit the clearing of the membrane.

2. The MF is dehydrated in a desiccator or dried in an oven for 5 minutes at 100° C.

3. The membrane is placed on a microscopic slide and covered with a few drops of "Tween 80" (polyoxythylene sorbitan monooleate, available from Atlas Powder Company, Wilmington, Delaware) which has been saturated with potassium thiocyanate and acidulated with hydrochloric acid (3 drops concentrated HCl per 100 ml of "Tween 80").

The "Tween 80" has an index of refraction close enough to that of the MF to clear the filters and render visible the deep red zones of iron thiocyanate complex which form about the iron particles. A typical distribution of iron particles in water taken from the pier of the Scripps Institution of Oceanography is shown in Fig. 2. A filter apparatus constructed completely of plastic, similar in design to that shown in Fig. 1, is utilized in these analyses.

The dried weight at 110° C and the ash weight of the sediment collected upon an MF from a given volume of sea water and subsequently washed free of soluble salts with distilled water can be used to define semiquantitatively the amount of inorganic and organic fractions. The MF is ashless and has a weight of about 95 mg reproducible to $\pm$ 0.2 mg after repeated washings and dryings at 100° C.

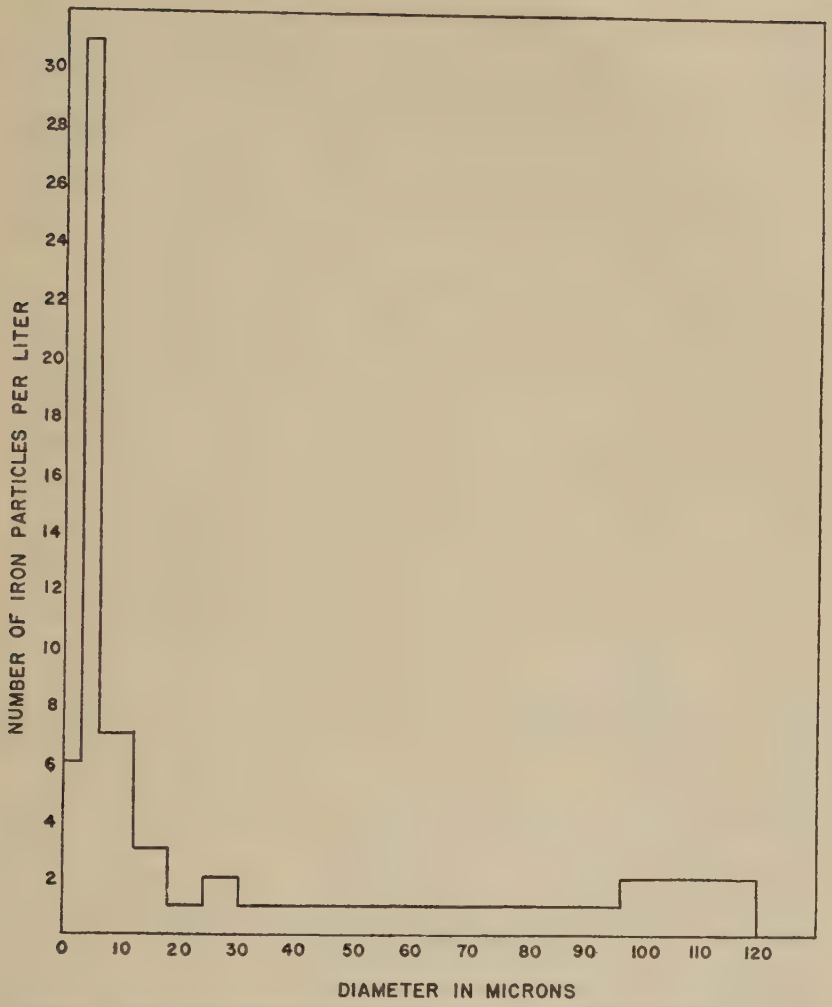


Figure 2. The size distribution of suspended particles, giving a positive thiocyanate test for iron in surface water collected six miles west of La Jolla, California.

Two inshore surface samples of one liter volume showed 1.9 and 6.2 mg of total dry weight and 1.3 and 4.4 mg of ash weight respectively. By difference the "organic content" would be 0.6 and 1.8 mg. A profile of suspended matter in the open ocean is given in Table III.

*Discussion.* The quantitative assay of both planktonic populations and suspended sediments has demonstrated that improvement in

sampling techniques is necessary for precision in the results. This is manifest in the volumetric analysis of plankton in Table I, where one large organism of diameter 64 $\mu$ accounts for one fourth of the volume estimated for a 500 ml sample. Duplicate assays of the same water sample differed by a factor of two. In other size distribution studies

TABLE III. The Distribution of Inorganic Suspended Matter

| *Depth* (*m*) | *Ash Weight at 400° C* (*mg*) | |
|---|---|---|
| | *Sample A* | *Sample B* |
| 0 | 1.2 | 2.7 |
| 10 | 2.1 | 7.7 |
| 25 | 1.2 | 1.3 |
| 50 | 1.3 | 0.4 |
| 75 | 0.0 | 0.2 |
| 100 | 1.6 | 0.2 |
| 150 | 6.0 | 1.0 |
| 200 | 1.0 | 7.3 |
| 300 | 2.4 | 0.5 |
| 400 | 0.8 | 3.8 |
| 500 | 1.0 | 0.7 |
| 600 | — | 0.8 |
| 800 | 4.7 | 1.6 |
| 1000 | 1.3 | 2.2 |
| 1200 | 1.6 | 0.5 |

Samples were 1.2 liters. Sample A collected 28 February 1952 at 1630. Sample B collected 29 February 1952 at 0700. Collections made in San Clemente Deep off San Diego, California.

of plankton, two similtaneously collected samples were often a whole order of magnitude apart. Comparison between pairs of samples subjected to the radiometric determination of carbon uptake show the same kind of deviation but to a less extent. The distribution of suspended sediment, as illustrated in Table III, exhibits considerable scatter.

These results emphasize the discontinuous arrays of suspended solid phases within natural waters. Thus, the amount of substance collected over a short time interval from a unique location will not necessarily represent conditions in the water region; rather, they may reflect the layering of the water masses or the turbulence of the area. To overcome these difficulties, two lines of approach, not mutually exclusive, are indicated. To secure more valid data for statistical representation of a given water mass would require the processing of voluminous samples from a considerable number of strata. Such a comprehensive survey would manifestly require much time and labor.

The collection of a sample integrated over time and space in a given locality is preferable where time is limited. A simple water sampler for volumes of one or two liters may be readily constructed by the use of a capillary bleeder. In the opening of the collection device two glass tubes may be held in place by a cork: one tube of large diameter for water inflow and a second tube of drawn capillary tubing for air release. By controlling the size of the capillary, filling times can be rigidly controlled.

*Acknowledgment.* The authors wish to acknowledge the generous donation of experimental molecular filters from Dr. Alexander Goetz of the California Institute of Technology during the initial stages of this investigation. James S. Kittridge aided in collection of the samples at sea.

*Summary.* 1. The standing crop of marine phytoplankton populations can be quantitatively estimated for all organisms larger than 0.5 $\mu$ by a filtering technique that utilizes the molecular filter, a cellulose acetate and nitrate membrane. The organisms are collected, fixed, dehydrated, stained, estimated as to size and number and preserved on one of these filter discs.

2. The molecular filter can be used in the quantitative assay of suspended organic and inorganic matter of natural waters.

3. The size distribution of suspended iron particles was studied by applying microchemical analyses to material collected on the molecular filter.

4. The suspended matter in marine waters was found to be inhomogeneously distributed. It is proposed that larger samples or integrating collecting devices be utilized to obtain the true picture of the dispersed suspensions.

## LITERATURE CITED

Armstrong, F. A. J. and W. R. G. Atkins
1950. The suspended matter of sea water. J. Mar. biol. Ass. U. K., *29:* 139–143.

Fox, D. L., J. D. Isaacs and E. F. Corcoran.
1952. Marine leptopel, its recovery, measurement and distribution. J. mar. Res., *11:* 29–46.

Goetz, A. and N. Tsuneishi
1951. The application of molecular filter membranes to the bacteriological analysis of water. J. Amer. Wat. Wks Ass., *43:* 943–969.

Goldberg, E. D.
1952. Iron assimilation by marine diatoms. Biol. Bull. Woods Hole, *102:* 243–248.

Harvey, H. W.
1937. The supply of iron to diatoms. J. Mar. biol. Ass. U. K., *22:* 205–219.

Jerlov, N. G.
1951. Optical measurement of particle size distribution in the sea. Tellus, *3:* 122–128.
Johansen, D. A.
1940. Plant Microtechnique. McGraw Hill Book Co., New York. 523 pp.
Krey, J.
1949. Uber Art und Menge des Seston im Meere. Verh. dtsch. Zool. Meere, 1949: 295.
Nielsen, E. S.
1951. Measurement of the production of organic matter in the sea by means of Carbon–14. Nature, London, *167:* 684.
Riley, G. A.
1944. The carbon metabolism and the photosynthetic efficiency of the earth as a whole. Amer. Sci., *32:* 129–134.
Riley, G. A., H. Stommel, and D. F. Bumpus
1949. Quantitative ecology of the plankton of the western North Atlantic. Bull. Bingham oceanogr. Coll., *12* (3): 1–169.

# ABRUPT CHANGE IN WIDTH IN TWO-LAYER OPEN CHANNEL FLOW[1]

By

HENRY STOMMEL AND HARLOW G. FARMER

*Woods Hole Oceanographic Institution*
*Woods Hole, Massachusetts*

## ABSTRACT

An abrupt widening in a channel can act as a control on the regime of two-layer flow immediately upstream. A simple explanation in terms of an interfacial Froude number is offered and a set of experimental verifications is described. Bernoulli's Principle is applied to an abrupt narrowing.

1. *The Interfacial Froude Number.* The ordinary Froude number, $F$, is defined by

$$F = u^2/gD \,, \tag{1}$$

where $u$ is the mean velocity of flow in a channel of depth $D$. A long wave of infinitesimal amplitude is stationary when $F = 1$, a condition which occurs in any channel transition which acts as a control.[2]

In a two layer system a transition may be expected to act as a control on the level of the interface when a long internal wave of infinitesimal amplitude is stationary.

For convenience we have defined the interfacial Froude number, $F_i$, in terms of $u_1$, the mean velocity of the upper layer, and $D_1$, the depth of the upper layer, and the quantity $\beta = (\rho_2 - \rho_1)/\rho_2$, where $\rho_1$ and $\rho_2$ are the densities of the upper and lower layers respectively:

$$F_i = u_1^2/g\beta D_1 \,. \tag{2}$$

The condition for a stationary internal wave also depends on $u_2$, the velocity, and $D_2$, the depth of the lower layer; hence it is not generally as simple as $F_i = 1$. The steady state equations of motion for the two layers are

$$u_1 \frac{\partial u_1}{\partial x} = -g \frac{\partial}{\partial x}(D_1 + D_2) \tag{3}$$

and

[1] Contribution No. 616 from the Woods Hole Oceanographic Institution. This work was supported from funds made available by the Office of Naval Research through their contract No. N6ONR-27701 (NR-083-004) with the Woods Hole Oceanographic Institution.

[2] "Engineering Hydraulics," edited by Hunter Rouse. John Wiley and Sons, New York. 1950.

$$u_2 \frac{\partial u_2}{\partial x} = -g\left[\alpha \frac{\partial (D_1 + D_2)}{\partial x} + \beta \frac{\partial D_2}{\partial x}\right], \tag{4}$$

where $\alpha = \rho_1/\rho_2$ and $\beta = (\rho_2 - \rho_1)/\rho_2$ .

The equations of mass continuity are

$$(\partial/\partial x)(D_1 u_1) = 0 \tag{5}$$

$$\text{and } (\partial/\partial x)\,(D_2 u_2) = 0\,. \tag{6}$$

TABLE I. Critical Interfacial Froude Number $F_i$ as a Function of $n$ and $q_2/q_1$

| $n$ \ $q_2/q_1$ | | .1 | .2 | .3 | .4 | .5 | .6 | .7 | .8 | .9 | 1.0 |
|---|---|---|---|---|---|---|---|---|---|---|---|
| 0 | 1 | 1 | 1 | 1 | 1 | 1 | 1 | 1 | 1 | 1 | 1 |
| .1 | 1 | 1 | 1 | 1 | 1 | 1 | 1 | 1 | .999 | .999 | .999 |
| .2 | 1 | 1 | 1 | .999 | .997 | .996 | .994 | .992 | .990 | .987 | .984 |
| .3 | 1 | .999 | .993 | .993 | .987 | .980 | .973 | .962 | .951 | .940 | .927 |
| .4 | 1 | .997 | .988 | .974 | .955 | .931 | .904 | .873 | .841 | .807 | .772 |
| .5 | 1 | .990 | .962 | .917 | .862 | .800 | .735 | .671 | .610 | .552 | .500 |
| .6 | 1 | .967 | .881 | .767 | .649 | .543 | .451 | .377 | .316 | .268 | .229 |
| .7 | 1 | .888 | .665 | .469 | .332 | .235 | .181 | .139 | .110 | | |
| .8 | 1 | .610 | .281 | .148 | | | | | | | |
| .9 | 1 | .121 | | | | Less than 0.1 | | | | | |
| 1.0 | | | | | | | | | | | |

Elimination of $\partial u_1/\partial x$, $\partial u_2/\partial x$, $\partial D_1/\partial x$, and $\partial D_2/\partial x$ from these four equations results in the following equation, which must hold for stationary interfacial waves:

$$G_2\,(G_1 - 1) = G_2 - \beta\,, \tag{7}$$

where we have written for simplicity $G_1 = u_1^2/gD_1$ and $G_2 = u_2^2/gD_2$ .

Since the regular Froude number in two-layer flow is very small, $G_1 << 1$, we may write the following very good approximation of (7): $G_1 + G_2 = \beta$ .

If we introduce the discharges per unit width, $q_1 = u_1 D_1$ and $q_2 = u_2 D_2$, and the quantity $n$ by $D_1 = nD$, then $D_2 = (1 - n)\,D$, where $D$ is the total depth. We write the interfacial Froude number for stationary interfacial waves in the following form:

$$F_i = \left[1 + \left(\frac{q_2}{q_1}\right)^2 \left(\frac{n}{1-n}\right)^3\right]^{-1}.$$

Values of the critical $F_i$ are given in Table I; for reasonably small values of both $q_2/q_1$ and $n$, $F_i$ is essentially unity.

2. *Experimental Runs on Control.* The flume shown in Fig. 1 was fitted with a transition in width. The lower layer of liquid was in all cases sea water; the upper layer was fresh water or a mixture of fresh and salt water (to provide various densities). The different widths of the flume used before the transition were 4.0, 8.5, 17.5, and 27.0 cm. The width of the flume after the transition was in every case 44.0 cm. The nature of the flow past the transition is shown in Figs. 2 and 3. Table II contains the data from the series of experiments: $W$ is the width before the transition, $W_1$ is that after the transition, $D_1$ is the depth of the upper layer measured upstream beyond the region of curvilinear flow. $D_{1T}$ is the depth of the upper layer at the beginning of the transition. $D_2$ is the depth of the lower layer at the point where $D_1$ was measured. $D_1{}^*$ is the depth of the upper layer computed from the assumption that $F_i = 1$. In most of the runs a slight counterflow in the lower layer was unavoidable due to some mixing across the interface. The velocity of flow in the lower layer was much less than that in the upper layer and exhibited a vertical distribution similar to that shown in Fig. 4.

Measurements of $D_1$ from photographs were made with a probable error of $\pm$ 0.3 cm. The standard deviation (all runs) of the observed depth of the upper layer, $D_1$, from computed depth $D_1{}^*$ on the assumption that $F_i = 1$ is $\pm$ 0.56 cm.

3. *Application to Estuaries.* Certain estuaries realize the conditions of this type of control. The Mississippi River enters the Gulf of Mexico through a number of passes, two of which, South Pass and Southwest Pass, are artificially confined by jetties so that the transition in width is very abrupt.[3] The flow in both passes is distinctly two-layered at low river discharges, the interface is very sharply defined, and there is negligible tidal mixing. The depth of the upper layer, as observed and computed, is given in Table III.

For model studies it is inferred that if the model is scaled properly for surface tides (Froude scaling) the action of controls on the two-layer flow will also be properly scaled, provided the densities of the model and their differences are the same as those in the prototype. A change of density difference precludes the possibility of scaled control of interfacial depth.

4. *Abrupt Contraction.* When the channel transition does not act as a control, the flow in the upper layer can be conveniently analyzed with Bernoulli's Theorem. We will neglect the velocity of the lower

[3] Mr. H. B. Simmons and Mr. G. H. Hudson of the U. S. Army Corps of Engineers very kindly provided the authors with data on the hydrography of these Passes.

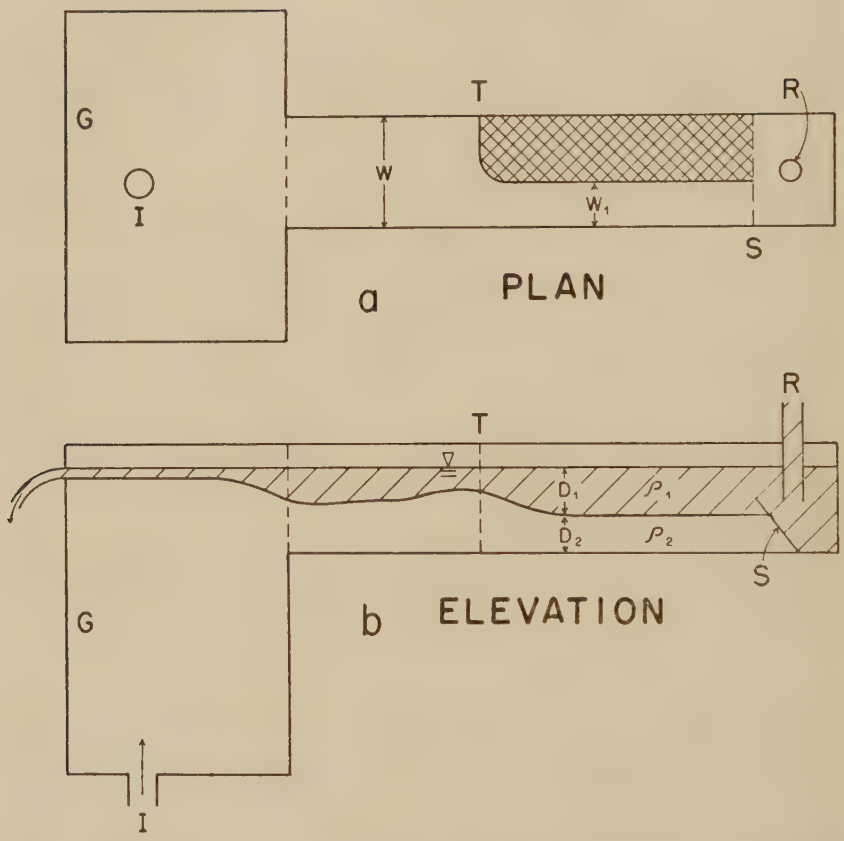


Figure 1. *a* and *b* show the plan and elevation of the set-up of the transition in the flume for an abrupt widening. The transition is at $T$, the river mixture enters at $R$, the separator, $S$, prevents mixing of the two layers at the river inlet, the heavy salt water is constantly replenished through inlet, $I$, at the bottom of the salt water tank. Both fluids flow out over the gate, $G$, which controls the free surface level. The upper fresh water layer is shaded. *c* and *d* (see opposite page) show the set-up for the abrupt narrowing of the flume. In all cases the edge of the transition is rounded with a three inch radius.

layer and assume that the velocity of the upper layer is uniform before and after the transition and that the pressure is everywhere hydrostatic. Using the same notation as before, the energy equation may be written as

$$\frac{\rho_1 u_1^2}{2} + (\rho_2 - \rho_1) gD_1 = \frac{\rho_1 u_1'^2}{2} + (\rho_2 - \rho_1) gD_1' + E .$$

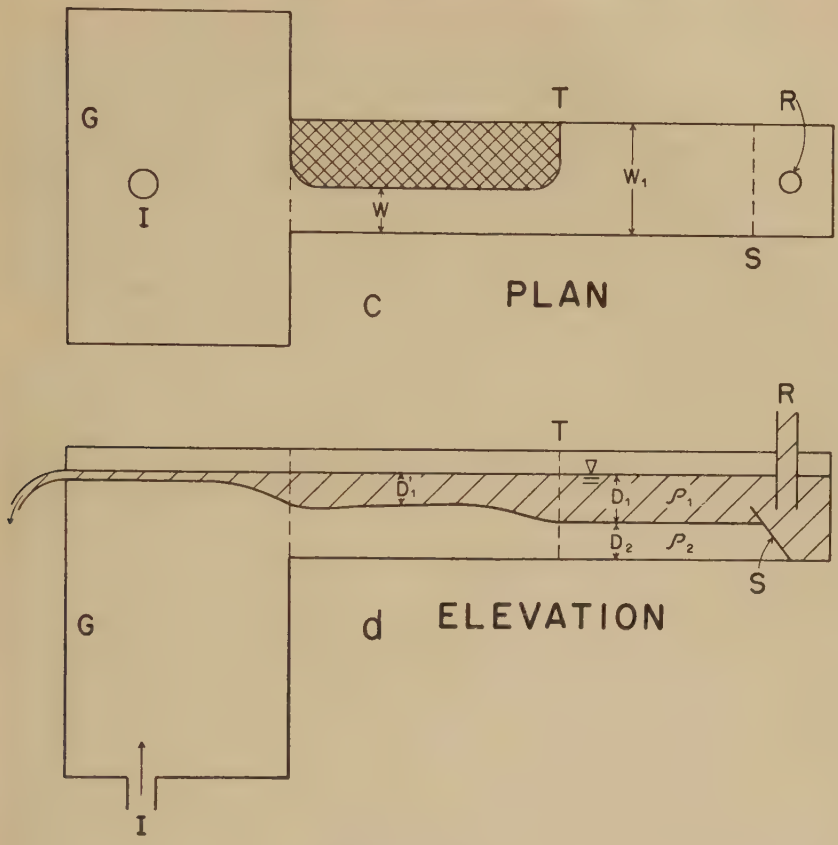


Figure 1 (*continued*)

The left-hand side of the equation refers to a section upstream of the transition, that on the right to a section downstream of the transition, both sections being beyond the region of curvilinear flow. $E$ represents the energy loss or change in total energy before and after the transition. Table IV contains 24 runs made through a narrowing. Fig. 4 shows a typical run. The quantity $(D_1 - D_1')^*$ is computed on the assumption of $E = 0$. Comparison with the measured $(D_1 - D_1')$ shows agreement well within the errors of measurement, which demonstrates the minor role of the turbulent energy loss in a narrowing.

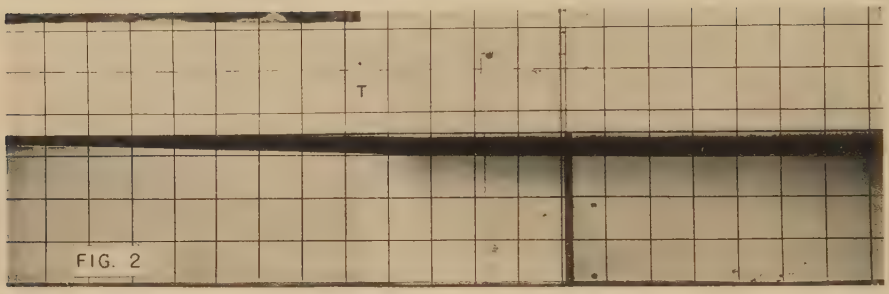


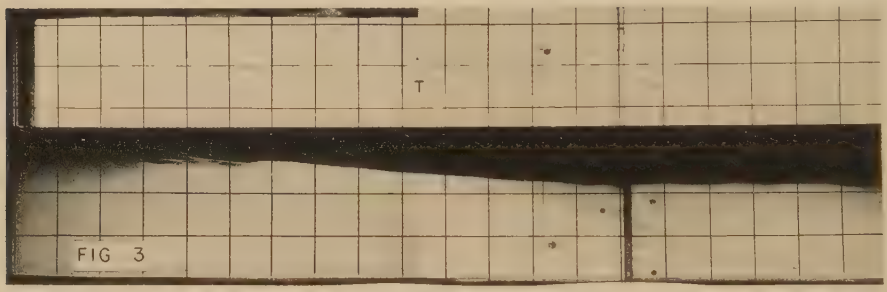


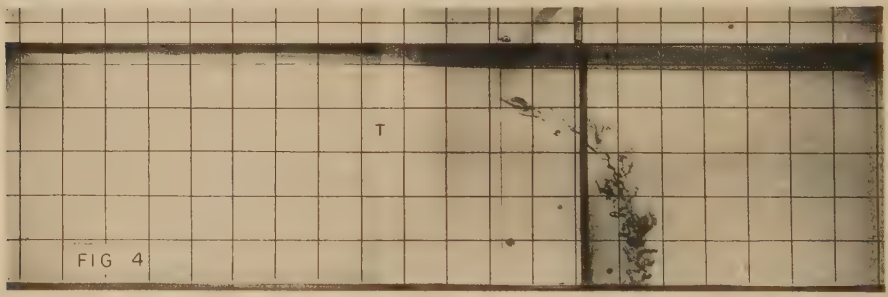


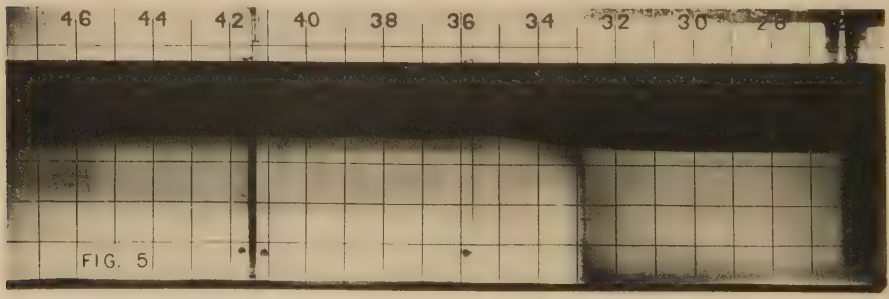


Figures 2 and 3. Illustrative examples of flow past sudden widening at T, runs C-3-16 and C-3-18 respectively. View through glass side of flume. The grid lines are 5 cm apart. The lower 5 cm of the flume are obscured by the shade on the photographic lamps. The upper fluid, dyed black, moves from right to left. Figure 4. The distribution of dye 10 seconds after release from the heavy vertical black line to illustrate the slow creeping motion of the lower layer, run C-3-21. Figure 5. Bernoulli flow through abrupt narrowing, run E-3-6.

TABLE II

| Run | $\beta \times 10^3$ | $q_1$ | $D_1$ | $D_2$ | $D_{1T}$ | $D_1^*$ |
|---|---|---|---|---|---|---|
| | | | $W_1/W = 0.091$ | | | |
| C–3–127 | 8.09 | 31.5 | 6.2 | 26.3 | 4.5 | 5.0 |
| 128 | 18.6 | 94.5 | 7.2 | 25.3 | 5.2 | 7.9 |
| 129 | 9.56 | 63.0 | 8.7 | 23.8 | 6.5 | 7.5 |
| 130 | 8.78 | 94.5 | 10.7 | 21.8 | 7.5 | 10.1 |
| 131 | 7.60 | 189. | 15.5 | 17.0 | 11.5 | 16.8 |
| 132 | 8.10 | 31.5 | 5.8 | 16.7 | 4.1 | 5.0 |
| 133 | 9.07 | 94.5 | 10.0 | 12.5 | 7.2 | 10.0 |
| 134 | 9.56 | 31.5 | 5.7 | 6.8 | 3.8 | 4.7 |
| 135 | 21.9 | 31.5 | 4.5 | 8.0 | 3.0 | 3.6 |
| 136 | 24.3 | 31.5 | 4.0 | 18.5 | 3.0 | 3.5 |
| 137 | 21.4 | 94.5 | 8.5 | 14.0 | 5.5 | 7.5 |
| 138 | 23.8 | 189. | 11.5 | 11.0 | 8.2 | 11.5 |
| | | | $W_1/W = 0.19$ | | | |
| C–3– 1 | 21.1 | 14.8 | 3.0 | 10.0 | 2.2 | 2.2 |
| 2 | 2.34 | 44.5 | 4.3 | 8.7 | 3.0 | 4.4 |
| 3 | 23.2 | 89.0 | 6.8 | 6.2 | 4.8 | 7.0 |
| 4 | 22.3 | 14.8 | 2.8 | 19.7 | 2.2 | 2.2 |
| 5 | 21.6 | 44.5 | 4.5 | 18.0 | 3.4 | 4.5 |
| 6 | 24.1 | 89.0 | 7.0 | 15.5 | 5.1 | 6.9 |
| 7 | 24.4 | 178. | 10.5 | 12.0 | 8.0 | 11.0 |
| 8 | 23.6 | 14.8 | 2.8 | 29.7 | 2.2 | 2.1 |
| 9 | 19.5 | 44.5 | 5.0 | 27.5 | 3.5 | 4.7 |
| 10 | 22.6 | 89.0 | 7.5 | 25.0 | 5.4 | 7.1 |
| 11 | 24.4 | 178. | 11.0 | 21.5 | 8.5 | 11.0 |
| 69 | 16.5 | 14.8 | 2.8 | 9.7 | 2.0 | 2.4 |
| 70 | 16.6 | 44.5 | 4.6 | 7.9 | 3.5 | 5.0 |
| 71 | 15.1 | 89.0 | 7.5 | 5.0 | 5.5 | 8.1 |
| 72 | 13.1 | 14.8 | 3.2 | 19.3 | 2.3 | 2.6 |
| 73 | 14.4 | 44.5 | 5.5 | 17.0 | 4.1 | 5.2 |
| 74 | 15.4 | 89.0 | 7.5 | 15.0 | 6.2 | 8.0 |
| 75 | 16.4 | 178. | 12.4 | 10.1 | 9.0 | 12.5 |
| 76 | 13.7 | 14.8 | 3.2 | 29.3 | 2.5 | 2.5 |
| 77 | 15.0 | 44.5 | 5.6 | 26.9 | 4.0 | 5.1 |
| 78 | 14.8 | 89.0 | 8.0 | 24.5 | 6.0 | 8.2 |
| 79 | 15.8 | 178. | 11.5 | 21.0 | 9.0 | 12.7 |
| 81 | 8.20 | 14.8 | 4.1 | 28.4 | 2.9 | 3.0 |
| 82 | 10.3 | 44.5 | 6.6 | 25.9 | 5.0 | 5.8 |
| 83 | 8.77 | 89.0 | 9.5 | 23.0 | 7.0 | 9.7 |
| 84 | 7.90 | 178. | 14.7 | 17.8 | 11.1 | 16.0 |
| 85 | 8.20 | 268. | 20.0 | 12.5 | 14.5 | 20.7 |
| 86 | 7.90 | 14.8 | 4.0 | 18.5 | 2.7 | 3.0 |
| 87 | 10.0 | 44.5 | 6.0 | 16.5 | 4.5 | 5.9 |
| 88 | 9.26 | 89.0 | 9.2 | 13.3 | 7.0 | 9.6 |

TABLE II (*Continued*)

| *Run* | $\beta \times 10^3$ | $q_1$ | $D_1$ | $D_2$ | $D_{1T}$ | $D_1^*$ |
|---|---|---|---|---|---|---|
| | | *$W_1/W$ = 0.19 (Continued)* | | | | |
| C–3– 89 | 7.90 | 178. | 15.0 | 7.5 | 11.0 | 16.0 |
| 90 | 8.10 | 14.8 | 3.4 | 9.1 | 2.5 | 3.0 |
| 91 | 11.6 | 44.5 | 6.0 | 6.5 | 4.7 | 5.6 |
| 92 | 6.05 | 14.8 | 4.0 | 18.5 | 3.1 | 3.3 |
| 93 | 8.10 | 44.5 | 6.2 | 16.3 | 4.5 | 6.3 |
| 94 | 8.00 | 89.0 | 9.0 | 13.5 | 6.9 | 10.0 |
| 95 | 7.90 | 178. | 15.1 | 7.4 | 11.0 | 16.0 |
| 96 | 7.12 | 14.8 | 4.5 | 28.0 | 3.5 | 3.2 |
| 97 | 9.75 | 44.5 | 6.0 | 26.5 | 4.5 | 5.9 |
| 98 | 10.2 | 89.0 | 9.1 | 23.4 | 7.3 | 9.3 |
| 99 | 8.00 | 178. | 14.5 | 18.0 | 11.5 | 15.9 |
| 100 | 8.00 | 268. | 20.0 | 12.5 | 15.0 | 20.9 |
| | | | *$W_1/W$ = 0.40* | | | |
| C–3– 12 | 23.0 | 21.6 | 2.8 | 9.7 | 2.7 | 2.8 |
| 13 | 23.6 | 43.2 | 4.5 | 8.0 | 3.5 | 4.3 |
| 14 | 24.1 | 86.4 | 7.0 | 5.5 | 5.6 | 6.8 |
| 15 | 19.6 | 7.2 | 2.0 | 20.5 | 1.5 | 1.4 |
| 16 | 22.0 | 21.6 | 3.0 | 19.5 | 2.5 | 2.8 |
| 17 | 22.8 | 43.2 | 4.5 | 18.0 | 3.6 | 4.4 |
| 18 | 23.6 | 86.4 | 6.7 | 15.8 | 5.9 | 6.8 |
| 19 | 24.0 | 130. | 9.0 | 13.5 | 7.7 | 9.0 |
| 20 | 23.0 | 7.2 | 2.0 | 30.5 | 1.5 | 1.3 |
| 21 | 20.7 | 21.6 | 2.7 | 29.8 | 2.4 | 2.8 |
| 22 | 21.9 | 43.2 | 4.7 | 27.8 | 3.9 | 4.4 |
| 23 | 23.3 | 86.4 | 7.0 | 25.5 | 5.9 | 6.9 |
| 24 | 23.6 | 130. | 9.2 | 23.3 | 8.0 | 9.0 |
| 53 | 14.9 | 21.6 | 3.3 | 9.2 | 2.5 | 3.2 |
| 54 | 15.5 | 43.2 | 5.0 | 7.5 | 4.0 | 5.0 |
| 55 | 16.1 | 86.4 | 7.8 | 4.7 | 6.3 | 7.8 |
| 56 | 15.2 | 21.6 | 3.5 | 19.0 | 2.6 | 3.2 |
| 57 | 15.4 | 43.2 | 5.7 | 16.8 | 4.0 | 5.0 |
| 58 | 16.0 | 86.4 | 7.6 | 14.9 | 6.2 | 7.8 |
| 59 | 15.9 | 130. | 10.4 | 12.1 | 8.5 | 10.2 |
| 60 | 16.2 | 172. | 12.2 | 10.3 | 10.0 | 12.3 |
| 61 | 15.0 | 21.6 | 3.4 | 29.1 | 2.7 | 3.2 |
| 62 | 16.0 | 43.2 | 5.1 | 27.4 | 3.6 | 4.9 |
| 63 | 16.1 | 86.4 | 7.7 | 24.8 | 6.4 | 7.8 |
| 64 | 16.0 | 130. | 9.8 | 22.7 | 8.0 | 10.2 |
| 65 | 16.2 | 172. | 12.5 | 20.0 | 10.0 | 12.3 |
| 66 | 11.7 | 7.2 | 2.5 | 30.0 | 1.8 | 1.7 |
| 67 | 14.6 | 7.2 | 1.9 | 20.6 | 1.4 | 1.5 |
| 68 | 16.4 | 7.2 | 2.1 | 10.4 | 1.5 | 1.5 |
| 101 | 6.60 | 7.2 | 2.2 | 30.3 | 2.2 | 2.0 |

TABLE II (*Continued*)

| *Run* | $\beta \times 10^3$ | $q_1$ | $D_1$ | $D_2$ | $D_{1T}$ | $D_1^*$ |
|---|---|---|---|---|---|---|
| | | $W_1/W = 0.40$ (*Continued*) | | | | |
| C–3–102 | 8.68 | 21.6 | 4.0 | 28.5 | 3.6 | 3.8 |
| 103 | 8.66 | 43.2 | 6.3 | 26.2 | 5.2 | 6.0 |
| 104 | 7.31 | 130. | 13.5 | 9.0 | 11.0 | 13.3 |
| 105 | 7.70 | 172. | 17.0 | 5.5 | 12.5 | 15.8 |
| 106 | 6.34 | 7.2 | 2.5 | 20.0 | 2.0 | 2.0 |
| 107 | 9.17 | 21.6 | 4.0 | 18.5 | 3.3 | 3.7 |
| 108 | 7.80 | 43.2 | 6.5 | 16.0 | 5.0 | 6.3 |
| 109 | 7.20 | 86.4 | 10.7 | 11.8 | 8.5 | 10.2 |
| 110 | 7.31 | 130. | 13.5 | 9.0 | 11.0 | 13.3 |
| 111 | 7.70 | 7.2 | 2.2 | 10.3 | 1.9 | 1.9 |
| 112 | 8.78 | 21.6 | 4.2 | 8.3 | 3.5 | 3.8 |
| 113 | 7.70 | 43.2 | 6.5 | 6.0 | 5.0 | 6.3 |
| | | $W_1/W = 0.61$ | | | | |
| C–3– 25 | 20.8 | 4.67 | 1.5 | 11.0 | 1.1 | 1.0 |
| 26 | 20.8 | 14.0 | 2.8 | 9.7 | 2.2 | 2.1 |
| 27 | 24.0 | 28.0 | 3.9 | 8.6 | 3.2 | 3.2 |
| 28 | 24.1 | 55.9 | 6.0 | 6.5 | 4.5 | 5.1 |
| 29 | 24.2 | 84.0 | 7.0 | 5.5 | 6.0 | 6.7 |
| 30 | 19.4 | 4.67 | 1.4 | 21.1 | 1.3 | 1.0 |
| 31 | 21.8 | 14.0 | 2.0 | 20.5 | 1.6 | 2.1 |
| 32 | 23.0 | 28.0 | 3.2 | 19.3 | 2.7 | 3.3 |
| 33 | 23.8 | 55.9 | 5.0 | 17.5 | 4.5 | 5.1 |
| 34 | 24.0 | 84.0 | 7.2 | 15.3 | 6.4 | 6.7 |
| 35 | 23.3 | 4.67 | 1.5 | 31.0 | 1.1 | 1.0 |
| 36 | 21.3 | 14.0 | 2.0 | 30.5 | 1.8 | 2.1 |
| 37 | 21.8 | 28.0 | 3.1 | 29.4 | 2.8 | 3.3 |
| 38 | 23.2 | 55.9 | 5.0 | 27.5 | 4.5 | 5.2 |
| 39 | 23.7 | 84.0 | 7.1 | 25.4 | 6.0 | 6.7 |
| 41 | 15.7 | 28.0 | 3.7 | 8.8 | 3.1 | 3.7 |
| 42 | 16.2 | 55.9 | 5.5 | 7.0 | 4.6 | 5.8 |
| 43 | 16.2 | 84.0 | 7.5 | 5.0 | 6.5 | 7.6 |
| 44 | 15.0 | 14.0 | 3.0 | 19.5 | 2.0 | 2.4 |
| 45 | 14.9 | 28.0 | 4.0 | 18.5 | 3.5 | 3.8 |
| 46 | 15.8 | 55.9 | 6.2 | 16.3 | 5.2 | 5.9 |
| 47 | 16.3 | 84.0 | 8.0 | 14.5 | 7.0 | 7.6 |
| 48 | 14.7 | 14.0 | 2.6 | 29.9 | 2.4 | 2.4 |
| 49 | 14.8 | 28.0 | 3.7 | 28.8 | 3.0 | 3.8 |
| 50 | 16.0 | 55.9 | 6.0 | 26.5 | 5.2 | 5.8 |
| 51 | 16.0 | 84.0 | 8.0 | 24.5 | 7.1 | 7.7 |
| 52 | 16.0 | 112. | 10.5 | 22.0 | 8.6 | 9.3 |
| 114 | 7.50 | 14.0 | 3.4 | 9.1 | 2.5 | 3.0 |
| 115 | 8.20 | 28.0 | 5.0 | 7.5 | 4.0 | 4.6 |
| 116 | 7.00 | 55.9 | 8.5 | 4.0 | 6.7 | 7.7 |

TABLE II (*Continued*)

$W_1/W = 0.61$ (*Continued*)

| *Run* | $\beta = 10^3$ | $q_1$ | $D_1$ | $D_2$ | $D_{1T}$ | $D_1$* |
|---|---|---|---|---|---|---|
| C–3–117 | 6.40 | 4.67 | 2.0 | 20.5 | 1.6 | 1.5 |
| 118 | 7.10 | 14.0 | 3.4 | 19.1 | 2.7 | 3.0 |
| 119 | 8.10 | 28.0 | 4.5 | 18.0 | 3.5 | 4.6 |
| 120 | 7.10 | 55.9 | 8.2 | 14.3 | 6.5 | 7.7 |
| 121 | 7.50 | 112. | 12.0 | 10.5 | 9.0 | 11.9 |
| 122 | 7.10 | 4.67 | 2.0 | 30.5 | 1.4 | 1.5 |
| 123 | 7.00 | 14.0 | 3.5 | 29.0 | 2.8 | 3.1 |
| 124 | 7.80 | 28.0 | 5.2 | 27.3 | 4.0 | 4.7 |
| 125 | 7.00 | 55.9 | 7.9 | 24.6 | 6.2 | 7.7 |
| 126 | 7.40 | 112. | 13.0 | 19.5 | 11.5 | 12.0 |

TABLE III

| Case number | 1 | 2 | 3 | 4 |
|---|---|---|---|---|
| River discharge $ft^3\ sec^{-1}$ | $3 \times 10^4$ | $6 \times 10^4$ | $10 \times 10^4$ | $20 \times 10^4$ |
| $q_1$ $ft^2/sec$ | 20 | 40 | 66 | 134 |
| $D_1$ measured ft. | 12 | 15 | 20 | 31 |
| $D_1$ computed ft. | 11 | 17 | 23 | 35 |

TABLE IV

| *Run* | $\beta \times 10^3$ | $q_1'$ | $D_1$ | $D_2$ | $D_1 - D_1'$ | $(D_1 - D_1')$* |
|---|---|---|---|---|---|---|
| | | | $W_1/W = 5.1$ | | | |
| E–3– 1 | 18.7 | 14.5 | 4.2 | 19.0 | 0.6 | 0.5 |
| 2 | 22.9 | 72.5 | 9.0 | 14.0 | 1.1 | 1.7 |
| 3 | 24.0 | 145. | 15.5 | 8.0 | 2.5 | 2.5 |
| 4 | 20.8 | 14.5 | 5.0 | 27.5 | 0.7 | 0.3 |
| 5 | 20.5 | 43.5 | 7.9 | 25.0 | 1.5 | 1.1 |
| 6 | 22.8 | 87.0 | 11.2 | 22.0 | 1.7 | 1.7 |
| 7 | 23.5 | 174. | 17.9 | 16.0 | 2.9 | 2.8 |
| 8 | 22.9 | 14.5 | 4.5 | 8.5 | 0.6 | 0.3 |
| 9 | 23.5 | 43.5 | 6.5 | 7.0 | 1.0 | 1.2 |
| 10 | 23.8 | 87.0 | 11.0 | 2.0 | 1.2 | 1.5 |
| 11 | 14.7 | 14.5 | 4.7 | 8.0 | 0.7 | 0.5 |
| 12 | 15.8 | 43.5 | 8.7 | 4.0 | 1.3 | 1.1 |
| 13 | 13.9 | 14.5 | 4.7 | 18.0 | 0.5 | 0.4 |
| 14 | 14.1 | 43.5 | 9.0 | 14.0 | 1.5 | 1.2 |
| 15 | 6.73 | 14.5 | 6.0 | 7.0 | 1.0 | 0.7 |
| 16 | 23.5 | 43.5 | 8.0 | 5.0 | 1.0 | 0.8 |
| 17 | 8.10 | 43.5 | 10.7 | 12.5 | 1.6 | 1.4 |
| 18 | 6.83 | 87.0 | 16.2 | 6.5 | 2.2 | 2.7 |
| 19 | 7.71 | 43.5 | 10.0 | 23.0 | 1.3 | 1.5 |
| 20 | 7.12 | 87.0 | 15.5 | 17.0 | 2.0 | 2.7 |
| 21 | 6.44 | 174. | 27.5 | 6.0 | 4.5 | 4.5 |
| | | | $W_1/W = 9.8$ | | | |
| E–3–22 | 7.12 | 84.0 | 18.1 | 15.0 | 2.1 | 3.1 |
| 23 | 7.12 | 168. | 27.0 | 6.0 | 4.0 | 3.8 |
| 24 | 7.02 | 42.0 | 11.0 | 21.5 | 1.5 | 1.4 |

# ABSORPTION OF NUTRIENTS BY AQUATIC PLANTS

By

WALTER H. MUNK

*Scripps Institution of Oceanography*[1]

and

GORDON A. RILEY

*Bingham Oceanographic Laboratory*

## ABSTRACT

Formulae are derived for the rate of nutrient absorption by aquatic plants approximating the shapes of spheres, discs, cylinders, and plates. Other parameters are the size and specific gravity of the plant, the nutrient concentration of the medium, and the physical properties affecting the transfer of nutrients toward the plant surface. The formulae allow for convection, i. e., the movement of water relative to the plant. Hence absorption is aided by a current in the case of attached plants and by a rapid sinking rate in the case of plankton. The results are not materially modified by turbulence.

The formulae are applied to problems of diatom growth and adaptation. Any division rate of diatoms corresponds to a certain *minimum* rate of nutrient absorption; this in turn requires a certain sinking rate and therefore a certain excess in specific gravity of the diatoms over that of the surrounding water. In well fertilized laboratory media the excess may be very small, and this is consistent with the slow sinking rates usually observed under laboratory conditions. Under impoverished natural conditions the excess must be much larger, and hence there is a flotation problem. Accordingly, the analysis was extended to take into account sinking rates and vertical overturn in addition to nutrient absorption. The results are realistic with regard to observed division rates and sizes of diatoms, but they indicate an inherent competitive advantage of small diatoms over large ones. The observed size-frequency distribution of diatom species can be accounted for if one introduces an arbitrary predation factor which assumes that small cells are eaten more readily than large ones and that spheres are more acceptable food for small animals than long cylinders and plates.

## 1. INTRODUCTION

It is commonly stated in the literature that the elaboration of diatoms into flat discs, plates, and more intricate shapes is a flotation device. However, this hypothesis ignores the existence of equally common adaptations that have the opposite effect. For example, the formation of centric diatoms into chains reduces the total surface area

[1] Contribution from the Scripps Institution of Oceanography, New Series No. 584. We are indebted to Marston C. Sargent for proposing the problem and examining the manuscript.

and thereby increases the sinking rate. While the necessity of adequate flotation cannot be denied, we must look further for a logical explanation of the whole array of observed morphological variations.

The absorption of essential nutrients is an aspect of phytoplankton ecology that involves both surface-volume relations and sinking rates. Ecological evidence indicates that the rate of absorption often puts an upper limit on plant growth in the sea. This is most likely to occur in warm and stable waters that are also critical from the standpoint of flotation. If variations in size and shape in the diatoms have survival value, the problem should be analyzed in terms of both sinking rates and absorption.

The coexistence of a variety of forms and sizes of diatoms in nature implies that each variety has a slight advantage over the other in a particular set of circumstances, but no single variety maintains an advantage in all circumstances. It remains to be seen whether slight differences of this sort can be detected experimentally. In the present paper we shall take the obvious preliminary step of investigating the underlying physical principles by theoretical methods. Brief attention will also be given to the related problem of absorption by attached plants.

A small grain of solid material sinking through water will absorb heat by *diffusion* and by *forced convection*. We shall assume that the physical laws governing these two processes give also an adequate description of the processes whereby sinking diatoms absorb nutrients. This permits us to be quantitative, within limits.

Unfortunately the theory of forced convection has not been developed to a point where it can easily be applied to our problem. Our knowledge of this subject rests mostly on experimental evidence guided by dimensional analysis. The experiments have been performed largely on wires, spheres and plates for which the Reynolds numbers are larger by at least one order of magnitude than those applicable to sinking diatoms. In order to extrapolate the experimental results into the region of interest, it is necessary to have some guidance from theory as to what should be expected at very small Reynolds numbers. The associated mathematical problem is surprisingly difficult, and there are several published accounts describing these difficulties without giving solutions. The first adequate approximation[2] has been found only very recently by Kronig and Bruijsten (1951), and this work makes it possible to discuss with confidence the relationships for the scale with which we are concerned.

The derivation of these relationships are cumbersome and uninteresting and are contained in Appendix I, pp. 235–239.

[2] See footnote 10 on p. 240.

## 2. THE ABSORPTION AND SINKING RATES

Consider a diatom of mass $m$, containing $rm$ grams of phosphate. Thus $r$ designates the fraction in body weight of phosphate. Suppose $q$ grams of phosphate are transferred each second from the surrounding water to the diatom. The relative rate of absorption may then be expressed by

$$\tau^{-1} = \frac{q}{rm}, \tag{1}$$

where $\tau$ is a measure of the time required to absorb as many grams of phosphate as are initially contained. The time required for a diatom to split in two cannot be much shorter than $\tau$, but it may be longer because of other limiting factors. We shall call $\tau$ the "absorption time."

Different nutrients lead to different absorption times. The nutrient with the largest absorption time imposes the most severe limitation on the possible rate of growth.

The problem is to obtain $q$. It depends on the dimensions of the plant and on the physical characteristics of the surrounding fluid. It will be much larger if the fluid moves past the plant (or vice versa) and continually renews the nutrients in an impoverished film immediately surrounding the plant than if there is no such relative motion. The effect of the moving water is designated as "forced convection," the remaining part as "diffusion."

The forced convection depends on the velocity $v$ of the fluid relative to the plant. This velocity is measured at some distance, say at least three diameters, from the plant, where the disturbing effect on the flow by the plant itself is negligible. We must distinguish between attached[3] plants and freely sinking plants. In the former case the velocity $v$ is an independent variable and is determined by wave action, currents, etc. In the latter case $v$ is dependent only on the properties of the plant and the fluid, provided the effect of turbulence does not have to be taken into account. Apparently this is the case, as will be shown.

The solutions have been derived for five cases: an attached plate, a freely sinking plate, disc, sphere and cylinder. The geometry and dimensions are given in Fig. 1. Such simple geometric arrays are quite inadequate to represent intricate plant forms. All that can be said is that this is the best that can be done and that it is better than making no calculations at all. An indication of the uncertainties arising from the representation of plants by simple geometric bodies

[3] The term "attached" has no bearing here on a flow of nutrients through the stem.

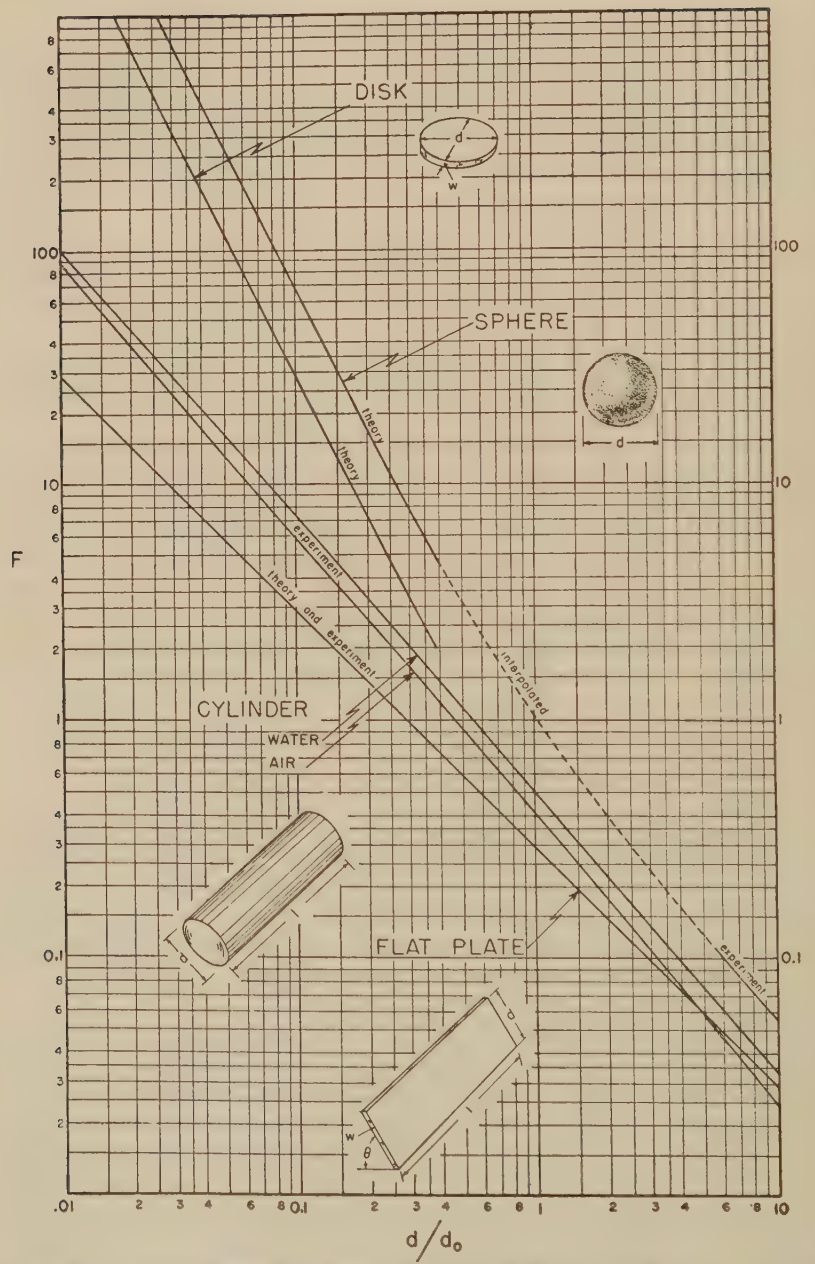


Figure 1. Plot of the relative absorption rate, $F$, as function of the diameter, $d$, for various geometric shapes: a flat plate sinking obliquely along a plane inclined by an angle $\theta$, a sphere, disc and cylinder sinking vertically as shown. In the case of a sphere, the theoretical relation for $d/d_0 < 0.4$ can be smoothly joined to the empirical relation for $d/d_0 > 5$. In the case of the flat plate the theoretical relation has been confirmed by experiment. In the case of the cylinder the relation is wholly empirical. In the case of the disc, it is theoretical. The relations hold for water and air, except for cylinders, where separate curves have been constructed.

is found in the variability of the results among the geometric bodies themselves. The terms of the equations are defined as follows:

| | | |
|---|---|---|
| $v$ | in cm sec$^{-1}$ | velocity of fluid relative to plant, at large distance from plant; |
| $\phi$ | in g cm$^{-3}$ | excess in concentration of nutrient at large distances from plant over concentration at surface of plant; |
| $m$ | in g | mass of plant; |
| $r$ | | mass of nutrient in plant divided by $m$; |
| $\rho$ | in g cm$^{-3}$ | density of surrounding fluid; |
| $\Delta\rho$ | in g cm$^{-3}$ | mean density of plant minus density of fluid. |

The absorption rates in sec$^{-1}$ are given by

attached plate:[4] $$\tau^{-1} = \frac{\phi}{r\rho}\frac{1}{wd^{\frac{1}{2}}}(k'v)^{\frac{1}{2}}\,; \tag{2}$$

sinking plate:[4] $$\tau^{-1} = \frac{\phi}{r\rho}\left(\frac{\Delta\rho}{\rho}\right)^{\frac{1}{3}}\tau_0^{-1}\left(\frac{d^2}{w^2}\sin\theta\right)^{\frac{1}{3}}F_p\,; \tag{3}$$

sinking disc: $$\tau^{-1} = \frac{\phi}{r\rho}\left(\frac{\Delta\rho}{\rho}\right)^{\frac{1}{3}}\tau_0^{-1}\frac{d}{w}F_d\,; \tag{4}$$

sinking sphere: $$\tau^{-1} = \frac{\phi}{r\rho}\left(\frac{\Delta\rho}{\rho}\right)^{\frac{1}{3}}\tau_0^{-1}F_s\,; \tag{5}$$

sinking cylinder: $$\tau^{-1} = \frac{\phi}{r\rho}\left(\frac{\Delta\rho}{\rho}\right)^{\frac{1}{3}}\tau_0^{-1}F_c\,. \tag{6}$$

The sinking rates[5] in cm sec$^{-1}$ are

plate: $$v = v_0\left(\frac{w}{d}\sin\theta\right)^{\frac{1}{3}}Pr^{\frac{1}{3}}F_p'\,; \tag{3a}$$

disc: $$v = v_0\frac{w}{d}F_d'\,; \tag{4a}$$

sphere: $$v = v_0F_s'\,; \tag{5a}$$

cylinder: $$v = v_0F_c'\,. \tag{6a}$$

We shall also need

[4] For the plate we have assumed diffusion negligible compared to forced convection, as will be the case except for extremely small values of $v$.

[5] The expressions for the sinking rate are more elaborate than ordinarily required in order to make it possible to plot the $F$ and $F'$ function against the same parameter $d/d_0$. Thus the diffusivity $k$ enters through $v_0$, and hence $v_0$ on one hand, and through $\delta_0$, and hence $d_0$ on the other hand, but actually the sinking rate is independent of $k$.

$$d_0 = \delta_0(\Delta\rho/\rho)^{-\frac{1}{3}}, \qquad v_0 = v_0(\Delta\rho/\rho)^{\frac{1}{3}}. \qquad (7)$$

Definitions and values are contained in Table I. Scale factors of time, $\tau_0$, of diameter, $\delta_0$, and of speed, $v_0$, depend only on the viscosity and diffusivity of the surrounding medium. The effect of size is contained in the $F$ and $F'$ functions. These are plotted in Figs. 1 and 2

TABLE I. Definitions and Values of Constants

| | | | *Water* | *Air* |
|---|---|---|---|---|
| $\nu$ | $cm^2\,sec^{-1}$ | viscosity at 20° C | 0.01 | 0.15 |
| $k$ | $cm^2\,sec^{-1}$ | diffusivity* at 20° C | $2x10^{-5}$ | 0.15 |
| $k'$ | $cm^2\,sec^{-1}$ | $1.8\,k^{4/3}\,\nu^{-1/3}$ | $4.5x10^{-6}$ | 0.27 |
| $Pr$ | | Prandtl number, $\nu k^{-1}$ | $5.0x10^{2}$ | 1.00 |
| $\tau_0$ | sec | $(\nu^2/g^2k)^{1/3}$ | $1.73x10^{-2}$ | $0.54x10^{-2}$ |
| $\delta_0$ | cm | $(72\nu\ k/g)^{1/3}$ | $0.24x10^{-2}$ | $12.0x10^{-2}$ |
| $v_0$ | $cm\,sec^{-1}$ | $(k^2\,g/72\nu)^{1/3}$ | $8.17x10^{-3}$ | 1.27 |

* The diffusion coefficient may vary by a factor of two depending on the nature of the solute.

against $d/d_0$, where $d$ is the diameter (the length in the direction of flow in the case of the plate). Numerical examples are given in Section 4. Table I and Figs. 1 and 2 deal with water and air, but no application will be made to conditions in air.

## 3. ATTACHED PLANTS

We shall represent a leaf by a thin plate of density $\rho$ and with the dimensions given in Fig. 1. The flow is along $d$. The surface area on both sides is $s = 2ld$, and the mass $m = \rho ldw = \rho(\frac{1}{2}\,s)w$. It follows from equation (1) that

$$\frac{q}{s} = \frac{r}{\tau}\frac{m}{s} = \frac{r\rho w}{2\tau}$$

is the absorption per unit surface area. Solving equation (2) for $v$ yields

$$v = \left(\frac{2q}{s}\right)^2 \frac{1}{\phi^2}\frac{d}{k'}.$$

Setting the absorption at $q/s = 10^{-10}$ g $sec^{-1}$ $cm^{-2}$, $\phi = 3.1x10^{-8}$ g $cm^{-3}$ (1 $\mu$g-at $P/l$), $d = 4$ cm, yields $v = 37$ cm/sec. If the nutrient concentration is reduced to 0.5 $\mu$g-at $P/l$, $v = 150$ cm/sec. It would appear that attached plants must obtain their nutrients from the sea bottom or a bacterial slime film, or otherwise exist in an environment rich in nutrients and exposed to high velocities such as are found in shallow

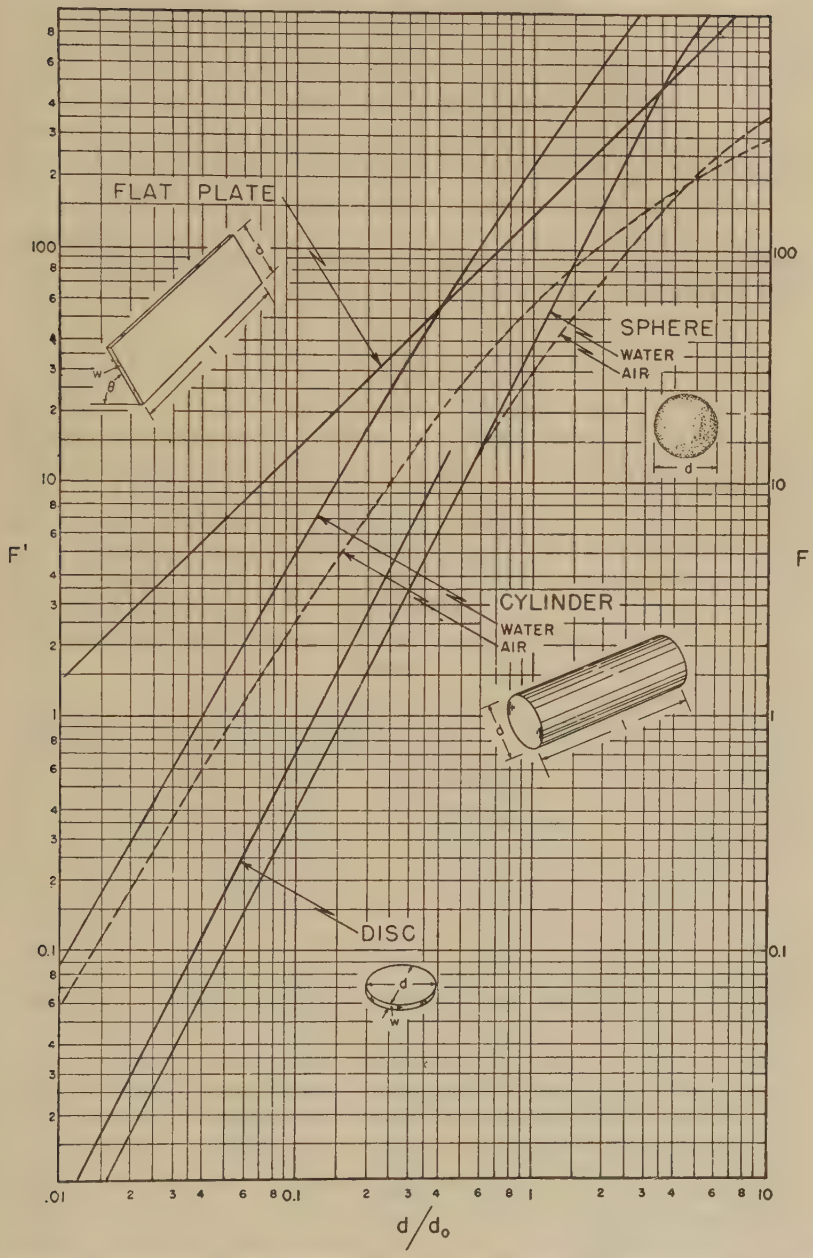


**Figure 2. Plot of the relative sinking rate, $F'$, as function of the diameter, $d$, for the various geometric shapes considered in Fig. 1. The curves are based on both theoretical and experimental considerations.**

water along open coast lines. Unattached plants can meet their nutrient requirements by being small, as will be shown next.

## 4. SINKING PLANTS

The curves in Fig. 1 show the effect of size on absorption time. For any given form and shape ($w/d$ constant), the absorption time always increases with increasing size. As far as absorption of nutrients is concerned, small size is therefore always an advantage. This factor is, of course, only a part of a complex problem which involves the merits of structural differentiation, the predator-prey relationships, etc.

Let the slope of the curves be denoted by

$$m = \frac{d \log F}{d \log x}, \tag{8}$$

where $x = d/d_0$. For the plate, $m_p = -1$. This means that the *absorption rate per unit mass is doubled when the dimension d is halved.* For cylinders, $m_c = -1.2$. For large spheres, $m_s - 1.1$; for small spheres, $m_s = -2.0$. The advantage of small size is most pronounced for small spheres. The change in slope[6] of the curve for spheres represents a marked change in the advantage of small size for spheres smaller than $d_0$ as compared to spheres larger than $d_0$. It may be significant that, in the case of water, $d_0$ is roughly 0.01 cm (100 $\mu$), a value fairly representative of the diameter of diatoms.

In the case of sinking plates, the absorption time varies as $w^{2/3}\ d^{1/3}$. It is remarkable how much more effectively the production of organic material is increased by splitting as compared to dividing lengthwise (in the direction of flow). Splitting increases $\tau^{-1}$ by $2^{2/3}$, dividing by $2^{1/3}$. The number of diatoms resulting from a single diatom by dividing after $n$ generations is $2^n$. In the same time interval the splitting diatoms will have gone through $2^{1/3}\ n$ generations, and the number of diatoms will equal $2^{2^{1/3}n}$. The ratio $2^{(2^{1/3}-1)n}$ equals 100 after 25 generations.

A few examples will illustrate the application of the formulae and the kind of information they provide on the problems of diatom existence. Assume an array of diatoms approximating the ideal shapes of spheres,[7] discs, and long cylinders and plates in which the dimension

[6] The physical interpretation of this change in slope is that for $d \ll d_0$ absorption is largely by diffusion, whereas for $d \gg d_0$ absorption is largely by forced convection. An increase in size leads to a smaller surface/volume ratio, and this is always unfavorable. In the case of convection, however, some of the disadvantage is offset by an increase in the sinking rate.

[7] While true spheres are rare, the specifications will be closely approximated by discs in which the thickness equals the diameter and perhaps also by more irregular shapes such as *Biddulphia.*

$d$ (Fig. 1) ranges from .0005 to .03 cm (5 to 300 $\mu$). Let the ratio of diameter to thickness in the discs be 3:1 and of width to thickness in the plates 5:1. The angle of the plate is 10°. Phosphorus is designated as the limiting nutrient, and its concentration $r$ in the diatom is assumed to be .001 (based on the estimate that phosphorus constitutes about 1% of the total organic matter and that the latter is about 10% of the wet weight).

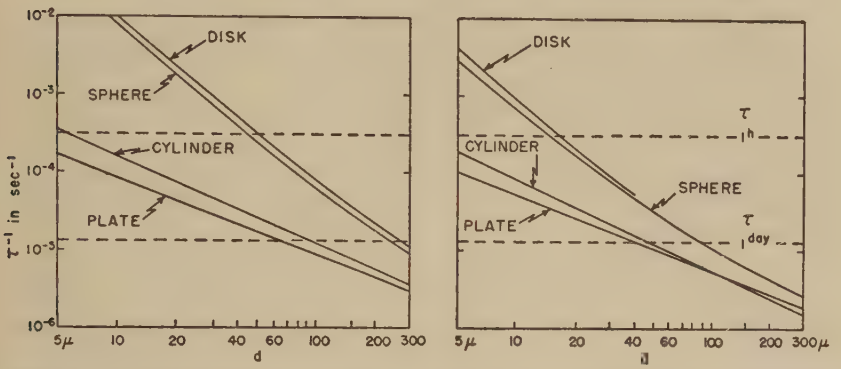


Figure 3. Absorption rates $\tau^{-1}$ (in sec$^{-1}$) for bodies of various sizes $d$ (in $\mu$) corresponding to example 1 (left) and example 3 (right).

*Example* 1. In well fertilized laboratory media, diatoms generally have a nearly negligible sinking rate. A similar condition may exist in the sea during flowerings. To simulate this condition in the model, let $\Delta\rho/\rho = .0001$; $\phi = 3.1 \times 10^{-8}$ g cm$^{-3}$ (1 $\mu$g-at $P/l$). This gives $d_0 = 0.052$ cm, $v_0 = 3.8 \times 10^{-4}$ cm sec$^{-1}$, according to equations (7). For a sphere in water with $d = 0.01$ cm (100 $\mu$), we find $d/d_0 = 0.19$, and hence $F_s = 19$, $F_s' = 1.5$, according to Figs. 1 and 2 respectively. From equation (5) we obtain $\tau^{-1} = 7.1 \times 10^{-5}$ sec$^{-1}$, or $\tau = 4$ hours; from (5a) $v = 5.6 \times 10^{-4}$ cm sec$^{-1}$, or 2 cm/hour. The computed absorption rates are plotted in Fig. 3 (left). They set a maximum limit to the size of diatoms that can absorb sufficient phosphorus to maintain an adequate division rate. For example, one division per day ($\tau^{-1} = 1.16 \times 10^{-5}$) requires that the width of a plate shall not exceed 76 $\mu$ and that the diameter of spheres, discs and cylinders shall not be greater than 260, 300, and 105 $\mu$ respectively. More than 90% of the marine diatom species fall within the prescribed maximum limits. Larger sizes require further reductions in specific gravity in order to maintain negligible sinking rates, and nutrient absorption then requires an increase in $\phi$ or a decrease in $r$.

*Example 2.* If $\phi$ is reduced to $3.1 \times 10^{-9}$ g cm$^{-3}$ (0.1 $\mu$g-at $P/l$) and other conditions remain the same, the value of $\tau^{-1}$ in Fig. 3 (left) will be reduced one order of magnitude. Plates and cylinders capable of maintaining one division per day will then have a maximum dimension $d$ of less than 10 $\mu$. Spheres and discs will have maximum diameters of 61 and 65 $\mu$ respectively. These are unrealistic results, particularly for plates and cylinders. Larger species have been observed in the sea under conditions of severe nutrient depletion.

*Example 3.* $\phi$ remains $3.1 \times 10^{-9}$ g cm$^{-3}$. Let $\Delta\rho/\rho$ increase to .02; i. e., the specific gravity of the diatoms is now about 1.045. Unfortunately the flat disc can no longer be included in the calculation, since the value of $d/d_0$ exceeds the limits of the curve in Fig. 1. The other calculations are illustrated in Fig. 3 (right). The relative effectiveness of plates and cylinders is now greatly increased. The maximum size permitting one division per day ranges between 48 and 95 $\mu$ in the different groups.

The change is due of course to the fact that the increase in specific gravity increases the sinking rate and thereby accelerates nutrient absorption. It should be pointed out in this connection that nutrient depletion in experimental cultures is commonly accompanied by an increased sinking rate. The same phenomenon may occur in the sea toward the end of a flowering and perhaps throughout the summer. There may be an increase in specific gravity due to the accumulation of storage products that cannot be used for reproduction because of nutrient deficiency. If so, we can postulate a self-regulatory device, since the accumulation of storage products will automatically increase the rate of nutrient absorption. However, the value of such a device is limited. It serves no useful purpose if the sinking rate is rapid enough to carry the diatoms below the euphotic zone before the necessary cell divisions occur. The calculated sinking speeds shown in Fig. 4 are by no means negligible for the larger size categories. Thus it becomes necessary to include the problem of flotation in the solution of the example.

It should be pointed out that values for $\Delta\rho/\rho$ have been so chosen as to yield realistic results with regard to absorption rates. These values of $\Delta\rho/\rho$ may be regarded as minimum values; if they were smaller it would be impossible to reconcile the computed absorption rate with the observed rate of division. In this regard it can be noted that the minimum value under natural conditions (example 3) is several hundred times the value corresponding to well fertilized laboratory media (example 1). Values of $\Delta\rho/\rho$ can be larger than those given. In that case conditions other than nutrient absorption must be limiting the

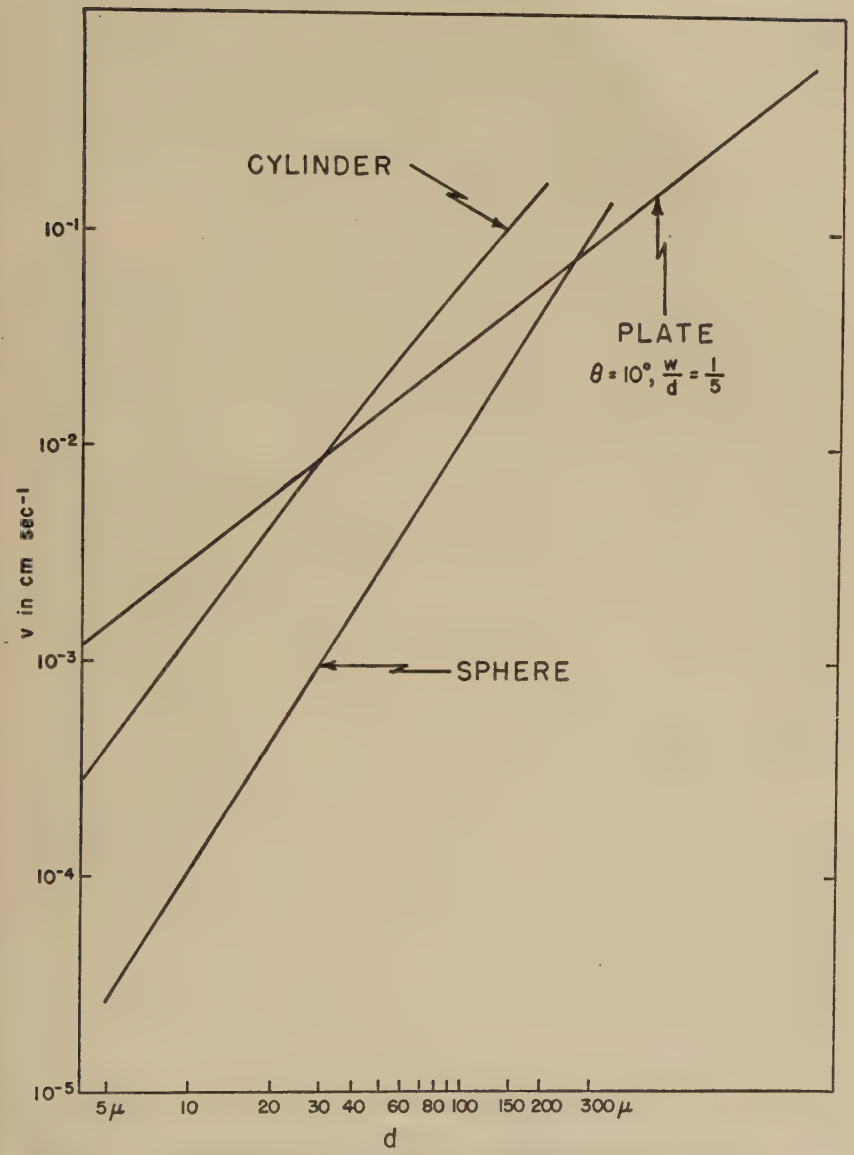


Figure 4. The sinking speed $v$ (in cm sec$^{-1}$) for bodies of various sizes $d$ (in $\mu$), corresponding to example 3, with $\Delta\rho/\rho = 0.02$.

rate of division. Apparently values of $\Delta\rho/\rho$ cannot be very much larger, or they would lead to unrealistic sinking rates. For the purpose of this paper we shall develop the implications of the hypothesis that nutrient absorption is one limiting factor. Our evidence does not permit us to say whether this is usually, or even sometimes, the case. On the other hand, there is nothing in our quantitative results that would make this hypothesis difficult to maintain.

## 5. THE FLOTATION PROBLEM

Perhaps the simplest way to analyze the flotation problem is to make use of a theoretical relationship derived by Riley, Stommel, and Bumpus (1949: 90). It postulates that a steady state, nonvanishing plankton distribution cannot occur if $v^2 > 4A\omega$, where $v$ is the sinking speed, $A$ is the coefficient of vertical eddy diffusivity, and $\omega$ is the mean coefficient of production in the euphotic zone.

Other factors may enter the situation and require a lesser sinking speed, but for present purposes it is sufficient to assume that equality exists in the steady state condition. In addition to the sinking speeds in Fig. 4, the analysis requires that we stipulate reasonable values for the eddy coefficient and utilize the calculated nutrient absorption rates to estimate the mean production coefficient $\omega$. The latter was originally defined as the net production coefficient, i. e., diatom multiplication minus predation. In the first approximation we shall assume that predation is negligible, but we shall have to revise the assumption subsequently in Section 6.

The following considerations enter into the calculation of $\omega$:

1. Although the absorption curves in Fig. 3 (right) theoretically permit the small cells to divide many times per day, there exists an inherent biological limit that cannot be surpassed. We shall simplify the situation by assuming that when nutrients are not limiting, the maximum production coefficient, occurring in the upper 20% of the euphotic zone, is $2.32 \times 10^{-5}$/sec (two divisions per day).

2. It will be assumed that in the remainder of the euphotic zone the limiting effect of light produces an exponential decrease with depth to 1% of the surface value. The resulting curve for maximum production is shown as a solid line in Fig. 5 (left).

3. When lack of nutrients reduces surface production, the form of the curve is assumed to change as shown by the dotted line in Fig. 5 (left). Fig. 5 (right) shows the relationship between surface and mean production that results from these assumptions.

Thus Figs. 3 (left) and 5 (left) may be used to estimate the mean production coefficient $\omega$ for various sizes and shapes of cells. Examples are given in Table II, which also lists a critical coefficient $\omega'$:

TABLE II. PRODUCTION COEFFICIENTS

| d | *Sphere* | | | *Cylinder* | | | *Plate* | | |
|---|---|---|---|---|---|---|---|---|---|
| | $10^6\,\omega$ | $10^6\,\omega'$ | | $10^6\,\omega$ | $10^6\,\omega'$ | | $10^6\,\omega$ | $10^6\,\omega'$ | |
| $\mu$ | $sec^{-1}$ | $sec^{-1}$ | | $sec^{-1}$ | $sec^{-1}$ | | $sec^{-1}$ | $sec^{-1}$ | |
| | | A ($cm^2sec^{-1}$) | | | A ($cm^2sec^{-1}$) | | | A ($cm^2sec^{-1}$) | |
| | | 10 | 50 | | 10 | 50 | | 10 | 50 |
| 5 | 9.2 | $1.8\times10^{-5}$ | $3.6\times10^{-6}$ | 9.2 | $4.2\times10^{-3}$ | $8.4\times10^{-4}$ | 9.2 | $5.6\times10^{-2}$ | $1.1\times10^{-2}$ |
| 10 | 9.2 | $3.0\times10^{-4}$ | $6.0\times10^{-5}$ | 9.2 | $4.9\times10^{-2}$ | $9.8\times10^{-3}$ | 9.2 | $2.2\times10^{-1}$ | $4.4\times10^{-2}$ |
| 20 | 9.2 | $4.8\times10^{-3}$ | $9.6\times10^{-4}$ | 9.2 | $5.1\times10^{-1}$ | $1.0\times10^{-1}$ | 9.2 | $9.0\times10^{-1}$ | $1.8\times10^{-1}$ |
| 30 | 9.2 | $2.5\times10^{-2}$ | $5.0\times10^{-3}$ | 8.9 | 2.2 | $4.4\times10^{-1}$ | 7.8 | 2.0 | $4.0\times10^{-1}$ |
| 40 | 9.2 | $8.1\times10^{-2}$ | $1.6\times10^{-2}$ | 7.3 | 5.6 | 1.2 | 6.6 | 3.6 | $7.2\times10^{-1}$ |
| 50 | 9.2 | $2.0\times10^{-1}$ | $4.0\times10^{-2}$ | 6.1 | 11 | 2.2 | 5.6 | 5.6 | 1.1 |
| 60 | 9.2 | $4.2\times10^{-1}$ | $8.4\times10^{-2}$ | 5.3 | 20 | 4.0 | 4.9 | 8.1 | 1.6 |
| 70 | 8.0 | $7.8\times10^{-1}$ | $1.6\times10^{-1}$ | 4.7 | 32 | 6.4 | 4.4 | 11 | 2.2 |
| 80 | 7.0 | 1.3 | $2.6\times10^{-1}$ | 4.2 | 48 | 9.6 | 4.1 | 14 | 2.8 |
| 90 | 6.3 | 2.2 | $4.4\times10^{-1}$ | 3.9 | 73 | 15 | 3.8 | 18 | 3.6 |
| 100 | 5.6 | 3.3 | $6.6\times10^{-1}$ | 3.5 | | | 3.5 | 22 | 4.4 |
| 150 | 3.7 | 17 | 3.4 | 2.5 | | | 2.6 | 50 | 10 |
| 200 | 2.9 | 58 | 12 | 1.9 | | | 2.0 | | |

$$\omega' = \frac{v^2}{4A}.$$

When $\omega$ exceeds $\omega'$, the cells will increase unless predation is equal to the difference between the two quantities. When $\omega$ is less than $\omega'$, the species must vanish. Lines in Table II indicate approximately the maximum size of cells that can exist in a steady state condition ($\omega = \omega'$).

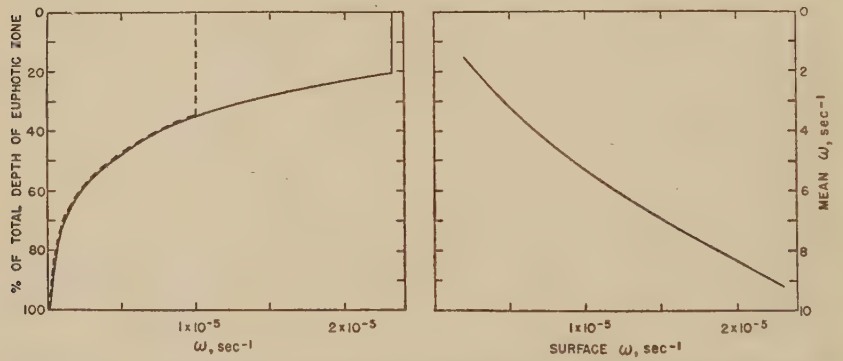


Figure 5. Left: Production coefficient as function of depth. Dashed line illustrates case where nutrient absorption limits production to 1 division in $10^5$ seconds in upper 35% of euphotic zone, and the light intensity limits production in lower 65%. Solid line represents conditions for unlimited nutrient supply. Right: Relationship between surface production and mean production in euphotic zone.

The results serve only to specify maximum size limits. They reveal no good reasons for the evolution of the diatoms into a variety of shapes and sizes. Fig. 3 and Table II indicate that it is an advantage for them to be small. In all size categories, a primitive centric type approximating a sphere appears to be slightly superior to the more elaborate shapes.

## 6. THE GRAZING FACTOR

The fact that neither flotation nor nutrient absorption imposes severe limits upon cells of less than 20 $\mu$ must mean that some other factor is decidedly unfavorable. Otherwise the larger species would not be able to compete with the small cells. Predation is a possible explanation. Although it has been demonstrated (Harvey, 1937) that a large copepod such as *Calanus finmarchicus* feeds most effectively on large cells, it seems likely that the small animals which constitute the major bulk of the zooplankton population would have definite limits as to the size of the food they encompass. Therefore, two hypotheses are proposed: (a) The average predation coefficient decreases with an

increase in the size of the food species; (b) the coefficient of predation on a sphere is larger than for a cylinder of the same diameter or for a plate of the same width.

An analysis of the hypotheses may be developed as follows:

1. Assume a diatom population of spheres, cylinders, and plates of varying sizes up to the maximum size that can maintain a steady state (cf Table II). In each size category, let the number of spheres, cylinders, and plates be initially equal.

2. Further assume that the total number of cells in the population has a steady state existence. This does not necessarily imply that any particular shape of cell exists in a steady state, but if, for example, the number of spheres of a particular size increases, there must be a corresponding decrease of plates or cylinders. The requirements of the first two assumptions will be fulfilled if, in each size category, the production coefficient equals the mean value of $\omega'$ (Table II) for the three shapes. This in turn requires that the predation coefficient equal the mean value of $\omega - \omega'$. The latter decreases with increasing size of the cells in accordance with hypothesis (a).

3. To fulfill hypothesis (b), a modification must now be introduced. It is arbitrarily assumed that the coefficient of predation on a cylinder of a given diameter and on a plate of the same width will be equal to the predation on a sphere with a diameter three times as large. This is readily accomplished in the model by comparing 10 $\mu$ cylinders and plates with 30 $\mu$ spheres, etc.

Thus in the two examples in Table II ($A = 10$ and $A = 50$ cm$^2$ sec$^{-1}$), positive values of $\omega - \omega'$ are averaged for each of the stipulated size groups. For each shape, the deviation of $\omega - \omega'$ from the mean is plotted in Fig. 6. Within the limits of the simplified assumptions, the deviations of each shape from the steady state existence of the population as a whole are indicative of the competition pressure exerted by a particular size and shape of diatom.

Cells of less than 20 $\mu$ show no striking differences in ability to compete. Within this range, competition must depend primarily upon factors that are not considered in the present analysis, namely inherent biological potentialities and reactions to the physical variations of the environment. In the larger size categories, cylinders appear to be particularly effective in the size range of 20 to 55 $\mu$, plates from 30 to 95 $\mu$. The spheroidal type appears to have a wider range of effectiveness than the other two shapes. In the present example it is not excessively dominant in any size category, but the form of the curve can be altered by changing assumption 3. If the spheres are compared with other shapes of half the size, instead of one-third, there is a strong peak of effectiveness centered at 60 $\mu$.

## 7. COMPARISON WITH OBSERVED SIZE-FREQUENCY DISTRIBUTIONS

To determine whether these results have any meaning, we must inquire as to whether they bear any relation to observed diatom speciation. A list of species was prepared, more or less approximating the ideal shapes under consideration. The list will not be reproduced in detail, but the following genera were included:

| Spheroids | Cylinders | Plates |
|---|---|---|
| *Thalassiosira* | *Rhizosolenia* | *Eucampia* |
| *Coscinodiscus* | *Lauderia* | *Climacodium* |
| *Hyalodiscus* | *Schroderella* | *Streptotheca* |
| *Lauderia* | *Dactyliosolen* | *Hemiaulis* |
| *Stephanodiscus* | *Leptocylindricus* | *Striatella* |
| *Biddulphia* | *Guinardia* | *Plagiogramma* |
| | *Ditylum* | *Pseudoeunotia* |
| | *Cerataulina* | *Achnathes* |
| 22 species | 31 species | 11 species |

*Lauderia glacialis* is placed among the spheroids, *L. borealis* with the cylinders.

The size limits of each species as listed by Cupp (1943) were then used to determine the size-frequency distribution of each shape, expressed as the percentage of the total number of species occurring in each size category. The results, plotted in Fig. 6, show that frequency modes of observed speciation correspond with favorable portions of the theoretical curves.

The large and important genus *Chaetoceros* is not included in the analysis. The individual species intergrade between plate-like and cylindrical form. The effect of the spines on its behavior is uncertain. However, examination of the genus shows a mode in the number of species at 12 $\mu$, with less than 20% of the species in any size category above 35 $\mu$. It could be placed with plates or cylinders without producing serious discord.

A small number of spheroids and cylinders (primarily *Coscinodiscus* and *Rhizosolenia*) greatly exceed the maximum size limits predicted by the example. They probably represent a special case that does not meet the initial assumptions. *Coscinodiscus* in particular has an unusually large vacuole, which probably gives it an abnormally low specific gravity and nutrient content. This appears on theoretical grounds to be virtually a necessity for large diatoms occurring in stable waters deficient in nutrients. For example, the 200 $\mu$ sphere in Table II requires an eddy coefficient of 200 $cm^2\ sec^{-1}$ in order to maintain

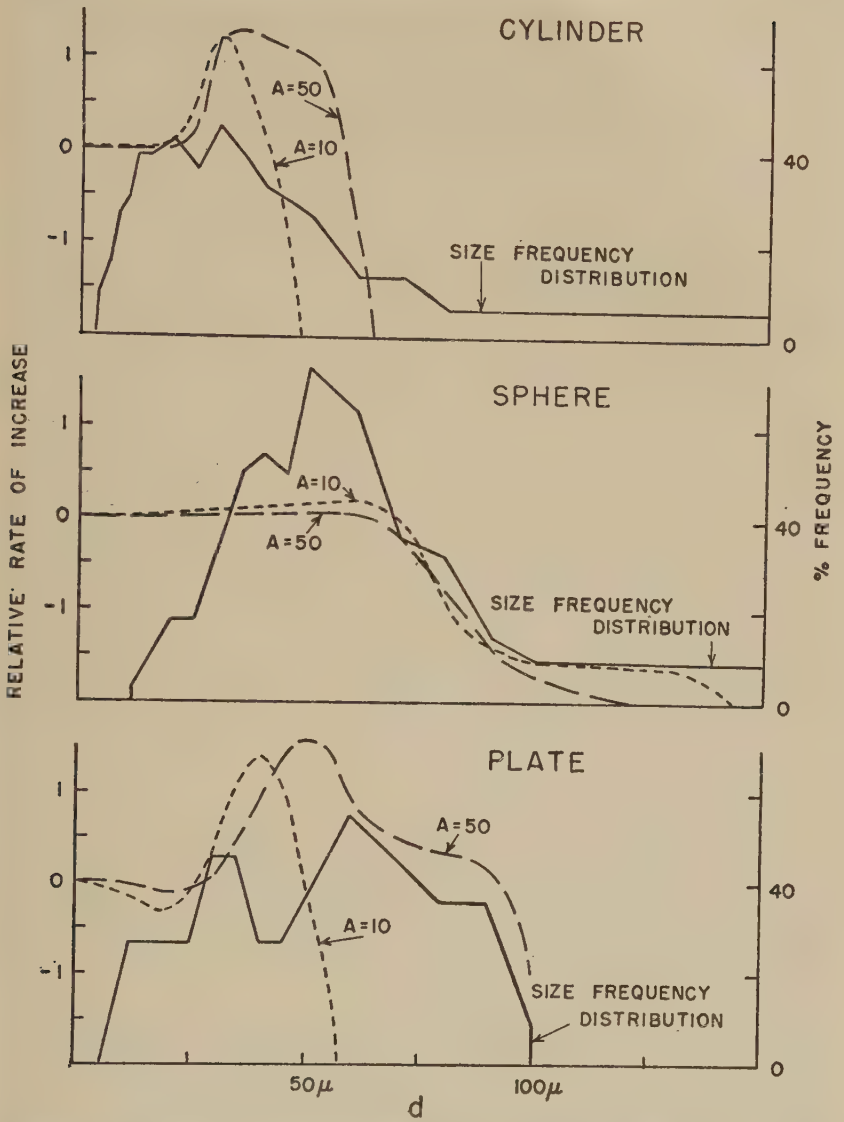


Figure 6. The dashed lines, corresponding to eddy viscosities of 10 and 50 $cm^2 sec^{-1}$, are indicative of the "competition pressure" exerted by diatoms of stated shapes and sizes. These curves are based on an analysis which takes into account nutrient absorption, the flotation problem (including sinking rates and vertical overturn), and the grazing factor. The solid curves give the observed size-frequency distribution for species resembling spheroids, cylinders, and plates, respectively.

a steady state in the absence of predation. If this cell is increased to a diameter of 300 $\mu$ solely by the addition of vacuolar space containing a fluid of the specific gravity and phosphorus content of the surrounding sea water, it will then be capable of maintaining a steady state in the absence of predation with an eddy diffusion coefficient of only 17 $cm^2\ sec^{-1}$.

In short, the analysis has revealed a situation too complicated to be tested easily by experiments or to be solved indisputably by theory. However, the calculated curves of competition pressure in relation to size and shape find some degree of support in the observable facts of nature. It seems likely that diatom speciation is the product of three essential ingredients—responses to problems of flotation, nutrient absorption, and predation. In large diatoms the chief problems are flotation and nutrient absorption, and adaptations that tend to reduce these difficulties have been noted. In small diatoms, predation appears to be more important, and it is common to find chain formation and elaboration of shape, which must be of some help in avoiding nauplii and other small predators. In the intermediate size range, the formation of chains is presumed to be advantageous from the standpoint of predation, but it tends to endanger flotation and nutrient absorption. Here some curious adaptations are found. *Thalassiosira* and some other genera succeed in forming chains without sacrificing the advantages of discoid shape. About half of the plate-like species form chains that are curved or twisted. This tends to impart lateral motion to the sinking cells, thus improving nutrient absorption without greatly affecting the vertical velocity.

## 8. THE EFFECT OF TEMPERATURE ON ABSORPTION

A change in temperature will effect the rate of absorption by varying the physical constants in the surrounding medium and possibly by changes inside the plankton. We shall consider the external effects only. These may be regarded as constituting a lower limit on the temperature effect.

By far the most important effect of temperature can be ascribed to variations in diffusion coefficient $k$ and viscosity $\nu$. In most substances the viscosity decreases with temperature by about 2.5%/°C whereas the diffusion coefficient *increases* by about the same amount:

$$\alpha = \frac{1}{k}\frac{dk}{dT} = -\frac{1}{\nu}\frac{d\nu}{dT} = 0.025\ (°C)^{-1}.$$

The coefficients appear in the combination $(\nu k)^{1/3}$ in the parameter $d_0$, and the temperature effects of $\nu$ and $k$ cancel in the first approximation.

The coefficients appear also in the constant $\tau_0^{-1}$ in the combination $k^{1/3}\ \nu^{-2/3}$. This leads to

$$\frac{1}{\tau^{-1}}\frac{d\tau^{-1}}{dT} = \frac{1}{\tau_0^{-1}}\frac{d\tau_0^{-1}}{dT} = \alpha \tag{9}$$

for sinking plates, spheres and cylinders alike. Goldberg's[8] very rough estimate on the basis of his experiments is a factor of 5–10%/°C, i. e., from 2 $\alpha$ to 4 $\alpha$. According to (9) the maximum absorption rate in the tropics might be roughly twice that in the arctic. Similar results have been obtained in studies of the photosynthesis and growth of natural phytoplankton populations (Riley, Stommel and Bumpus, 1949: 94).

## 9. THE EFFECT OF TURBULENCE AND NOISE ON ABSORPTION

In our discussion we have dealt with sinking through still water. Yet whenever suitable measurements have been made, it has been found that the ocean is in turbulent motion.

Turbulence enters the general problem in a number of ways: it brings about the replenishment of the nutrients in the euphotic zone, i. e., it affects the value of $\phi$ in our equation (1); large eddies help maintain the sinking diatoms in the euphotic zone (Section 5); turbulence also erases the tiny trails of impoverished water left behind the individual diatoms sinking through the water. These effects enter only indirectly into the problem concerning the absorption of nutrients by sinking diatoms.

Here we shall be concerned only with the effect of turbulence in increasing the volume of water with which plankton are in immediate contact. For this purpose turbulence can be regarded to include all the unsteady motion. This motion can be resolved into many different frequencies. Low frequencies, with periods of, say, 10 seconds, are due largely to ocean waves (whether the waves are regular or not is of no consequence here); noise in the sea is associated with frequencies above 100 cycles/sec. Consider now a small sphere slowly sinking through water. The sphere can follow low frequency oscillations of the surrounding water without appreciable lag. However, with increasing frequency a condition is reached where the sphere is no longer able to follow the water motion without lag. For even higher frequencies the sphere will remain virtually stationary, while the water will wash back and forth along its sides. Such high frequency turbulence is therefore associated with a "forced draft" which can be expected to increase the nutrient made available to plankton.

[8] Personal communication.

For any *fixed* amplitude of oscillation, the most effective forced draft is associated with the highest frequencies, i. e., acoustic noise. However, it is found that amplitude of oscillations in the ocean drops off so rapidly with increasing frequency that the most effective portion of the turbulence spectrum lies in the low frequencies. Even there, as will be shown, the effect is quite small.

TABLE III. VALUES OF PERTINENT PARAMETERS

| | *Surface waves* | *Sound waves* | |
|---|---|---|---|
| Frequency $\sigma/2\pi$ in cycles per second | $10^{-1}$ | $10^{3}$ | $10^{4}$ |
| Wave length $L$ in cm | 15,000 | 1500 | 15 |
| $\beta$ for $d = 10^{-2}$cm (100$\mu$) | $2\times10^{-6}$ | $2\times10^{-5}$ | $2\times10^{-3}$ |
| $\gamma$ for $d = 10^{-2}$cm (100$\mu$) | 0.03 | 0.9 | 9 |

The theory is rather involved. Fortunately it is closely related to the problem of the attenuation of sound by fog, which has received the attention of the mathematicians and experimentalists (Epstein, 1941). Let us define the ventilation

$$h = \frac{v_{water} - v_{sphere}}{v_{Stokes}}$$

as the ratio between the mean slippage through the water associated with turbulence, and the sinking velocity $v_{Stokes}$ according to Stokes' law. The slippage depends on three dimensionless quantities,

$$\frac{\Delta\rho}{\rho}, \quad \beta = \frac{\pi d}{L}, \quad \gamma^2 = \frac{\sigma d^2}{8\nu},$$

where $L$ is the wave length, $\sigma$ frequency, and $C = L\sigma/2\pi$ the wave velocity. Some values of $\beta$ and $\gamma$ are given in Table III. It appears that $\gamma$ may be large or small compared to unity but that $\beta \ll 1$. In addition $(\Delta\rho/\rho) \ll 1$. With these approximations it can be shown (Appendix 2) that

$$h = \frac{48\nu}{\pi g d^2} f(\gamma) V, \tag{10}$$

where

$$f = \gamma^2/3, \qquad f = \tfrac{1}{2},$$

according to whether the frequency is small ($\gamma \ll 1$) or large ($\gamma \gg 1$). Here $V$ is the amplitude of the velocity of oscillation of the water.

*Surface Waves.* For very low frequencies equation (10) gives the ventilation arising from the viscous effects only. This can be used to analyze the effect of surface waves whose height $H$ equals $2V/\sigma$, and wave length $L = 2\pi g/\sigma^2$. Equation (10) then becomes simply

$$h = 2H/L.$$

The theoretical maximum for $H/L$ equals 1/7 and leads to $h = 0.28$. This value is attained only under extreme conditions; furthermore it applies only to a thin upper layer of thickness, say $L/10$, and diminishes rapidly with increasing depth. Thus under extreme conditions the absorption may be increased by something like 25% in the upper 10 or 20 feet.

*Noise.* For ambient sound it is convenient to convert the amplitude of oscillation to pressure amplitude $P$ and express these in the customary units (see, for example, Knudsen and Harris, 1950). Thus

$$V = \frac{P}{\rho C}, \qquad P = \frac{1}{5000}\, 10^{L'/20},$$

where $L'$ is the sound level in *db*'s above 0.002 dynes cm$^{-2}$. Measurements of ambient noise (Knudsen, et al., 1948) are well represented by straight lines on a graph $L'$ against log $\sigma$, such as

$$L' = 20\, a - 20\, b \log(\sigma/1000)\ .$$

This leads to

$$\delta h = \frac{48 \nu f(\gamma)}{5000\, \pi \rho g C d^2}\, 10^{a+3b}\, \sigma^{-b}\, \delta\sigma$$

for each frequency band $\delta\sigma$. We shall overestimate the effect by setting $f(\gamma) = \frac{1}{2}$. Integrating from $\sigma_1$ to $\sigma_2$, this gives

$$h = h_0 \frac{10^{a+3b}}{1 - b} \left( {\sigma_2}^{1-b} - {\sigma_1}^{1-b} \right),$$

where

$$h_0 = \frac{24 \nu}{5000\, \pi \rho g C d^2}$$

equals $10^{-9}$ for $d = 0.01$ cm (100 $\mu$).

For ordinary water noises from 100 to 25,000 cycles, $a = 2.25, b = 0.8$. Since $1 - b$ is positive, the larger contribution is made by the higher frequencies. Between the stated limits, this gives $h = 10^{-3}$.

In a very noisy croaker bed one may set $a = 4$, $b = 0$ from $\sigma = 10^2$ to $10^3$ sec$^{-1}$, and $a = 4$, $b = 3$ from $10^3$ to $10^4$ sec$^{-1}$. These values lead to $h = 10^{-2}$ for either range of frequencies. The effect of ambient noise is therefore negligible.

## APPENDIX I: DERIVATION OF ABSORPTION RATES

The three nondimensional numbers that are encountered in problems of forced convection are the Reynolds, Prandtl, and Nusselt numbers

$$Re = \frac{vd}{\nu} \qquad Pr = \frac{\nu}{k} \qquad Nu = \frac{9d}{ks\phi}. \tag{11}$$

In some texts the Péclet number $Pe = Re\ Pr$ is referred to. Here $v$ is the velocity at large distances, $\nu$ the kinematic viscosity, $k$ the diffusivity, $q$ the grams of a concentrate transferred each second to an immersed body of surface area $s$, $\phi$ the concentration at large distances over that at the surface of the body (in g cm$^{-3}$), and $d$ a representative dimension of the body. Let $p$ be the volume, $\rho$ the density, and $m = \rho p$ be the mass of the body. Then equation (1) can be written

$$\tau^{-1} = \frac{\phi}{r\rho}\frac{ks}{vd}Nu = \frac{\phi}{r\rho}\left(\frac{\Delta\rho}{\rho}\right)^{2/3}\tau_0^{-1}\,GF, \tag{12}$$

where

$$G = sd/cp \tag{13}$$

depends on the geometric dimensions, and

$$F = 72^{-2/3}\,c\,Nu(d/d_0)^{-2}. \tag{14}$$

The constant $c$ is so chosen as to make $G$ a ratio of dimensions only.

With regard to sinking rate, it is convenient to define a quantity $u_0 = k/d_0$. Then it follows from (11) that

$$\frac{u}{u_0} = \frac{Re\ Pr}{d/d_0}. \tag{15}$$

*Attached Plate.* This problem has been studied theoretically by Pohlhausen with regard to a flat plate thermometer oriented parallel to flow (Goldstein, 1938: Chap. 14). For one side of the plate

$$Nu = 0.67\ Pr^{\frac{1}{3}}\,Re^{\frac{1}{2}}, \tag{16}$$

where $d$ in the Reynolds number now represents the length of a thin plate in the direction of flow. The equation has been verified experimentally. For the dimension as given in Fig. 1, substitution of (16) into (1) leads at once to equation (2).

*Sinking Plate.* The quantity $v$ is no longer an independent variable but equals the sinking speed. Consider the plate slicing obliquely downward and forming an angle $\theta$ with the horizontal (Fig. 1). Then after the plate has reached its terminal velocity, the frictional forces on its sides is balanced by the pull of gravity:

$$2Tld = g \sin\theta\ \Delta\rho\ lwd,$$

where $T$ is the frictional stress per unit surface area and $\Delta\rho$ the density of the diatom minus the density of the surrounding medium. The stress can be equated to

$$T = \nu\rho\left(\frac{dv}{dy}\right)_{y=0} = 2v\nu\rho\,\frac{2}{5.83}\sqrt{\frac{v}{\nu d}}$$

according to Von Kárman's boundary layer theory (Goldstein, 1938: Chap. 4). This leads to the dimensionless expression

$$Re^{3/2} = 0.73(\Delta\rho/\rho)g\sin\theta\, wd^2\nu^{-2}$$
$$= (0.73)(72)\sin\theta\,(w/d)\,Pr^{-1}(d/d_0)^3 \quad (17)$$

for the sinking rate $v = Re\ \nu/d$ along an axis inclined by an angle $\theta$. Combining equations (13) to (17) leads to

$$G_p = (d^2\sin\theta/w^2)^{1/3},$$
$$F_p = (1.34)(0.73)^{1/3}(72)^{-1/3}(d/d_0)^{-1} = 0.29(d/d_0)^{-1},$$
$$F_p' = (0.73)^{2/3}(72)^{2/3}(d/d_0) = 14(d/d_0).$$

*Sinking Sphere.* For $Pr$ from 0.7 to 400 and $Nu$ from 10 to 40, the following relationship is in agreement with experimental evidence and dimensional considerations (Kramer, 1946):

$$Nu = 2.0 + 1.3\,Pr^{0.15} + 0.66\,Pr^{0.31}\,Re^{0.15}. \quad (18)$$

Note the combination $Pr^{0.31}\,Re^{0.5}$, which is similar to the one encountered for the flat plate. For water and air this becomes, respectively

$$Nu = 5.3 + 4.6\,Re^{0.5} \quad (18w)$$
$$Nu = 3.3 + 0.66\,Re^{0.5}. \quad (18a)$$

In these experiments the rate of flow past the sphere, as expressed by $Re$, could be varied independently. For freely falling spheres, it is already determined by the balance between the gravitational force and the drag:

$$\frac{1}{6}\pi\,\Delta\rho\,gd^3 = \frac{1}{2}C_D\,\rho v^2\left(\frac{\pi d^2}{4}\right).$$

The drag coefficient in the range over which Stokes' law is applicable equals $C_D = 24\,Re^{-1}$. We shall write, in general,

$$C_D = 24\,Re^{-1}f_s, \quad (19)$$

where the function $f_s(Re)$ can be taken from experimental data (Goldstein, 1938: 493). This leads to the dimensionless expression

$$f_s\,Re\,Pr = 4(d/d_0)^3 \quad (20)$$

for the sinking rate $v = \nu\,Re/d$ of a freely falling sphere. Thus $F_s' = 4(d/d_0)^2/f_s$. The absorption rate for the sphere (eq. 5) is now obtained

in the following manner: in eq. (13) we set $s = \pi d^2$, $p = \pi d^3/6$, and $c = 6$. This leads to $G_s = 1$, and

$$F_s = 6 \times 72^{-2/3}\, Nu(d/d_0)^{-2} = 0.345\, Nu(d/d_0)^{-2}\,. \tag{21}$$

We then substitute for $Nu$ in terms of $Re$ according to (18) and for $Re$ in terms of $d/d_0$ according to (20).

For small values of $Pe = Re\, Pr$, Kronig and Bruijsten (1951) obtain from theory[9]

$$Nu = 2 + \frac{1}{2} Pe + \frac{581}{1920} Pe^2 + \ldots \tag{22}$$

The empirical and experimental curves are shown in Fig. 1.

*Sinking Disc.* According to Oberbeck (Lamb, 1932: 597–604), $Nu = 8/\pi$ for a disc at rest. This compares to $Nu = 2$ for a resting sphere. Setting $s = \pi d^2/2$, $p = w\pi d^2/4$, and $c = 2$ gives $G_d = d/w$ and $F_d/F_s = 4/3\pi$. This ratio applies only to small discs (Fig. 1). We know of no empirical or theoretical evidence which would permit us to extend these calculations into a more pertinent range.

In computing the sinking rate of a small disc, we note that, according to theory and observations, small (but not too small) objects sink with the flat side horizontal. Equating the resistance to the force of gravity,

$$6\pi\mu \left(\frac{4d}{3\pi}\right) v = \pi \left(\frac{d}{2}\right)^2 w\, \Delta\rho\, g$$

leads to

$$Re\, Pr = \frac{9\pi}{4} \frac{w}{d} \left(\frac{d}{d_0}\right)^3$$

for the sinking speed. This yields $F_d' = (9\pi/4)(d/d_0)^2$.

*Sinking Cylinder.* Because of the relative ease with which measurements can be made with fine wires, the empirical evidence is more complete than for other shapes. For $Re > 50$, Ulsamer (Kramer, 1946) finds

$$Nu = 0.60\, Pr^{0.31}\, Re^{0.5}\,. \tag{23a}$$

The occurrence of $Pr^{0.31}\, Re^{0.5}$ should be noted. For $Re$ from 0.1 to 50, Ulsamer finds, on the average,

$$Nu = 0.91\, Pr^{0.31}\, Re^{0.385}\,. \tag{23b}$$

At $Re = 0.1$, $Nu \sim Re^{0.3}$ approximately. There is also some theoretical evidence that, for very small Reynolds numbers, $Nu$ should be a function of $(Pr\, Re)$ only, hence the exponent of $Re$ would approach 0.31. Apparently we shall not be far amiss if we set

[9] See footnote 10 on p. 240.

$$Nu = 0.8\, Pr^{0.31}\, Re^{0.31} \tag{23c}$$

for $Re \ll 1$. For the long cylinder (unlike the sphere), $Nu$ must approach zero as $Re$ approaches zero, in agreement with the foregoing type of equations. These three equations (23) define the relationship $Nu(Re)$ with sufficient accuracy for our purposes.

We can again express the sinking rate in nondimensional form. Using the relationships given by Lamb (1932: 616) we obtain

$$\frac{Re\, f_c\, Pr}{\kappa - ln\, Re} = \frac{9}{2}\left(\frac{d}{d_0}\right)^3,$$

where

$$C_D = \frac{8\pi f_c}{Re(\kappa - ln\, Re)}$$

is the drag coefficient, and $f_c(Re)$ can again be determined from empirical data (Goldstein, 1938: 16). For $Re \ll 1$, Oseen's investigations (Lamb, 1932: 616) lead to $f_c(Re) = 1$. Here $\kappa = 0.5 + \log 8 - \eta = 2.00$, and $\eta = 0.577$ is Euler's number. Setting $s = \pi d$, $p = \pi d^2/4$, and $c = 4$ gives $G_c = 1$, and

$$F_c = 4 \times 72^{-2/3}\, Nu\, (d/d_0)^{-2} = 0.23\, Nu\, (d/d_0)^{-2}. \tag{25}$$

We then substitute for $Nu$ in terms of $Re$ according to (23) and for $Re$ in terms of $d/d_0$ according to (24).

## APPENDIX II.

The ratio "$R$" between the displacement of a rigid sphere of density $\rho + \Delta\rho$ to that of the water (density $\rho$) at the position of its center when the sphere is absent is given by (Lamb, 1932: 659–661)

$$R = 1 - \frac{\Delta\rho}{\rho f' + \Delta\rho}, \tag{26}$$

where

$$f' = \frac{3}{4\gamma^2}\left[2\gamma^2 + 3\gamma - i\,(4\beta\gamma + 3\gamma + 3)\right]. \tag{27}$$

According to Table II, $\beta \ll 1$. Furthermore, $\beta \ll \alpha$, provided $2\nu\sigma/C^2 \ll 1$ or $\sigma \ll 10^{12}$ sec$^{-1}$. The simplifications resulting from these approximations have been incorporated in equations (26) and (27).

The following extreme cases should be noted:

1. The sphere oscillates essentially with the surrounding water ($R = 1$) (a) if its density equals that of the surrounding water ($\Delta\rho = 0$), (b) for low frequencies ($\sigma = 0$, $\beta = 0$), (c) for small spheres ($d = 0$, $\beta = 0$), and (d) for very viscous fluids ($\nu = \infty$, $\gamma = 0$). 2. The sphere does

not partake in the oscillation of the surrounding water ($R = 0$) if its density is large ($\Delta\rho = \infty$).

If $\Delta\rho \ll \rho$, $R = 1 - \Delta\rho/\rho f'$, then the mean value of $v_{sphere} - v_{water}$ equals

$$\frac{2}{\pi} V \frac{\Delta\rho}{\rho} (f_r'^2 + f_i'^2)^{-1/2},$$

where $f_r'$ and $f_i'$ are the real and imaginary parts of $f'$. Combining this with Stokes' equation for a small sinking sphere leads to

$$f(\gamma) = \gamma^2(4\gamma^4 + 12\gamma^3 + 18\gamma^2 + 18\gamma + 9)^{-1/2}. \qquad (28)$$

## REFERENCES


Cupp, E. E.
1943. Marine plankton diatoms of the west coast of North America. Bull. Scripps Inst. Oceanogr., *5* (1): 1–238.

Davis, A. H.
1921. Convection from wires in a stream of air. Phil. Mag., (6) *41:* 899–908.

Epstein, P.
1941. On the absorption of sound waves in suspensions and emulsions. Karman Anniversary Volume, Calif. Inst. Techn. 337 pp.

Goldstein, S.
1938. Modern developments in fluid dynamics. Oxford Press, New York. 702 pp.

Harvey, H. W.
1937. Note on selective feeding by *Calanus.* J. Mar. biol. Ass. U. K., *22:* 97–100.

Knudsen, V. O., R. S. Alford and J. W. Emling
1948. Underwater ambient noise. J. Mar. Res., *7* (3): 410–429.

Knudsen, V. O., and C. M. Harris
1950. Acoustical designing in architecture. Wiley and Sons, New York. 45 pp.

Kramer, H.
1946. Heat transfer from spheres to flowing media. Physica, *12:* 61–80.

Kronig, R., and J. Bruijsten
1951. On the theory of the heat and mass transfer from a sphere in a flowing medium at low values of Reynolds number. Appl. Sci. Res., A, *2*, 5–6: 439–446.

Lamb, Horace
1932. Hydrodynamics. Cambridge University Press, London. 738 pp.

Riley, G. A., Henry Stommel and D. F. Bumpus
1949. Quantitative ecology of the plankton of the western North Atlantic. Bull. Bingham oceanogr. Coll., *12* (3): 169 pp.


---

Footnote 10 (added in page proof). Prof. Paul Epstein has just drawn our attention to the fact that the method used by Kronig and Bruijsten (1951) leads to a divergent series, and that only the first two terms in equation (22) of Appendix I, p. 238, are correct. The third term should be $-\frac{1}{4} Pe^2 \ln(\frac{1}{2}\Gamma e^{1/4} Pe)$ instead of $+ (581/1920) Pe^2$, where $\Gamma = 1.781$ is Euler's number. Actually the numerical values and the curve in Fig. 1 are not appreciably affected by this correction.

# DETERMINATIONS OF FREE AND BOUND ASCORBIC ACID IN FISHERY PRODUCTS[1]

By

W. H. HASTINGS AND C. FLOYD SPENCER

*School of Fisheries, University of Washington, Seattle*

## ABSTRACT

Asorbic acid is found in two different forms in fish tissue. One form, soluble in 95% ethanol, constitutes approximately 85% of the total vitamin C content, and the other form, which is insoluble in 95% ethanol, constitutes approximately 15% of the total. Certain fish products have sufficient ascorbic acid to be of importance as dietary sources. Retention of the vitamin on processing varies with different fish products.

## INTRODUCTION

Fresh and processed fish products have been assayed for ascorbic acid, but few have been found to be major dietary sources of this nutrient. In view of the fact that scurvy-free inhabitants of arctic regions exist largely on whole fish or animal diets, it has been suggested that ascorbic acid is bound in animal tissues but is not available for assay by standard acid extraction procedure. It has also been suggested that visceral organs of fish may contain a higher proportion of vitamin C than muscle tissue.

This is a preliminary report of a survey of ascorbic acid in fish and shellfish. A modification of the method used by Roe and Kuether (1943), by which amounts of "bound" and "free" ascorbic acid are determined separately, has been used. The procedure, obtained from Sumerwell and Sealock (1952), has been further modified for use with the materials studies.

## METHOD

The residue from ethanol extractions, from which free ascorbic acid is determined, was digested with trichloracetic acid. The alcoholic and acidic extracts containing free and bound ascorbic acid were cleared, chilled, saturated with carbon dioxide, treated with thiocarbamide and dinitrophenylhydrazine, and incubated. They were then chilled again, sulfuric acid was added, and after aging, the color of the mixture was read in a spectrophotometer at 540 m$\mu$, using a blank with dye addition at the end of incubation as 100% transmitancy. The ascorbic acid osazones which were measured at this wave length

[1] Research carried out with salary assistance from the Biological and Medical Research Fund of the State of Washington.

include l-ascorbic acid, dehydroascorbic acid and diketogulonic acid. Measurements of degradation products of ascorbic acid by the method of Roe, et al. (1948) showed that 0–4% of the total osazone color is due to diketogulonic acid. We believe that the modified Roe and Kuether method as used gives values of ascorbic acid that are more in line with actual *in vivo* levels than does a substraction of diketo form when it shows up in such small amounts.

## RESULTS

Table I presents data on samples assayed for bound, free and total ascorbic acid as well as the percentage of moisture. Fresh silver salmon muscle is typical of fish products, being low in total ascorbic acid and showing no appreciable proportion in the bound form. Fresh Pacific herring contains about 3 mg/100g, with one fifth bound. Fresh tuna muscle appears fairly high with five mgs%, one third of this being in the bound complex.

TABLE I.—Free, Bound and Total Ascorbic Acid and Moisture in Fish and Shellfish
(Ascorbic acid expressed in mgs/100g material)

| *Product* | *Ascorbic Acid* | | | *Moisture* |
|---|---|---|---|---|
| | *Free* | *Bound* | *Total* | (%) |
| Albacore (*Thunnus germo*) | | | | |
| Fresh muscle | 3.5 | 1.6 | 5.1 | 63 |
| Pre-cooked muscle | 3.5 | 1.9 | 5.6 | 55 |
| Canned muscle | 3.0 | 2.1 | 5.1 | — |
| Liver | 10.5 | 11.5 | 22.0 | — |
| Silver salmon (*Oncorhynchus kisutch*) | | | | |
| Fresh muscle | 1.13 | 0.17 | 1.3 | 67 |
| Liver | 8.1 | 1.8 | 9.9 | 75 |
| Roe | 11.5 | 6.5 | 18.0 | 57 |
| Milt | 7.1 | 2.7 | 9.8 | 72 |
| Pacific herring (*Clupea pallasii*) | | | | |
| Fresh muscle | 2.0 | 0.63 | 2.6 | 78 |
| | 3.0 | 0.81 | 3.8 | 73 |
| Canned muscle | 0.25 | 0 | 0.25 | 79 |
| Fresh roe | 11.8 | 2.2 | 14.0 | 75 |
| Canned roe | 1.5 | 0.62 | 2.12 | 75 |
| Pacific oysters (*Ostrea gigas*) | | | | |
| Fresh | 20.0 | 2.3 | 22.3 | 80 |
| Canned meat | 10.5 | 3.3 | 13.8 | 76 |
| Canned liquor | 11.7 | 0.13 | 11.8 | 93 |
| Olympia oysters (*Ostrea lurida*) | | | | |
| Fresh | 36.2 | 1.9 | 38.1 | 83 |

Whole fresh Pacific oysters show significant amounts of ascorbic acid, mostly in the free form. Whole fresh Olympia oysters give even higher amounts, assaying 38 mgs%, which is equal to the average for citrus fruit juices. Tuna liver is high in total ascorbic acid, with 52% present in the bound form. Salmon and herring eggs are high in total amounts, salmon sperm and liver being somewhat less. All these organs contained significant amounts in the bound form.

Canned Pacific oysters, processed at the time when the fresh material was assayed, showed a retention of 80% found in fresh material (see calculations for the free, bound and total ascorbic acid content of oyster meat, oyster liquor and moisture in Table I). Retorting was done at 250° F for 13 minutes in 211 x 309 cans, as recommended by the National Canners Association. Note that 99% of the total ascorbic acid in canned oyster liquor was in the free form as compared to 76% in canned oyster meat. Canned herring and their eggs showed considerable loss after retorting.

## DISCUSSION

The chief purpose of the data shown in Table I is to add information on ascorbic acid sources. The value of determining "free" and "bound" ascorbic acid is not understood. Total levels obtained by adding free and bound ascorbic acid are not significantly different from those determined by the photometric method recommended by The Association of Vitamin Chemists, Inc. (1951, pp. 81–87), which uses a single acid extraction. Yet, up to 15 extractions with ethanol, with no appreciable ascorbic acid after the fifth, have been followed by acid extraction resulting in considerable amounts of "bound" ascorbic acid. It is inconceivable that a single chemical would show this property. More ascorbic acid is recovered from the ethanolic extracted residue by a short heat digestion than by a cold extraction. This is true of canned as well as fresh fish products.

Recent tests with sand sole, *Psettichthys melanostictus*, not shown in Table I, showed 6.0 mgs% ascorbic acid in the liver. After the same species, caught at the same time, had lived in a salt water aquarium for five months, with little food intake, it showed 6.4 mgs% ascorbic acid in liver samples.

## BIBLIOGRAPHY

Roe, J. H. and C. A. Kuether

1943. The determination of asorbic acid in whole blood and urine through the 2, 4-dinitrophenylhydrazine derivative of dehydro-asorbic acid. J. biol. Chem., *147:* 399.

Roe, J. H., M. B. Mills, M. J. Oesterling and C. M. Damron
1948. The determination of diketo-l-gulonic acid, dehydro 1-ascorbic acid and 1-ascorbic acid in the same tissue extract by the 2, 4-dinitrophenylhydrazine method. J. biol. Chem., *174:* 201–208.

Sumerwell, W. N. and R. R. Sealock
1952. The determination of bound ascorbic acid in liver tissue. J. biol. Chem., *196:* 753–759.

The Association of Vitamin Chemists, Inc.
1951. Methods of vitamin assay. pp. 81–87. Interscience Publishers, Inc., New York, 301 pp.

## NOTE TO AUTHORS

The pages of this Journal are open to all contributors, and manuscripts may be submitted to any member of the Board of Editors or to the Managing Editor. Publication will be made only in the English language, but copy may be submitted for consideration in other languages. Aid in translation of accepted manuscripts will be given when possible.

All manuscripts should be typewritten with double space, carefully corrected, with footnotes continuously numbered and set off in the body of the text. If an article is to appear as a contribution from another institution, it should be approved by that institution before submission; contribution numbers of such institutions are submitted with the return of galley proofs.

The author (or authors) of each article will receive a total of 50 free reprints (with covers). Additional reprints with or without covers may be ordered by authors or institutions at the cost of printing. Orders for reprints are given when galley proofs are returned.

Both galley and page proofs are submitted to the senior author of each article.

Tables should be prepared for clarity and as near as practicable to Journal pattern, without ruled lines if possible. Table footnotes should appear at the base of each Table.

Figures are required for consideration simultaneously with the manuscript. Original figures of inconvenient size for forwarding may be represented by photographs on first submission of a manuscript; originals are required for line cuts. Illustrations requiring half-tone reproduction should be avoided as far as possible, but they will be accepted when necessary. *It is very important that the proper size of characters and symbols should be used for the lettering of illustrations.* A diagram for determining suitable heights of letters for original drawings that will be reduced, together with an explanatory note, has been published in this Journal, Vol. III, No. 1: 89–91; reprints will be submitted to authors on request. Mechanical lettering is recommended. If facilities for lettering are not available to the author, it is preferable to receive illustrations with lettering indicated in pencil only, to be finished in ink in the editorial office. All illustrations will be subject to at least a minimum reduction at the rate of 1 : 1.2. Drawings which have been heavily patched and pasted must *not be rolled* for mailing. The legends for the figures, identified by corresponding figure numbers on the illustrations also, should be typed in sequence at the end of the manuscript.

*A complete* and *accurate list of references* in alphabetical order at the end of each article is essential. References may be indicated in the text by author's name (or names) and *year of publication*, or by italicized numbers which correspond to the numbers given in sequence in the list of references. Each reference should include the last name followed by at least two initials or first name; co-authors should be listed with the initials or first name preceding the last name. The date should be indented on the line below, followed by a complete title *verbatim* in lower case except for the first word. Publisher, city and pagination should be indicated for books; for periodicals (abbreviations from "World List of Scientific Periodicals," Oxford, as far as possible), the volume (italicized), number and pagination should be given.

Additional information regarding the preparation of manuscripts will be furnished by the Managing Editor.

TABLE OF CONTENTS

Page

1. **W. V. R. Malkus and M. E. Stern:** Determination of ocean transports and velocities by electromagnetic effects ..... 97
2. **D. W. Pritchard:** Salinity distribution and circulation in the Chesapeake Bay estuarine system ..... 106
3. **T. J. Chow and T. G. Thompson:** The determination and distribution of copper in sea water. Part I. The spectrophotometric determination of copper in sea water ..... 124
4. **G. H. Jung:** Note on the meridional transport of energy by the oceans ..... 139
5. **F. A. Richards:** The estimation and characterization of plankton populations by pigment analyses. I. The absorption spectra of some pigments occurring in diatoms, dinoflagellates, and brown algæ ..... 147
6. **F. A. Richards with T. G. Thompson:** The estimation and characterization of plankton populations by pigment analyses. II. A spectrophotometric method for the estimation of plankton pigments ..... 156
7. **J. V. Griel and R. J. Robinson:** Titanium in sea water ..... 173
8. **Marie P. Fish, A. S. Kelsey, Jr., and W. H. Mowbray:** Studies on the production of underwater sound by North Atlantic coastal fishes ..... 180
9. **E. D. Goldberg, Majorie Baker, and D. L. Fox:** Microfiltration in oceanographic research. I. Marine sampling with the molecular filter ..... 194
10. **Henry Stommel and H. G. Farmer:** Abrupt change in width in two-layer open channel flow ..... 205
11. **W. H. Munk and G. A. Riley:** Absorption of nutrients by aquatic plants ..... 215
12. **W. H. Hastings and C. F. Spencer:** Determinations of free and bound ascorbic acid in fishery products ..... 241